AFCRL-65-99

SMALL SCALE WIND SHEARS FROM ROSE BALLOON TRACKED BY AN/FPS 16 RADAR

William E. Brockman

University of Dayton
Research Institute
Dayton, Ohio

Contract No. AF 19(604)-7450
Project No. 6682
Task No 668203

Final Report

December 1964

Prepared
for

Air Force Cambridge Research Laboratories
Office of Aerospace Research
United States Air Force
Bedford, Massachusetts

DISCLAIMER NOTICE

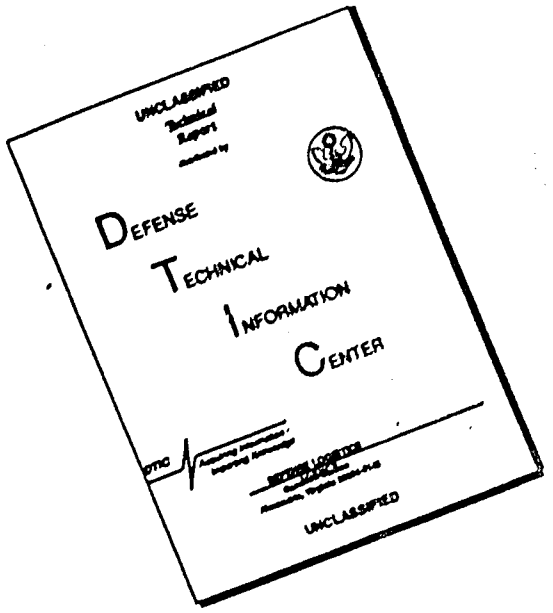

THIS DOCUMENT IS BEST QUALITY AVAILABLE. THE COPY FURNISHED TO DTIC CONTAINED A SIGNIFICANT NUMBER OF PAGES WHICH DO NOT REPRODUCE LEGIBLY.

AFCRL - 65 - 99

SMALL SCALE WIND SHEARS FROM ROSE BALLOON TRACKED BY AN/FPS 16 RADAR

William E. Brockman

University of Dayton
Research Institute
Dayton, Ohio

Contract No. AF 19(604)-7450
Project No. 6682
Task No. 668203

Final Report

December 1964

Prepared
for

Air Force Cambridge Research Laboratories
Office of Aerospace Research
United States Air Force
Bedford, Massachusetts

ABSTRACT

The ROSE balloon/AN-FPS-16 radar system is designed to report small-scale winds and shears by polynomial smoothing of the radar tracking data. The most successful mathematical technique for fitting the data and computing winds and shears is presented along with other techniques which were considered but ultimately rejected.

Analysis of the self-induced balloon motion is attempted by classical physical methods and by a Power Spectral Density Technique.

A criterion for evaluating the effect of modification to the standard ROSE is developed and applied to modified ROSEs and the newer small lightweight balloon.

TABLE OF CONTENTS

TABLE OF CONTENTS (Cont'd)

LIST OF FIGURES

LIST OF FIGURES (Cont'd)

LIST OF TABLES

LIST OF SYMBOLS

(Not applicable to Appendix 2)

Symbols Relating to Balloon Motion:

x, y, z	Cartesian coordinates
$\dot{x}, \dot{y}, \dot{z}$	First derivative with respect to time of x, y, z
$\ddot{x}, \ddot{y}, \ddot{z}$	Second derivative with respect to time of x, y, z
$\dot{x}_i, \dot{y}_i, \dot{z}_i$	First derivative evaluated at index i
A, E, R,	Polar coordinates
h	Altitude of balloon above surface of earth
$\dot{h}$	First derivative of altitude with respect to time
$\|v\|$	Magnitude of velocity of balloon
q	A general Cartesian coordinate representing x, y, or z
q_i	The ith x, y, or z value in a layer
$\bar{q}$	Average coordinate value in a layer
$\dot{q}$	First derivative of q with respect to time
$\ddot{q}$	Second derivative of q with respect to time
g	Gravitational acceleration of balloon
Re	Reynold's Number
$\sigma_x, \sigma_y, \sigma_z$	Errors in Cartesian coordinates due to errors in radar
$\sigma_A, \sigma_E, \sigma_R$	Errors in polar coordinates of radar

Symbols Relating to the Balloon:

m	Mass of balloon
M	Total effective mass of moving balloon
A_B	Cross sectional area of balloon
V_B	Volume of balloon
C_D	Drag coefficient of balloon
a	Radius of balloon
D	Diameter of balloon

Symbols Relating to Atmosphere:

ρ	Density of the air
ρ_m	Density from the model atmosphere

LIST OF SYMBOLS (Cont'd)

μ	Coefficient of viscosity of the air
μ_m	Coefficient of viscosity from the model atmosphere

Symbols Relating to Meteorological Data:

W_x, W_y, W_z	Components of wind in Cartesian coordinates
W_q	W_x, W_y, or W_z
$\overline{W}_q$	An average component wind in a layer
W_{q_i}	A component wind evaluated at the index i
σ_W	Error in a component wind
S_x, S_y	Component shear in Cartesian coordinates
S_q	S_x, or S_y
σ_s	Error in component shear
σ^2	Variance of wind vector over 10,000-foot layer
σ^2_{WE}, σ^2_{WN}	Variance of component wind over 1,000-foot layer
σ^2_{Std}	σ^2 for standard ROSE balloon
σ^2 modified	σ^2 for modified ROSE balloon
$\overline{R}$	Percent change of variance
WE	East wind
WN	North wind
WT	Wind vector
A_x, A_y	Component aerodynamic force on balloon

Symbols Relating to Data Smoothing:

n + 1	Number of data points in fit
i	Index of data i = 0, n
$P_{m,n}(i)$	The Legendre polynomial, degree m, for n + 1
$P'_{m,n}(i)$	First derivative of a Legendre polynomial

LIST OF SYMBOLS (Cont'd)

$P''_{m,n}(i)$	Second derivative of a Legendre polynomial
A_m	The m th coefficient in the orthogonal polynomial
$A_{m,q}$	The m th coefficient in the orthogonal polynomial for the q coordinate
σA_m	Standard Error of Estimate of the m th degree coefficient
$\hat{q}_i$	The predicted value of the q coordinate evaluated at index i
$\dot{\hat{q}}_i$	First derivative of q_i evaluated at i
$\ddot{\hat{q}}_i$	Second derivative of q_i evaluated at i
$\sigma_{\dot{\hat{q}}}$	Error in $\dot{\hat{q}}$
$\sigma_{\ddot{\hat{q}}}$	Error in $\ddot{\hat{q}}$
$R_{m,q}$ or σ^2_e	Residual of m th degree fit in q coordinate

LIST OF SYMBOLS
(Appendix 2)

x, y, z	Cartesian coordinates
r, θ, ϕ	Polar coordinates
$\bar{\Omega}$	Angular velocity of balloon
$\bar{W}$	Vertical velocity
$\bar{d}$	Radius of spiral
R	Radius of balloon
$\bar{V}$	Velocity of fluid relative to moving axes
V_r	Radial component of velocity relative to balloon
U	Velocity potential
V_θ, V_ϕ	Velocity of fluid at stagnation point
p	Pressure
ρ	Density
D	Perpendicular distance from axis of spiral

INTRODUCTION

The standard ROSE balloon is a metalized nonexpanding sphere having a diameter of two meters. When tracked by AN/FPS-16 radar, the space-time coordinates of this rising balloon can be determined accurately at a frequency of 10/sec.

This report is a chronological presentation of part of the work performed under AF 19(604)-7450 sponsored by AFCRL. The first section describes only the mathematics which were developed and used in an attempt to accurately describe the balloon's velocity and acceleration. As the reader will note, the author became increasingly aware that the velocities and accelerations of the standard ROSE balloon did not represent the wind. In particular, the acceleration of the balloon in no way represents the wind shear. Consequently, Sections 2 and 3 deal with the unsuccessful effort to eliminate "noise" (regardless of cause) from the balloon motion in order to find the proper wind.

Concurrent with the work described in Sections 1-3, Murrow and Henry (working independently) determined by physical experiments that the standard ROSE balloon was definitely not a proper wind sensor--at least over the first 200 feet of its ascent. Reid of AFCRL, who was also aware of this, showed that unpredictable aerodynamic forces were acting on the standard ROSE over at least the first 20,000 feet of its ascent. Our study, especially the work described in Sections 2 and 3, indicated that there was no good way to mathematically separate the aerodynamic forces acting on the balloon from those induced on the balloon by the wind. It thus became apparent to all concerned that the standard ROSE was not an adequate wind sensor.

A physical modification of the standard ROSE balloon was therefore undertaken by AFCRL. Such work had already been started by Scoggins of NASA. His modified ROSEs are called "Jimspheres." Reid and Lenhard of AFCRL devised several different modifications and developed some smaller smooth ROSEs. The description of these balloons, the mathematical treatment used in describing their motion, and the statistics employed in comparing the modified balloons to the standard and to the smaller ROSEs is described in Sections 4, 5, and 6.

The conclusion reached in these sections is that the modification has improved the wind sensitivity and will permit use of the techniques for predicting wind and wind shear which are described in Section 1.

1. MATHEMATICAL TECHNIQUES FOR COMPUTING WINDS AND SHEARS

That the ROSE balloon constituted a good wind sensing system was the basic assumption for the various mathematical techniques developed for computing winds and shears. Sections 1.1 and 1.2 describe two of these techniques and the empirical basis on which they were rejected. Sections 1.3 and 1.4 describe the other techniques which seem preferable. Although none of these methods were acceptable prior to balloon modification, it now appears that the techniques described in Sections 1.3 and 1.4 will provide valid wind and shear values when applied to radar tracking data from the modified balloon.

The mathematical rationale upon which all these techniques are based is as follows. The standard equations of motion for a balloon moving in the atmosphere without external forces are:

$$M\ddot{x} = 1/2\ \rho\ A_B\ C_D\ |v|\ (\dot{x} - W_x) \tag{1}$$

$$M\ddot{y} = 1/2\ \rho\ A_B\ C_D\ |v|\ (\dot{y} - W_y) \tag{2}$$

$$M\ddot{z} = 1/2\ \rho\ A_B\ C_D\ |v|\ (\dot{z} - W_x) + (m - \rho\ V_B)\ g, \tag{3}$$

where m is the mass of the balloon and M is the total effective mass (see Appendix 1). Combining the first and third equations and then the second and third gives the equations for the component wind in the x and y directions:

$$W_x = \dot{x} - \frac{M\ddot{x}\ (\dot{y} - W_y)}{M\ddot{y} - (m - \rho V_B)\ g} \quad \text{and} \quad W_y = \dot{y} - \frac{M\ddot{y}\ (\dot{z} - W_z)}{M\ddot{z} - (m - \rho V_B)\ g} \tag{4a, 4b}$$

The second term in both equations may be neglected because of its insignificance when compared with the first term. The wind equations modified in this way would be

$$W_x = \dot{x} \quad \text{and} \quad W_y = \dot{y} \tag{5a, 5b}$$

Winds computed by this equation are known as point winds. The average wind in a layer is given by the equations

$$W_x = \frac{x_2 - x_1}{t_2 - t_1} \quad \text{and} \quad W_y = \frac{y_2 - y_1}{t_2 - t_1}\ , \tag{6a, 6b}$$

where x_i, y_i, and t_i are the space-time coordinates.

The wind shear in the component directions is defined by the equations

$$S_x = \frac{d(W_x)}{dh} \quad \text{and} \quad S_y = \frac{d(W_y)}{dh}\ . \tag{7a, 7b}$$

The chain rule of differentiation gives

$$S_x = \frac{d(W_x)}{dt} \cdot \frac{dt}{dh} \quad \text{and} \quad S_y = \frac{d(W_y)}{dh} \cdot \frac{dt}{dh} \tag{8a, 8b}$$

If the approximations $\dot{x} = W_x$, $\dot{y} = W_y$, and $\dot{z} = \dot{h}$ are made the equations are:

$$S_x = \frac{\ddot{x}}{\dot{z}} \quad \text{and} \quad S_y = \frac{\ddot{y}}{\dot{z}} \tag{9a, 9b}$$

Quite often it is difficult to compute the second derivative accurately. In such cases $d(W_x)$ is replaced by ΔW_x, and dh is replaced by Δh which are finite differences. The component shear equations then become:

$$S_x = \frac{W_{x_2} - W_{x_1}}{h_2 - h_1} \quad \text{and} \quad S_y = \frac{W_{y_2} - W_{y_1}}{h_2 - h_1} \; . \tag{10a, 10b}$$

1.1 NINTH-DEGREE POLYNOMIAL METHOD

It has been suggested by Scoggins (May, 1963) that a polynomial approximation to the FPS-16 radar tracking data will yield valid accelerations and velocities which will in turn give realistic values of winds and shears from a rising sphere[1]. It is most economical to use the lowest possible degree polynomial in approximating the radar tracking data. In order to determine the lowest degree necessary the data was approximated by a zero degree polynomial, and the residual was compared with the theoretical tracking error inherent in the radar. The degree of the polynomial was then increased until the residual was less than the tracking error. The maximum degree used was the ninth degree even though the residual of the ninth was occasionally larger than the tracking error. Since the radar tracking data is equally spaced at one-tenth second, orthogonal polynomials are used in the approximations. The orthogonal polynomials are especially desirable in this application because they allow the next higher power term to be added without recalculating all the previous coefficients as is the case with ordinary least-squares polynomials. Later work indicated that it was also desirable to compute the analysis of variance (ANOVA) table to determine whether the higher degree polynomial terms were statistically significant.

1.1.1 ORTHOGONAL POLYNOMIALS

The general form of the orthogonal polynomial for n+1 data points, evaluated at the i th point, is:

$$\hat{q}_i = A_0 P_{0,n}(i) + A_1 P_{1,n}(i) + \ldots + A_m P_{m,n}(i) \tag{11}$$

where i takes on all integral values from 0 to n, and q is x, y, or z depending on which axis is being considered and m is the degree of the polynomial.

A_m is the coefficient of the form

$$A_m = \frac{\sum_{i=0}^{n} q_i P_{m,n}(i)}{\sum_{i=0}^{n} P_{m,n}(i)^2} \qquad \text{where } q_i \text{ is the i th data point.} \tag{12}$$

$P_{m,n}(i)$ is a Legendre polynomial of degree m, of the form

$$P_{m,n}(i) = \sum_{k=0}^{m} (-1)^k \binom{m}{k} \binom{m+k}{k} \frac{i^{[k]}}{n^{[k]}} \quad \text{where} \tag{13}$$

$$i^{[k]} = i(i-1)(i-2)(i-3)\cdots(i-k+1), \quad i^{[0]} = 1 \text{ and } \binom{m}{k} = \frac{m!}{(m-k)!\,k!}. \tag{14a, 14b}$$

The evaluation of these expressions for each degree from zero to nine is given in Appendix 6.

The Legendre polynomials were generated in a computer program instead of being obtained from standard tables so that transcription errors and costly key punching might be avoided. The generating program was written in BALGOL and run on the University of Dayton's Burroughs 220 computer. Every foreseeable error-producing operation was eliminated. When possible, integer arithmetic was used. When it was not possible to use integer arithmetic, 18-digit, double-precision arithmetic was used. The orthogonality of each set of numerical values of Legendre polynomials was checked using this property of orthogonality:

$$\sum_{i=0}^{n} P_{1,n}(i) \cdot P_{m,n}(i) = 0 \qquad m=2,5 \tag{15}$$

and

$$\sum_{i=0}^{n} P_{6,m}(i) \cdot P_{m,n}(i) = 0 \qquad m=7,10 \tag{16}$$

The values of the coefficients used in the standard reduction program were limited to 8 digits; therefore the results of the generating program were truncated after the 8th digit. The maximum deviation from zero occurring in the largest sets was less than 9×10^{-6}. It was felt that these coefficients would produce satisfactory results in the data reduction program.

The sums of squares of the coefficients $\sum_{i=0}^{n} P^2_{m,n}(i)$ were also computed in double precision and included at the end of the list of each set.

A sample printout of one set of coefficients is presented in Figure 1.

DEGREE 1	DEGREE 2	DEGREE 3	DEGREE 4	DEGREE 5		DEGREE 6	DEGREE 7	DEGREE 8	DEGREE 9	DEGREE 10	
.10000000. 01	.10000000. 01	.10000000. 01	.10000000. 01	.10000000. 01	0	.10000000. 01	.10000000. 01	.10000000. 01	.10000000. 01	.10000000. 01	0
0	0				0	0	0				0
.91666666. 00	.75000000. 00	.50000000. 00	.16666666. 00	-.25000000. 00	1	-.75000000. 00	-.13333333. 01	-.20000000. 01	-.27500000. 01	-.35833333. 01	1
6666666670	0	0	6666666670	0	1	0	3333333333	0	0	3333333333	1
.83333333. 00	.52173913. 00	.10869565. 00	-.34057971. 00	-.73913043. 00	2	-.97826086. 00	-.92753623. 00	-.43478260. 00	.67391304. 00	.25942028. 01	2
3333333340	0434782608	2173913043	0144927530	4782608700	2	9565217400	1884057970	8695652180	3478260860	9855072470	2
.75000000. 00	.31521739. 00	-.18379446. 00	-.59090909. 00	-.74407114. 00	3	-.51482213. 00	.14229249. 00	.11304347. 01	.21413043. 01	.25760869. 01	3
0	1304347826	6403162055	0909090910	6245059291	3	4387351784	0118577070	8260869558	4782608700	5652173920	3
.66666666. 00	.13043478. 00	-.38735177. 00	-.64690382. 00	-.48221343. 00	4	.10671936. 00	.88801054. 00	.13913043. 01	.99999999. 00	-.81159420. 00	4
6666666670	2608695652	8656126483	0816864294	8735177866	4	7588932813	0184453190	4782608690	9999999990	2898550700	4
.58333333. 00	-.32608695.-01	-.51185770. 00	-.56455862. 00	-.11758893. 00	5	.58399209. 00	.10171277. 01	.60869565. 00	-.85869565. 00	-.27644927. 01	5
3333333340	6521739140	7509881427	9776021078	2806324108	5	4861659994	9973649542	2173913030	2173913170	5362318700	5
.50000000. 00	-.17391304. 00	-.56719367. 00	-.39328063. 00	-.23320158. 00	6	.78749739. 00	.63074682. 00	-.46224256. 00	-.18112128. 01	-.18100686. 01	6
0	3478260870	5889328065	2411067193	1027667921	6	9625946142	7543166205	2929061860	1464530976	4988558410	6
.41666666. 00	-.29347826. 00	-.56324110. 00	-.17588932. 00	.49505928. 00	7	.70912211. 00	.83211982.-03	-.11670480. 01	-.13792906. 01	.63367658. 00	7
6666666670	0869565218	6719367591	8063241109	8537549320	7	3584356079	5254865100	5491990851	1784896977	2761251210	7
.33333333. 00	-.39130434. 00	-.50988142. 00	.51383399.-01	.62845849. 00	8	.41751612. 00	-.58310796. 00	-.12021806. 01	-.66361556.-01	.23852021. 01	8
3333333340	7826086960	2924901193	2094861720	8023715479	8	2321614316	7547326941	4342441801	0640727820	3577422157	8
.25000000. 00	-.46739130. 00	-.41699604. 00	.25889328. 00	.62351778. 00	9	.20334928.-01	-.90784272. 00	-.63427109. 00	.12151029. 01	.22173913. 01	9
0	4347826090	7430830044	0632410974	6561264800	9	2296651500	9353026852	9744246048	7482837746	0434781782	9
.16666666. 00	-.52173913. 00	-.29446640. 00	.42358366. 00	.49407114. 00	10	-.36665279. 00	-.88066014. 00	.21537219. 00	.17162471. 01	.43020594. 00	10
6666666670	0434782610	3162055340	2714097460	6245059220	10	8002912430	8394702070	0065956862	3958810516	9656741817	10
.83333333.-01	-.55434782. 00	-.15217391. 00	.52898550. 00	.27173913. 00	11	-.64359267. 00	-.53396355. 00	.94225333. 00	.12013729. 01	-.16178489. 01	11
3333333400	6086956530	3043478260	7246376860	0434782610	11	7345537440	4538518500	1538566260	9771165929	7025171599	11
.00000000. 00	-.56521739. 00	.00000000. 00	.56521739. 00	.00000000. 00	12	-.74370709. 00	.00000000. 00	.12249293. 01	.00000000. 00	-.24988558. 01	12
0	1304347830	0	1304347900	0	12	3821511070	0	3100012858	0	3524031592	12
-.83333333.-01	-.55434782. 00	.15217391. 00	.52898550. 00	-.27173913. 00	13	-.64359267. 00	.53396355. 00	.94225333. 00	-.12013729. 01	-.16178489. 01	13
3333333400	6086956530	3043478260	7246376860	0434782610	13	7345537440	4538518500	1538566260	9771165929	7025171599	13
-.16666666. 00	-.52173913. 00	.29446640. 00	.42358366. 00	-.49407114. 00	14	-.36665279. 00	.88066014. 00	.21537219. 00	-.17162471. 01	.43020594. 00	14
6666666670	0434782610	3162055340	2714097460	6245059220	14	8002912430	8394702070	0065956862	3958810516	9656741817	14
-.25000000. 00	-.46739130. 00	.41699604. 00	.25889328. 00	-.62351778. 00	15	.20334928.-01	.90784272. 00	-.63427109. 00	-.12151029. 01	.22173913. 01	15
0	4347826090	7430830044	0632410974	6561264800	15	2296651500	9353026852	9744246048	7482837746	0434781782	15
-.33333333. 00	-.39130434. 00	.50988142. 00	.51383399.-01	-.62845849. 00	16	.41751612. 00	.58310796. 00	-.12021806. 01	.66361556.-01	.23852021. 01	16
3333333340	7826086960	2924901193	2094861720	8023715479	16	2321614316	7547326941	4342441801	0640727820	3577422157	16
-.41666666. 00	-.29347826. 00	.56324110. 00	-.17588932. 00	-.49505928. 00	17	.70912211. 00	-.83211982.-03	-.11670480. 01	.13792906. 01	.63367658. 00	17
6666666670	0869565218	6719367591	8063241109	8537549320	17	3584356079	5254865100	5491990851	1784896977	2761251210	17
-.50000000. 00	-.17391304. 00	.56719367. 00	-.39328063. 00	-.23320158. 00	18	.78749739. 00	-.63074682. 00	-.46224256. 00	.18112128. 01	-.18100686. 01	18
0	3478260870	5889328065	2411067193	1027667921	18	9625946142	7543166205	2929061860	1464530976	4988558410	18
-.58333333. 00	-.32608695.-01	.51185770. 00	-.56455862. 00	.11758893. 00	19	.58399209. 00	-.10171277. 01	.60869565. 00	.85869565. 00	-.27644927. 01	19
3333333340	6521739140	7509881427	9776021078	2806324108	19	4861659994	9973649542	2173913030	2173913170	5362318700	19
-.66666666. 00	.13043478. 00	.38735177. 00	-.64690382. 00	.48221343. 00	20	.10671936. 00	-.88801054. 00	.13913043. 01	-.99999999. 00	-.81159420. 00	20
6666666670	2608695652	8656126483	0816864294	8735177866	20	7588932813	0184453190	4782608690	9999999990	2898550700	20
-.75000000. 00	.31521739. 00	.18379446. 00	-.59090909. 00	.74407114. 00	21	-.51482213. 00	-.14229249. 00	.11304347. 01	-.21413043. 01	.25760869. 01	21
0	1304347826	6403162055	0909090910	6245059291	21	4387351784	0118577070	8260869558	4782608700	5652173920	21
-.83333333. 00	.52173913. 00	-.10869565. 00	-.34057971. 00	.73913043. 00	22	-.97826086. 00	.92753623. 00	-.43478260. 00	-.67391304. 00	.25942028. 01	22
3333333340	0434782608	2173913043	0144927530	4782608700	22	9565217400	1884057970	8695652180	3478260860	9855072470	22
-.91666666. 00	.75000000. 00	-.50000000. 00	.16666666. 00	.25000000. 00	23	-.75000000. 00	.13333333. 01	-.20000000. 01	.27500000. 01	-.35833333. 01	23
6666666670	0	0	6666666670	0	23	0	3333333333	0	0	3333333333	23
-.10000000. 01	.10000000. 01	-.10000000. 01	.10000000. 01	-.10000000. 01	24	.10000000. 01	-.10000000. 01	.10000000. 01	-.10000000. 01	.10000000. 01	24
0	0				24	0	0				24
.90277777. 01	.63586956. 01	.57806324. 01	.62088274. 01	.76199245. 01	25	.10519814. 02	.16208307. 02	.27761633. 02	.52783632. 02	.11143211. 03	25
7777777776	5217391297	1106719362	0447957829	4186130042	25	8533388809	3295887887	6614064019	4223161294	2890923096	25

Figure 1. Tabular Listing of Orthogonal Polynomial Coefficients for 25 Points

The physical size of the computer used in the computation of winds and shears imposes a practical limit on the maximum number of Legendre polynomials that can be used in the approximation of the data. The maximum number of data points to be approximated can be determined by considering the vertical velocity of the balloon. The average vertical velocity of the balloon is about 20 feet per second, producing an average of 50 tenth-second data points per 100-foot layer. In order to include all reasonable vertical velocities, the lower limit was set at 10 feet per second and the upper limit at 40 feet per second. This corresponds to 100 points and 25 points for the upper and lower limits respectively. The Legendre polynomials were computed to cover the range of 25 to 100 data points per fit and the degrees from one to ten.

It was desirable to associate an altitude in the layer with the meteorological parameters. The altitude chosen was the mid-point of the 100-foot layer. The accelerations and velocities were evaluated at mid-point of the data, and these values were associated with the altitude 50 feet above the bottom of the layer. It is much more convenient to evaluate the polynomials at one of their original data than between two of them. The mid-point coincides with an original data point only when there is an odd number of data points in the layer. The program is designed to assemble an odd number of data points over the nominal 100-foot layer which might be as much as 103 feet in depth. Each layer was considered individually. That is, there was no overlapping of data from layer to layer.

1.1.2 TRACKING ERRORS

The theoretical tracking errors to be used in the determination of the degree of polynomial approximating the data is a function of the errors in the parameters reported by the radar, namely elevation and azimuth angles and the slant range distance. These radar parameter errors are related to the space-time coordinate errors by the geometry of the coordinate systems.

The space-time coordinate system used is earth fixed, Euclidian 3-space, such that

i) The x-axis is oriented north - south, with north positive.
ii) The y-axis is oriented east - west, with east positive.
iii) The z-axis is perpendicular to the x - y plane with upwards positive.
iv) The x - y plane is tangent to the earth at the launch site.

The equations of transformation from radar parameters--Range (R), Elevation (E), and Azimuth (A, positive clockwise from north)--to a Euclidian 3-space are:

$$x = R \cos E \cos A \tag{17}$$
$$y = R \cos E \sin A \tag{18}$$
$$z = R \sin E \tag{19}$$

Since there exists an error inherent in the radar, the errors of x, y, and z with respect to the error in A, E, and R are given by

$$\sigma_x^2 = R^2\left[\sigma_E^2 \sin^2 E \cos^2 A + \sigma_A^2 \cos^2 E \sin^2 A\right] + \sigma_R^2 \cos^2 E \cos^2 A \quad (20)$$

$$\sigma_y^2 = R^2\left[\sigma_E^2 \sin^2 E \sin^2 A + \sigma_A^2 \cos^2 E \cos^2 A\right] + \sigma_R^2 \cos^2 E \sin^2 A \quad (21)$$

$$\sigma_z^2 = R^2 \sigma_E^2 \cos^2 E + \sigma_R^2 \sin^2 E \quad (22)$$

where σ_A^2, σ_E^2 and σ_R^2 are the errors in Azimuth, Elevation, and Range respectively and are constant with respect to the radar system tracking the balloon.

Since the data is given in x, y, and z, the transformation equation can be used to give the errors σ_x^2, σ_y^2, and σ_z^2 in terms of x, y, and z and the constant radar errors. The tracking errors in this more useful form are:

$$\sigma_x^2 = \left[\frac{x^2}{x^2 + y^2 + z^2}\right]\sigma_R^2 + \left[\frac{x^2 z^2}{x^2 + y^2}\right]\sigma_E^2 + \left[y^2\right]\sigma_A^2 \quad (23)$$

$$\sigma_y^2 = \left[\frac{y^2}{x^2 + y^2 + z^2}\right]\sigma_R^2 + \left[\frac{y^2 z^2}{x^2 + y^2}\right]\sigma_E^2 + \left[y^2\right]\sigma_A^2 \quad (24)$$

$$\sigma_z^2 = \left[\frac{z^2}{x^2 + y^2 + z^2}\right]\sigma_R^2 + \left[x^2 + y^2\right]\sigma_E^2 \quad (25)$$

The errors must be computed for each layer since the errors are functions of the x, y, and z values.

1.1.3 DETERMINATION OF DEGREE OF THE POLYNOMIAL

As outlined in a previous section, the lowest degree polynomial possible in approximating the radar tracking data is determined by comparing the residual of the m th degree polynomial fit with the independent, theoretical tracking error described in Section 1.1.2. The residual of the zero-degree fit is compared to the tracking error; if the tracking error is larger, a "good" fit has been obtained, in this case the mean. If the tracking error is smaller than the residual, the sum of squares accounted for by the first-degree fit is subtracted; this new residual is then compared with the tracking error. If the residual is now smaller than the tracking error, the linear fit is "good"; if the residual is still larger, the next degree (the second) must be added.

This process continues until the residual is finally smaller than the tracking error, or until the ninth degree has been reached. If the residual is still larger than the theoretical tracking error, the process is discontinued, and the ninth-degree polynomial fit is accepted as being "good."

The equation of the residual of the zero-degree fit is

$$R_{0,q} = \frac{\sum_{i=0}^{n} (q_i - \overline{q})^2}{n+1} \tag{26}$$

where q_i are the data points and $\overline{q} = A_0$ since $P_{0,n}(i) = 1$. $R_{0,q}$ is compared to σ_q^2 (in calculating σ_q^2, the mean of q_i in the 100 foot layer is used). If $R_{0,q}$ is less than or equal to σ_q^2, a zero-degree polynomial is a "good" fit. If $R_{0,q}$ is greater than σ_q^2, a higher degree fit is necessary.

The expression for the residual of the j + 1 st degree fit is given by the recurrence relation

$$R_{j+1,q} = R_{j,q} - \frac{\sigma_{j+1,q}^2}{n+1} \tag{27}$$

where

$$\sigma_{j+1,q}^2 = \sum_{i=0}^{n}\left[A_{j+1}P_{j+1,n}(i)\right]^2 = A_{j+1}^2 \sum_{i=0}^{n}\left[P_{j+1,n}(i)\right]^2 \tag{28}$$

The coefficients $A_1, A_2, \ldots, A_{j+1}$ are of course available from the polynomial without further computation.

An alternate method of determining the lowest degree of the polynomial is the standard statistical technique of the analysis-of-variance table (Crow, Davis, Maxfield)[2]. This table is presented as Figure 2. The analysis of variance is performed to test the significance of the terms $A_m P_{m,n}(i)$ of the polynomial. First, the total sum of squares (which is the sum of squared deviations of q from the average q) is computed. As shown earlier in this section, the average q is just A_0, the first term of the polynomial. Computed next is that part of the total sum of squares accounted for by the linear, quadratic, cubic, quartic terms, etc, up to the m th degree. These sums of squares,

$$\left[\sum_{i=0}^{n} q_i P_{m,n}(i)\right]^2 \Big/ \sum_{i=0}^{n}\left[P_{m,n}(i)\right]^2 ,$$

their degrees of freedom, and the corresponding mean squares are shown in Figure 2. That part of the total not accounted for by the sums of squares of the various degree terms is the residual sum of squares. An "F" value is

Quantity	Equation		Degrees of Freedom	Mean Square	$F = \frac{\text{Mean Square}}{\text{Residual MS}}$
Total	$\sum_{i=0}^{n} (q_i - A_0)^2$	(1)	n		
Linear	$\left[\sum_{i=0}^{n} q(i)P_{1,n}(i)\right]^2 \Big/ \sum_{i=0}^{n} P_{1,n}(i)^2$	(2)	1	(2)	(2)/Res MS
Quadratic	$\left[\sum_{i=0}^{n} q(i)P_{2,n}(i)\right]^2 \Big/ \sum_{i=0}^{n} P^2_{2,n}(i)$	(3)	1	(3)	(3)/Res MS
Cubic	.	(4)	1	(4)	(4)/Res MS
Quartic	.	(5)	1	(5)	(5)/Res MS
.	.	.	.	.	.
.	.	.	.	.	.
.	.	.	.	.	.
m th	$\left[\sum_{i=0}^{n} q_i P_{m,n}(i)\right]^2 \Big/ \sum_{i=0}^{n} P^2_{m,n}(i)$	(m+1)	1	(m+1)	(m+1)/Res MS
Residual	(1) -(2) -(3) -(4) -. . . -(m+1)		n-m	Residual MS = $\frac{\text{Residual}}{(n-m)}$	

Figure 2. Analysis of Variance Table for Orthogonal Polynomials

computed for each term by computing the ratio of the mean square of each term to the mean square of the residual. Each computed F value is then compared with the tabular value of the "F Distribution" at the 5 percent significance level. If the F of the jth term is larger than the corresponding tabular value, then the data are significantly better represented by including this term than by omitting it.

The analysis-of-variance criterion was not applied in this problem because it was felt that the independent estimate of error was more meaningful. In order to become familiar with the contribution to the fit of each term in the polynomial, a modified form of this table was computed and printed out for several early flights. The modification was to reduce the size of the tables by printing out only the sum of squares of the residual after each term had been added to the polynomial. Some "F" values were then computed by hand and checked for significance.

1.1.4 COMPUTATION OF WINDS AND SHEARS

1.1.4.1 Winds

There are two ways to describe the wind in the 100-foot layer: 1) the average wind in the layer; 2) the wind evaluated at a given altitude known as the Point Wind.

1.1.4.2 Average Wind

The average wind in the layer is determined by a simple finite difference between the highest fitted coordinate point in the layer and the lowest point divided by the time needed to traverse the layer. In terms of the evaluated polynomial fit, the average wind is given by:

$$\overline{W}_q = \frac{\hat{q}_n - \hat{q}_0}{t_n - t_0} \tag{29}$$

1.1.4.3 Point Wind

Using the equation developed in Section 1, the wind is given by $W_{q_i} = 10 \cdot \dot{\hat{q}}_i$; the factor of 10 is necessary because the points are 0.1 second apart instead of 1.0 second apart. Note that $\dot{\hat{q}}_i$ is the first derivative of the polynomial evaluated at the point i. The mid-point of the layer was chosen as the altitude to be assigned to the point wind. This corresponds to evaluating the polynomial at the point (i=n/2) where n is always even.

The equation for the first derivative is

$$\dot{\hat{q}}_{n/2} = A_1 P'_{1,n}(\tfrac{n}{2}) + A_3 P'_{3,n}(\tfrac{n}{2}) + \ldots + A_j P'_{j,m}(\tfrac{n}{2}) \tag{30}$$

where j is an odd number either equal to m (if m is odd) or m-1 (if m is even). The point wind is then given by

$$W_{q_{n/2}} = 10 \cdot \dot{\hat{q}}_{n/2} \tag{31}$$

Obviously, if m = 1 (the polynomial is of the first degree), then the point wind, $W_{q_{n/2}}$, will be equal to the average wind, $\overline{W}_q$.

The derivatives of the Legendre polynomials are developed and presented in Appendix 6.

1.1.4.4 Shears

During the examination of the results of preliminary computations (particularly the ANOVA tables) it was decided that accurate second derivatives of the polynomial would be difficult to obtain, especially in the higher degrees. Therefore, the simplified form of the shear equations was chosen:

$$S_x = \frac{W_{x2} - W_{x1}}{h_2 - h_1} \tag{10a}$$

$$S_y = \frac{W_{y2} - W_{y1}}{h_2 - h_1} \tag{10b}$$

It was thought that the point wind (Section 1.1.4.3) was a better representation of the wind at the center of the layer; therefore point winds were used in the computation of the shears. The altitude layer was always 100 feet; consequently the denominator, $h_2 - h_1$, always equals 100 feet.

The equations for shear then reduce to

$$S_x = \frac{(\dot{x}_{n/2})_{\ell+1} - (\dot{x}_{n/2})_{\ell}}{100} \tag{32a}$$

$$S_y = \frac{(\dot{y}_{n/2})_{\ell+1} - (\dot{y}_{n/2})_{\ell}}{100} \tag{32b}$$

where the subscript, ℓ, denotes any given layer and $\ell+1$, the layer immediately above it. The units of shear are sec^{-1}.

1.1.5 RESULTS AND CONCLUSIONS

The computer program was written to compute the winds and shears as outlined in the previous sections. The program was written in FORTRAN II for the IBM 7094 computer, checked out at the Wright-Patterson A.F.B. facility, then forwarded to Eglin A.F.B. for operation on their system. Through the very fine cooperation of PGVMS, Eglin A.F.B., Florida the program with all of the polynomial coefficients was implemented. A test ROSE balloon was launched and tracked, the data were reduced in manner that has been outlined, and the results were forwarded to the University of Dayton.

The results of this test run were quite surprising in that while the average winds looked reasonable, the point winds (and therefore the shears) were quite erratic and did not agree with the average winds. A sample of this output is shown in Figure 3. As indicated on the tabulation shown in Figure 3, the output parameters are:

ALTITUDE	WIND EAST	NORTH	TOTAL	ANG	M	PT SHEAR EAST	NORTH	TOTAL	PT * E	PT * N
1050.	0.00	-9.03	5.35	C	5					
1100.						C.13273865	-0.03317297	0.13632103	13.27	-26.20
1150.	13.27	-19.15	13.80	325	3					
1200.						-C.13273865	0.32083193	0.36720697	0.00	5.88
1250.	0.00	1.05	0.62	175	7					
1300.						C.00000000	-0.30340336	0.30340336	0.00	-24.46
1350.	0.00	-16.83	9.97	C	7					
1400.						C.23803916	0.60513848	0.65120384	23.80	36.16
1450.	23.80	-8.49	14.96	285	9					
1500.						-C.15395639	-2.53183237	2.53650865	8.41	-217.03
1550.	8.41	8.34	7.01	225	9					
1600.						C.04514764	3.53530994	3.53559819	12.92	136.50
1650.	12.92	-23.29	15.77	330	9					
1700.						-C.05502044	1.12945595	1.13079518	7.42	249.45
1750.	7.42	-6.10	5.69	305	9					
1800.						C.32949221	4.01847482	4.03136043	40.37	651.30
1850.	10.81	-20.13	13.53	331	9					
1900.						5.93384427	-7.43480539	9.51245701	633.75	-92.18
1950.	19.94	24.88	18.88	218	9					
2000.						-2C.822093C1	7.04525435	21.93170066	-1448.45	612.34
2050.	10.43	-15.33	10.98	325	9					
2100.						14.62306941	-5.62501782	15.65754128	13.95	49.84
2150.	13.85	-19.14	13.99	324	9					
2200.						C.06438351	2.14214444	2.14311177	20.29	264.05
2250.	15.52	-17.64	13.91	318	9					
2300.						C.09589146	-2.53924125	2.54135121	29.88	10.13
2350.	29.88	2.35	17.75	265	5					
2400.						6.08669555	-0.15326882	6.08852543	638.55	-5.20
2450.	25.60	-9.06	16.08	285	9					
2500.						-6.26437831	-0.09468655	6.25539386	12.11	-14.67
2550.	12.11	-14.67	11.26	320	1					
2600.						-C.81219283	0.17102312	0.83000367	-69.11	2.44
2650.	12.65	-4.81	8.01	290	9					
2700.						-C.41916125	-0.27325223	0.53036285	-111.02	-24.89
2750.	21.19	-24.89	19.35	315	9					
2800.						2.41098812	0.15240891	2.41533213	130.07	-9.60
2850.	26.71	-9.60	16.80	285	9					
2900.						-3.69375536	-0.16162071	3.69728955	-239.30	-25.76
2950.	-1.22	-25.76	15.27	2	9					
3000.						4.92421752	0.21165040	4.92876434	253.12	-4.60
3050.	18.00	-4.60	11.00	284	9					
3100.						-13.13959372	-0.27324076	13.14243436	-1060.84	-31.92
3150.	6.03	-31.92	19.23	349	9					
3200.						12.94904721	0.21192632	12.95078123	234.07	-10.73
3250.	31.04	-10.73	19.44	285	9					
3300.						17.30752563	-0.13470572	17.30934968	1964.82	-24.20
3350.	11.50	-11.05	9.45	313	9					
3400.						-22.78912926	0.15713237	22.78957071	-314.09	-8.48
3450.	34.28	-8.48	20.91	283	9					
3500.						3.75974229	0.05484935	3.76014233	61.88	-3.00

Figure 3. Sample Printout of Ninth-Degree Method

Altitude	ft
Wind East	ft/sec
Wind North	ft/sec
Wind Total	Knots
Angle	degrees
M	Highest degree polynomial used
Shear East	Sec^{-1}
Shear North	Sec^{-1}
Shear Total	Sec^{-1}
Point Wind East	ft/sec
Point Wind North	ft/sec

As will be noted, the highest degree used by either component is quite often the ninth, which was the maximum. The component data were plotted vs. time and although ragged, they resembled a parabola--indicating a second-degree polynomial fit. It was then decided to add monitor variables to the printout to check intermediate computations and to add the Residuals of the fits as successively higher degree terms were added. A sample of another test flight is presented in Figure 4. The monitor parameters, indicated by the *, are

q^{-2}	ft^2
$\overline{q}_2$	ft (average space coordinate)
σ_q	Tracking error for this layer
$R_{0,q}$	Residual for zero degree
$R_{1,q}$	Residual for first degree
$R_{2,q}$	Residual for second degree
$R_{3,q}$	Residual for third degree
$R_{5,q}$	Residual for fifth degree
$R_{7,q}$	Residual for seventh degree
$R_{9,q}$	Residual for ninth degree

The monitor parameters are always arranged: North East, and vertical. The Residual for the Vertical is always zero because the Vertical is only used for finite differences and therefore is not fitted. It can be seen that the only significant reduction of the Residual occurs when the linear effect is removed, i.e., the linear fit is significantly better than the average. In order to verify these results, the first flight was rerun. The sums of squares needed in the ANOVA table were printed out with the altitude and number of points preceding each group. A sample of this printout is shown in Figure 5. Each group consists of 10 lines. These correspond to: the total sums of squares; that part accounted for by the linear term; the part accounted for by the quadratic etc., up to the ninth. The criteria for stopping the fit at a certain degree was removed for this, allowing each of the three coordinates to go to the ninth degree. When the horizontal components of the entire flight were considered, approximately 75% of the sum of the squares of the degree higher than first were small, i.e., (did not explain much of variation), and about 95% of the sums of the squares of the degrees higher than the second were not significant. The vertical component was almost never significant above the first degree.

Figure 4. Sample Printout of Ninth Degree Method

	1050. 47			
0	0.128986376 05	0.26705527E 04	0.42727653E 05	
1	0.11635142E 05	0.12977353E 04	0.42480990E 05	
2	0.10459229E 03	0.23804767E 03	0.10786510E 02	
3	0.82027593E 03	0.23133238E 03	0.27255104E 02	
4	0.10682093E 03	0.43456020E 02	0.32711781E 01	
5	0.11788232E 03	0.17714383E 02	0.20607188E-01	
6	0.18607964E 02	0.55114378E 02	0.30641113E-00	
7	0.58518855E 00	0.15111933E 03	0.18432444E 02	
8	0.17832662E 02	0.42238697E 01	0.35851125E 01	
9	0.16974244E 02	0.45423881E 02	0.28217219E 02	
	1150. 43			
	0.31787438E 06	0.12226278E 05	0.36050505E 05	
	0.31396449E 05	0.11667465E 05	0.35832722E 05	
	0.93727569E 01	0.20531458E 03	0.13878377E 03	
	0.24401158E 03	0.31985190E 02	0.78863400E 01	
	0.10767385E 02	0.43988150E-00	0.18527291E 01	
	0.13834375E 02	0.28060341E 02	0.19699720E 02	
	0.19689167E 02	0.29546902E 02	0.50272697E 00	
	0.27116477E 01	0.52196701E 02	0.53465224E 01	
	0.90405026E 01	0.42081892E-02	0.41583557E 01	
	0.40712259E-00	0.26569420E-01	0.61865373E 00	
	1250. 47			
	0.19473188E 04	0.13654891E 04	0.37924461E 05	
	0.10700502E 04	0.33180430E 03	0.37736554E 05	
	0.50462514E 03	0.38977972E 03	0.46845157E 02	
	0.21806452E 03	0.30315685E 01	0.40882799E 02	
	0.36134019E 02	0.15453888E 02	0.15454812E-03	
	0.20474964E 02	0.62593009E 01	0.95965384E 00	
	0.21827787E 02	0.42586818E 01	0.34621612E 02	
	0.87548620E 01	0.21561760E 02	0.50338188E 01	
	0.20862719E-02	0.12169160E 02	0.11070099E 02	
	0.99910565E 01	0.10171815E 02	0.81580595E 01	
	1350. 43			
	0.23397625E 05	0.13184604E 03	0.32368275E 05	
	0.22565093E 05	0.13929126E 01	0.32198616E 05	
	0.59844577E 03	0.72520565E 03	0.10084382E 02	
	0.19809570E 03	0.85497833E 01	0.32914955E 01	
	0.87413991E-02	0.20404538E 01	0.54184658E 02	
	0.26387259E 01	0.48819278E 01	0.70242788E 02	
	0.57707421E 00	0.22549401E 02	0.36788028E 01	
	0.94424308E 01	0.17545099E 01	0.90313151E 01	
	0.16191162E-00	0.32889096E 01	0.46806868E 01	
	0.61291972E 01	0.51228204E 01	0.16754898E 01	
	1450. 43			
	0.76814406E 04	0.38166504E 05	0.32498693E 05	
	0.73215506E 04	0.37522002E 05	0.32242788E 05	
	0.20618086E 03	0.12770844E 03	0.22693055E-01	
	0.10074470E 03	0.92479887E 02	0.61138853E 01	
	0.40704094E-01	0.30697029E 02	0.83017248E 02	
	0.42015298E 01	0.12078739E 02	0.11504110E 03	
	0.31877830E 01	0.53903448E 02	0.13661620E 02	
	0.15856502E-00	0.46356085E-00	0.33246574E 01	
	0.58482970E 01	0.44811297E 02	0.29104852E 01	

Figure 5. Sample Printout of Modified ANOVA Table for Ninth Degree Method

With this in mind, the plots of the raw data were studied again. Almost without fail, whenever the degree of the polynomial above the second was required (by the tracking error criteria), the coordinate value plot showed either a rough section of data or a relatively smooth section with one or two slightly skew points.

These findings were the basis for discarding this long and rather elaborate method in favor of a simpler one. The ANOVA table indicated that the degree of the polynomial fit should probably not be higher than two.

1.2 SECOND-DEGREE POLYNOMIAL METHOD

The study of the ninth-degree polynomial fit indicated that in 25% of the cases the second degree polynomial term was statistically significant in the approximation. Another program was then written to compute the wind and shears based on the second degree fit. Similar expressions were used for the winds, but the original form of the shear was used because the component accelerations were significant in the second-degree fit. Furthermore, since the degree of the polynomial was reduced, the sampling frequency was also reduced to 0.2 second.

1.2.1 ORTHOGONAL POLYNOMIALS AND DERIVATIVES

The orthogonal polynomial for the second-degree fit will be repeated here for ease of reference, and the second derivative will be added. The number of points in the layer is n+1, and the index (i) takes on all integral values from zero to n. The Legendre polynomials are:

$$P_{0,n}(i) = 1 \qquad (33a)$$

$$P_{1,n}(i) = 1 - \frac{2i}{n} \qquad (33b)$$

$$P_{2,n}(i) = 1 - \frac{6i}{n} + \frac{6i\,(i-1)}{n\,(n-1)} \qquad (33c)$$

The first derivatives are:

$$P'_{0,n}(i) = 0 \qquad (34a)$$

$$P'_{1,n}(i) = -\frac{2}{n} \qquad (34b)$$

$$P'_{2,n}(i) = \frac{-6}{n} - \frac{6}{n(n-1)} + \frac{12i}{n(n-1)} \qquad (34c)$$

The second derivatives are:

$$P''_{0,n}(i) = 0 \qquad (35a)$$

$$P''_{1,n}(i) = 0 \qquad (35b)$$

$$P''_{2,n}(i) = \frac{12}{n(n-1)} \qquad (35c)$$

The first derivative (the velocity) is:

$$\dot{\hat{q}}_i = A_1 P'_{1,n}(i) + A_2 P'_{2,n}(i) \qquad (36)$$

The second derivative (the acceleration) is:

$$\ddot{\hat{q}}_i = A_2 P''_{2,n}(i) \tag{37}$$

where in all cases

$$A_m = \frac{\sum_{i=0}^{n} q_i \, P_{m,n}(i)}{\sum_{i=0}^{n} P_{m,n}^{2}(i)} \tag{12}$$

1.2.2 WINDS

In the second-degree fit, as in the ninth, we can compute two values for wind. One is an average over the layer, and the other is assigned to a particular altitude point in the layer known as the average wind and point wind respectively. In working with the second-degree polynomial, the values of the two types of winds are exactly the same. This is due to the property of the Legendre polynomial of the even degrees being zero when evaluated at the mid-point. Thus, since

$$P'_{2,n}(\tfrac{n}{2}) = 0 \tag{38}$$

then

$$\dot{\hat{q}}_{n/2} = A_1 P'_{1,n}(\tfrac{n}{2}) \tag{39}$$

The quadratic term is lost, and the answer is the same as if we had fitted a linear equation. However, for the linear equation the slope is the same at any point in the layer and is equivalent to the ratio of difference in space coordinate to the difference in time, i.e.,

$$\text{slope} = \frac{\Delta \hat{q}}{\Delta t} = \overline{W}_q = W_{q_{n/2}} \tag{40}$$

The equations for the component winds are:

$$W_x = \frac{-10}{n} A_{1x} \tag{41a}$$

$$W_y = \frac{-10}{n} A_{1y} \tag{41b}$$

where the 10 (instead of 2) is necessary to convert to the correct units of ft/sec from ft/0.2 sec for 0.2 sec spaced data.

1.2.3 SHEARS

Since the second degree was often found to be significant, it was decided to use the following form for shear:

$$S_x = \frac{\ddot{x}}{\dot{z}} \qquad \text{and} \qquad S_y = \frac{\ddot{y}}{\dot{z}} \tag{9a}$$ (9b)

This equation implies that within the layer there is a constant acceleration in the horizontal components and a constant velocity in the vertical component. The equations for shears of the component directions in terms of the polynomial coefficients are:

$$S_x = \frac{A_{2x} \cdot P''_{2,n}(i)}{A_{1z} \cdot P'_{1,n}(i)} \cdot 5 \qquad S_y = \frac{A_{2y} \cdot P''_{2,n}(i)}{A_{1z} \cdot P'_{1,n}(i)} \cdot 5 \tag{42a}$$ (42b)

where the factor 5 converts to normal shear units of sec^{-1}. Substitution for the Legendre polynomials gives:

$$S_x = -\frac{30}{n-1} \cdot \frac{A_{2x}}{A_{1z}} \qquad S_y = -\frac{30}{n-1} \cdot \frac{A_{2y}}{A_{1z}} \tag{43a}$$ (43b)

where again -30 is used in place of -6 to correct for the 0.2 sec interval.

1.2.4 ERROR ANALYSIS OF WINDS AND SHEARS

The second-degree method does not compare the residual to the tracking error, as does the ninth degree. The error in the value of a parameter was included with the parameter itself in the output of the program to provide confidence limits on the parameters.

1.2.4.1 Standard Error of Estimate of the Coefficients

The standard error of estimate (σ_{A_m}) of the m th polynomial coefficient (A_m) is given by

$$\sigma_{A_m}^2 = \frac{\sigma_e^2}{\sum_{i=0}^{n} P_{m,n}^2(i)} \tag{44}$$

where σ_e^2 is the residual variance of the m th degree fit. Therefore, the squares of the error in A_1 and A_2 are given by

$$\sigma_{A_1}^2 = \frac{\sigma_{e_1}^2}{\sum_{i=0}^{n} P_{1,n}^2(i)} \qquad \sigma_{A_2}^2 = \frac{\sigma_{e_2}^2}{\sum_{i=0}^{n} P_{2,n}^2(i)} \tag{45a, 45b}$$

The expression for the residual variance of the first degree fit is given by

$$\sigma_{e_1}^2 = \left[\sum_{i=0}^{n} (q_i - \bar{q})^2 - A_1^2 \sum_{i=0}^{n} P_{1,n}^2(i) \right] \Big/ \left[n-1 \right] \tag{46}$$

and for the second degree by

$$\sigma_{e_2}^2 = \left[\sum_{i=0}^{n} (q_i - \bar{q})^2 - A_1^2 \sum_{i=0}^{n} P_{1,n}^2(i) - A_2^2 \sum_{i=0}^{n} P_{2,n}^2(i) \right] \Big/ \left[n-2 \right] \tag{47}$$

1.2.4.2 Errors in Winds and Shears

If the errors in the coefficients of the fitting polynomial are known, the errors in the wind and shears can be computed. The expression for the wind is given by

$$W_q = \dot{\hat{q}}_{n/2} = A_1 P'_{1,n}\left(\frac{n}{2}\right) \tag{48}$$

and the error in the wind (σ_W) is given by

$$\sigma_W = P'_{1,n}\left(\frac{n}{2}\right) \cdot \sigma_{A_1} = \left(-\frac{2}{n}\right) \sigma_{A_1} \tag{49}$$

since $P'_{1,n}\left(\frac{n}{2}\right) = -2/n$

The wind can then be reported as a value plus or minus the error by using the following expression:

$$W = -\frac{10}{n} \left[A_1 \pm \sigma_{A_1} \right] \tag{50}$$

The expression for shear is given by

$$S_q = \ddot{q}/\dot{z} \tag{51}$$

Assuming that the interaction between the component acceleration and the vertical velocity is zero, the error in shear (σ_s) is given by

$$\sigma_s^2 = \frac{1}{\dot{z}^2} \sigma_{\ddot{q}}^2 + \frac{\ddot{q}}{\dot{z}^4} \sigma_{\dot{z}}^2 \tag{52}$$

The square of the error in the component acceleration ($\sigma_{\ddot{q}}^2$) is given by

$$\sigma_{\ddot{q}}^2 = \left[\frac{12}{n(n-1)}\right]^2 \sigma A_{2q}^2 \tag{53}$$

since $$\ddot{q} = \left[\frac{12}{n(n-1)}\right] A_{2q}$$

The square of the error in the vertical velocity ($\sigma_{\dot{z}}^2$) is given by

$$\sigma_{\dot{z}}^2 = \frac{4}{n^2} \sigma A_{1z}^2 \tag{54}$$

since $$\dot{z} = -\frac{2}{n} A_{1z}$$

Making these substitutions the error (σ_s) becomes

$$\sigma_s^2 = \frac{\left[\frac{12}{n(n-1)}\right]^2 \sigma A_{2q}^2}{\left[-\frac{2}{n} A_{1z}\right]^2} + \frac{\left[\frac{12}{n(n-1)}\right]^2 A_{2q}^2}{\left[-\frac{2}{n} A_{1z}\right]^4} \left[\frac{4}{n^2}\right] \sigma A_{1z}^2 \tag{55}$$

Simplifying this expression gives

$$\sigma_s = \left[\frac{-6}{n-1}\right] \cdot \frac{\left[\sigma A_{2q}^2 + \left(\frac{A_{2q}^2}{A_{1z}^2}\right) \cdot \sigma A_{1z}^2\right]^{1/2}}{A_{1z}} \tag{56}$$

The shear can then be reported as a value plus or minus the error, using the following expression:

$$S_q = -\left[\frac{30}{n-1}\right]\cdot\frac{A_{2q}}{A_{1z}} \pm \left[\frac{30}{n-1}\right]\cdot\frac{\left[\sigma A_{2q}^{\,2} + \left(\frac{A_{2q}}{A_{1z}}\right)^2 \sigma A_{1z}^{\,2}\right]^{1/2}}{A_{1z}} \qquad (57)$$

1.2.4.3 ANOVA Table for Second-Degree Fit

The analysis of variance table was constructed to determine the significance of each term in the second-degree fit. A sample of an ANOVA Table was given in Figure 2. For the second-degree, the table contains only four lines: the total sums of squares, that part due to the linear term, that part due to the quadratic term, and the residual. For ease of computation, the linear and quadratic effect terms can be simplified by the following relationship.

The sum of squares for the m th degree is given by

$$\left[\sum_{i=0}^{n} q_i P_{m,n}(i)\right]^2 \Big/ \left[\sum_{i=0}^{n} P_{m,n}(i)^2\right]$$

$$\text{since } A_m^{\,2} = \left[\sum_{i=0}^{n} q_i P_{m,n}(i)\right]^2 \Big/ \left[\sum_{i=0}^{n} P_{m,n}(i)^2\right]^2 \qquad (58)$$

The sum of squares is just $A_m^{\,2}\left[\sum_{i=0}^{n} P_{m,n}(i)^2\right]$

The A_m's are computed in the fits. The second factor is a constant for a given number of points and will therefore be designated as SS1 for the first degree and SS2 for the second. The sums of squares column then becomes

(1) $\sum_{i=0}^{n} (q_i - \bar{q})^2$ Total

(2) $A_1^{\,2} \cdot$ SS1 Linear

(3) $A_1^{\,2} \cdot$ SS2 Quadratic

(4) Residual = (1) - (2) - (3)

1.2.5 ELIMINATION OF STRAY DATA POINTS

It is always a problem with a completely automatic system to eliminate the obviously bad data before it can contaminate the results of the analysis. This obviously bad data can be the result of a variety of events such as momentary radar failure, read-out failure, a bad spot on the radar tape, computer error, etc. The condition usually exists for only one data point, and the result is a value of a coordinate that bears little relationship to the surrounding points. If the error is in the radar system, the stray point contaminates all of the coordinates; if it occurs in computer processing, it usually contaminates only one of the coordinates.

Scoggins uses the common technique of fitting a simple function to the data and rejecting a point if it falls outside a tolerance, replacing it by a predicted value. As he points out, this method is adequate and requires little computer time.

In our previous work with radar tracking data, we have developed a simpler and faster method of editing the radar tapes[3]. It is based on the idea that, in the great majority of cases, there are only one or two consecutively bad points, and the surrounding data is normal. If the maximum velocity in all components is known, then the maximum average change in any component from one point to the next can be computed. This point-to-point difference is multiplied by 10 as a safety factor against discarding valid data to establish a maximum, reasonable point-to-point change. This maximum value is called the tolerance. In the editing process, finite differences are computed and compared to the component tolerances. If the difference is less than the tolerance, the point is accepted as valid. If the difference is greater, the point is discarded, and the next point is read in and checked to see if the new differences are less than twice the tolerances (the time interval has now doubled). If the difference is still larger this point is discarded; the next point is then read in, checked against three times the tolerance, etc. until a "good" point is found. The discarded values are then replaced with values computed by linear interpolation between two good points. Even if only one coordinate is in error, the complete data point is replaced. If a maximum number (50) of interpolated points is exceeded, the technique considers that a loss of track had occurred; the flight is therefore processed in separate batches each having continuity of track. This method also allows the program to discard data in a time inversion or to fill in a small portion of missing data.

While this method has less statistical basis than the method commonly employed, it has proved very satisfactory in our use and takes very little time to perform.

1.2.6 RESULTS AND CONCLUSIONS FOR SECOND-DEGREE METHOD

The basic program was written as outlined in this section. It contains the editing procedure and the computations for the wind and the shears. Two minor modifications were made to the basic program in actual operation: one was the addition of the errors in the coefficients and the variables necessary for the ANOVA Tables; the other was the addition of the errors in winds and shears to the computer output.

A printout of a test flight with the modifications of computing the errors in the coefficients and parameters in the ANOVA Table is presented in Figure 6. Each altitude layer presented has four lines of output associated with it (except the first 1050 feet, which has only two lines). The first two lines of each printout are bracketed and are the variables for use in the ANOVA Table (these two lines are missing for the first printout). The last two lines contain the normal printout.

The variables printed out for use in the ANOVA Table are:

1st line A_{1x}, A_{2x}, A_{1y}, A_{2y}, A_{1z}

2nd line
1) Total sums of Squares for x = $\Sigma (x - \bar{x})^2$
2) Total sums of Squares for y = $\Sigma (y - \bar{y})^2$
3) Total sums of Squares for x = $\Sigma (z - \bar{z})^2$
4) $\sum_{i=0}^{n} P_{1,n}(i)^2 = SS1$
5) $\sum_{i=0}^{n} P_{2,n}(i)^2 = SS2$

The ANOVA Table can be constructed using this information and the value of "N" in the normal output. The normal printout consists of two lines: the fist line having its title at the top of the figure, and the second line having its title at the bottom of the figure.

The ANOVA Tables were constructed for the first 46 altitude layers for each coordinate, with the following results:

X	Y	
33	38	first degree only significant
13	6	both first and second degree significant
0	2	second degree only significant

This indicates that since the second-degree term is not significant in at least 70% of the layers, the second derivative is not representative of the balloon's acceleration.

Further evidence of this is provided by examining the one sigma level of the shears. These values are printed out as normal output in the second modification of the basic program. A sample of this output is presented on Figure 7. The sigmas of the shears appear as the sixth and seventh data fields in the second card whose title, as before, appears at the bottom of the figure. Upon examining the relative magnitude of the shear and its one sigma level, it becomes evident that in some cases the one sigma value is larger than the value of the shear itself. In fact, in most levels, the value of sigma is much too large to produce confidence in the values of shear.

Figure 6. Sample Printout of Second Degree Method with Modified ANOVA Table

ALTITUDE FEET	WIND EAST FT/SEC	WIND NORTH FT/SEC	WIND TOTAL KNOTS	WIND ANG DEG	SHEAR EAST /SEC	SHEAR NORTH /SEC	SHEAR TOTAL /SEC	
1050.	-3.77	-11.39	7.10	18	-0.097071	0.071269	0.120436	1
1050.	-1263.	240.	3.70110		3.58702	0.28589	0.27805	24 2
1150.	13.25	-22.05	15.23	328	-0.123863	-0.032512	0.128059	1
1150.	-1236.	178.	2.28821		2.07965	0.21976	0.20623	21 2
1250.	2.26	3.30	2.37	214	-0.172853	-0.181940	0.250958	1
1250.	-1202.	147.	2.35547		2.10501	0.20431	0.18734	24 2
1350.	-0.58	-17.72	10.50	1	-0.281947	0.259625	0.383274	1
1350.	-1197.	97.	1.07468		1.77396	0.14117	0.18015	22 2
1450.	23.79	-10.27	15.34	293	-0.126037	0.180152	0.219863	1
1450.	-1151.	46.	2.69779		1.52341	0.26959	0.19263	21 2
1550.	8.37	5.76	6.01	235	-0.153442	-0.509116	0.531736	1
1550.	-1078.	70.	4.11808		2.11217	0.35258	0.20864	22 2
1650.	13.04	-24.87	16.62	332	-0.132182	0.400622	0.421865	1
1650.	-1034.	11.	2.89717		1.94122	0.30298	0.25201	19 2
1750.	7.72	-5.61	5.65	305	0.180518	-0.247111	0.306024	1
1750.	-1005.	-27.	2.95227		1.24920	0.28764	0.19433	20 2
1850.	13.26	-17.80	13.14	323	-0.724653	-2.088568	2.210710	1
1850.	-953.	-48.	9.21212		19.15512	0.71850	1.42455	23 2
1950.	22.38	32.38	23.31	214	-0.013240	-0.339513	0.339771	1
1950.	-906.	-85.	7.09919		6.52922	0.61380	0.57151	21 2
2050.	10.03	-15.96	11.16	327	-0.357206	-0.583537	0.684186	1
2050.	-823.	-54.	5.21431		2.92302	0.42738	0.28860	22 2
2150.	14.19	-20.39	14.71	325	-0.079421	0.470663	0.477317	1
2150.	-791.	-161.	4.36600		2.12627	0.36171	0.21602	21 2
2250.	17.54	-19.34	15.55	318	0.105096	-0.723498	0.731091	1
2250.	-731.	-209.	2.78618		3.28117	0.23547	0.27017	26 2
2350.	29.96	3.70	17.87	262	0.102181	0.321901	0.337729	1
2350.	-620.	-280.	2.34028		2.59697	0.22845	0.24467	21 2
2450.	24.48	-7.08	15.09	286	-0.288604	-0.192118	0.346701	1
2450.	-488.	-279.	3.90560		2.26113	0.34506	0.23735	23 2
2550.	12.06	-12.97	10.49	317	-0.028184	0.761253	0.761775	1
2550.	-420.	-368.	1.91151		1.31036	0.21099	0.18003	21 2
2650.	9.16	-5.00	6.18	298	-0.448890	-0.547282	0.707827	1
2650.	-343.	-363.	3.06118		2.79198	0.25146	0.23380	24 2
2750.	20.45	-24.91	19.09	320	0.342176	0.224292	0.409135	1
2750.	-294.	-466.	3.00891		1.40556	0.30074	0.19877	23 2
2850.	27.24	-9.65	17.11	289	-0.063558	0.012304	0.064738	1
2850.	-161.	-541.	2.11733		0.80556	0.18282	0.10481	27 2
2950.	-3.75	-25.70	15.38	8	-0.085229	0.430074	0.438438	1
2950.	-99.	-632.	3.34216		1.93475	0.33658	0.25865	20 2
3050.	15.12	-4.85	9.40	287	-0.456624	0.109639	0.469602	1
3050.	-54.	-690.	2.92402		2.44531	0.25180	0.22191	24 2
3150.	8.13	-31.30	19.15	345	-0.209228	0.370255	0.425283	1
3150.	-8.	-786.	5.45893		2.27604	0.45200	0.24236	22 2
3250.	31.52	-11.04	19.77	289	0.570326	-0.058156	0.573284	1
3250.	45.	-860.	3.29948		1.49146	0.32449	0.20464	19 2
3350.	13.03	-15.71	12.09	320	0.208994	0.001909	0.209002	1
3350.	137.	-908.	5.42828		3.94457	0.42163	0.32017	22 2
3450.	36.50	-8.91	22.24	283	-0.049491	-0.204518	0.210421	1
3450.	262.	-949.	3.41827		1.64858	0.29809	0.19693	23 2
3550.	13.82	-2.91	8.36	281	0.309200	-0.299871	0.430729	1
3550.	364.	-970.	4.76414		1.53951	0.37926	0.17345	21 2
ALTITUDE	E BAR	N BAR	SIG EE		SIG NN	SIG SE	SIG SN	N

Figure 7. Sample Printout of Second Degree Method with One Sigma Level for Winds and Shears

The winds computed by the second-degree fit agree, for the most part, with the winds produced by the ninth-degree method, but the shears produced by the two methods do not agree with each other or with values generally thought to be realistic.

In general, if the second degree is not significant, the accelerations predicted by the fit are smaller in magnitude than the noise level of the data. The noise can be attributed either to the actual random motion of the balloon itself or to the random tracking errors of the radar which will produce an apparent random motion of the balloon. It is impossible to determine which of these factors is the primary cause of the noise. Thus, we must conclude that with the present data, only linear smoothing is valid.

1.3 LINEAR FIT METHOD

The results of the work with the second-degree polynomial indicated that, in most cases, the linear fit was sufficient to describe the motion of the balloon. Since an acceleration term could no longer be computed, it was necessary to go back to the finite difference between winds to compute the shear. In computing the linear fit, one of the steps produces the mean over the interval. A finite difference between this mean and the one from the previous layer gives a type of average wind over a 200-foot layer. A shear can then also be computed from these winds. It was also desired to compute the one sigma level of the linear winds and include it in the printout. The sampling frequency was 0.2 sec for this degree also.

1.3.1 WINDS

The orthogonal polynomials for the first-degree fit were given in Section 1.2.1.

In the linear fit the point wind and the average wind in the layer, as defined in the section on the ninth-degree polynomial are identical. In this section, we will introduce a slightly different definition of the average wind which will include data from a deeper layer and will be different from the point wind.

1.3.1.1 Point Winds and Errors

The point wind is the first derivative evaluated at the mid-point of the layer. The equations for the component winds, derived in Section 1.2.2, are

$$W_x = -\frac{10}{n} A_{1x} \qquad (41a)$$

$$W_y = -\frac{10}{n} A_{1y} \qquad (41b)$$

The errors derived in Section 1.2.4 are

$$\sigma_{W_x} = -\frac{10}{n} \sigma_{A_{1x}} \qquad \sigma_{W_y} = -\frac{10}{n} \sigma_{A_{1y}} \qquad (59)$$

The point wind can then be reported as a value plus or minus the error using the following expression

$$W = -\frac{10}{n} A_1 \pm \frac{10}{n} \sigma_{A_1} \tag{50}$$

1.3.1.2 Average Winds

When a linear fit is performed, the simple mean of the data points in the layer is obtained. It was decided to compute a wind from the finite differences of these values from consecutive layers. Hence, for this section the definition of the average wind will be:

$$\overline{W}_q = (\overline{q}_{\ell + 100} - \overline{q}_\ell) / \Delta t \tag{60}$$

where ℓ is the altitude of the center of a certain layer, and $\ell + 100$ is the altitude of the center of the next 100-foot layer. Δt is of course the time difference between $\overline{q}_{\ell+100}$ and $\overline{q}_\ell$. The value reported for the wind is then actually using data over a 200-foot layer. As one would expect, this deeper layer has a smoothing effect on the winds which also reduces the magnitude of the shear.

1.3.2 SHEARS

Since there are two distinct types of winds computed by this method, it was desired to compute the shear associated with each type wind.

1.3.2.1 Shears from Point Winds

Since the second derivative is not obtained in this method, the alternate method of computing shears is used:

$$S_q = \frac{W_{q_{\ell+100}} - W_{q_\ell}}{\Delta h} \tag{61}$$

where again the ℓ is the altitude of the mid-point of the layer.

The component shears are given by the equations:

$$S_x = \frac{W_{x_{\ell+100}} - W_{x_\ell}}{100} \tag{62a}$$

$$S_y = \frac{W_{y_{\ell+100}} - W_{y_\ell}}{100} \tag{62b}$$

The point winds are computed for the mid-point of the layer--for example, at altitudes of 1050, 1150, 1250 feet, etc. The shears are then assigned an altitude exactly between the two winds used in their computation. For the example above, the shears will be reported at 1100, 1200 feet, etc.

1.3.2.2 Shears from Average Winds

The equations for the shears from average winds are identical to the shears from point winds. However, the altitudes to which the winds and shears are assigned are reversed. Since the winds are computed from the mean space-coordinates assigned to the mid-point of the layer (e.g., 1050, 1150, 1250 etc.), the average winds are assigned to altitudes of 1100, 1200 etc. The shears are then assigned to the mid-point of the wind data so that the altitudes of the shears are 1150, 1250 etc.

1.3.3 RESULTS AND CONCLUSIONS FOR THE FIRST DEGREE

The computer program was written as described in the previous sections; it included the Technique for Eliminating Stray Data Points given in Section 1.2.5. Also, a test run of the check-out flight was made. A sample of the result is presented in Figure 8. The title at the top of the page is for the data appearing on the odd lines (those with 50 foot altitudes), while the title at the bottom is for the data on the even lines (those with 100 foot altitudes). The parameters for the 50 foot altitudes are:

Parameter	Description
Alt	Altitude
Wind East	Point wind in East direction
Wind North	Point wind in North direction
Wind Total	Point wind Vector
Wind Angle	Angle of wind Vector
Average East	Mean of East components in this layer
Average North	Mean of North components in this layer
Sigma East	One sigma level of wind East
Sigma North	One sigma level of wind North
N	Number of 0.2 sec data points in this layer

The parameters for the 100 foot altitudes are:

Parameter	Description
Alt	Altitude
East Shear	Shear from East Point wind
North Shear	Shear from North Point wind
Total Shear	Magnitude of Vector sum of East and North Shears
Avg WE	Average wind in East Direction
Avg WN	Average wind in North Direction
Shear Avg WE	Shear from Avg WE
Shear Avg WN	Shear from Avg WN
N	Number of 0.2 sec data points in this layer

The point winds of this method are identical to the point winds of the second-degree method, as they should be. The shears from the point winds seem to be less erratic than the shears obtained from the second-degree method, but they are still sufficiently unstable to cause some questions about their reliability. The average winds are smoother than the linear winds--mainly due to the deeper layer over which the wind is measured. The shears from the average winds are also smoother (as expected) but still somewhat erratic.

ALT	WIND EAST	WIND NORTH	WIND TOTAL	WIND ANG	AVERG EAST	AVERG NORTH	SIGMA EAST	SIGMA NORTH	N			ID
FEET	FT/SEC	FT/SEC	KNOTS	DEG	FT	FT	WIND	WIND				
1050	-3.77	-11.39	7.1	18	-1263	240	3.933	3.218	24	1	11	02263
1100	0.1702	-0.1066	0.2008		6.07	-13.70	5.3239	-1.1375	21	2	11	02263
1150	13.25	-22.05	15.2	329	-1239	178	2.768	2.120	21	1	11	02263
1200	-0.1099	0.2535	0.2363		2.45	-7.11	0.0138	0.0659	26	2	11	02263
1250	2.26	3.30	2.4	214	-1202	146	3.251	3.161	24	1	11	02263
1300	-0.0285	-0.2102	0.2121		1.23	-10.66	-0.0622	-0.0356	22	2	11	02263
1350	-0.58	-17.72	10.5	1	-1196	97	3.714	3.224	22	1	11	02263
1400	0.2438	0.0745	0.2549		10.62	-11.88	0.0966	-0.0122	21	2	11	02263
1450	23.79	-10.27	15.3	293	-1150	46	3.081	2.616	21	1	11	02263
1500	-0.1542	0.1603	0.2224		16.93	5.45	0.0626	0.1753	22	2	11	02263
1550	8.37	5.76	6.0	235	-1078	69	4.539	6.675	22	1	11	02263
1600	0.0467	-0.3063	0.3098		10.27	-14.65	-0.0616	-0.1990	19	2	11	02263
1650	13.04	-24.87	16.8	332	-1033	10	3.356	5.670	19	1	11	02263
1700	-0.0531	0.1926	0.1998		7.62	-9.53	-0.0335	0.0492	20	2	11	02263
1750	7.72	-9.61	5.7	305	-1006	-24	3.728	3.358	20	1	11	02263
1800	0.0553	-0.1219	0.1339		12.00	-6.92	0.0456	0.0462	23	2	11	02263
1850	13.26	-17.80	13.1	323	-993	-67	13.519	34.352	23	1	11	02263
1900	0.0913	0.5618	0.5100		10.25	-8.51	-0.0125	-0.0360	21	2	11	02263
1950	22.38	37.38	23.3	214	-906	-85	2.101	7.228	21	1	11	02263
2000	-0.1235	-0.4834	0.4989		19.22	7.17	0.0847	0.1568	22	2	11	02263
2050	10.03	-15.96	11.2	327	-823	-54	7.151	8.511	22	1	11	02263
2100	0.0415	-0.0443	0.0602		2.44	-24.83	-0.1178	-0.3200	21	2	11	02263
2150	14.19	-20.39	14.7	329	-791	-161	8.489	6.541	21	1	11	02263
2200	0.0335	0.0085	0.0346		12.87	-10.26	0.0538	0.1458	26	2	11	02263
2250	17.54	-19.54	15.5	318	-731	-209	3.102	10.010	26	1	11	02263
2300	0.1242	0.2324	0.2635		23.62	-15.06	0.1080	-0.0681	21	2	11	02263
2350	29.96	3.70	17.9	262	-620	-280	2.683	4.884	21	1	11	02263
2400	-0.0548	-3.1078	0.1210		30.12	0.16	0.0650	0.1522	23	2	11	02263
2450	24.48	-7.08	15.1	286	-607	-229	5.159	3.329	23	1	11	02263
2500	-0.1242	-0.0589	0.1395		15.34	-20.23	-0.1478	-0.2039	21	2	11	02263
2550	12.06	-12.97	10.5	317	-470	-368	1.944	9.718	21	1	11	02263
2600	-0.0290	0.0798	0.0849		13.15	1.31	0.0180	0.2153	24	2	11	02263
2650	9.16	-5.00	6.2	298	-342	-362	6.814	7.930	24	1	11	02263
2700	0.1130	-0.1991	0.2289		10.46	-21.98	-0.0667	-0.2328	23	2	11	02263
2750	20.45	-24.91	19.1	320	-291	-605	5.032	2.994	23	1	11	02263
2800	0.0678	0.1526	0.1670		26.51	-16.96	0.1603	0.0701	27	2	11	02263
2850	27.24	-9.65	17.1	289	-161	-560	2.274	0.822	27	1	11	02263
2900	-0.3099	-0.1605	0.3490		13.25	-19.41	-0.1326	-0.0665	20	2	11	02263
2950	31.75	-25.70	15.4	0	-90	-631	3.512	5.726	20	1	11	02263
3000	0.1887	0.2086	0.2813		10.12	-13.22	-0.0313	0.0616	24	2	11	02263
3050	15.12	-4.85	9.4	287	-56	-690	6.812	2.052	24	1	11	02263
3100	-0.0700	-0.2645	0.2736		10.09	-20.25	-0.0003	-0.0762	22	2	11	02263
3150	8.13	-31.30	19.1	345	-7	-785	6.099	5.326	22	1	11	02263
3200	0.2339	0.2027	0.3095		12.94	-18.06	0.0284	0.0268	19	2	11	02263
3250	31.52	-11.04	19.8	289	45	-859	7.432	1.639	19	1	11	02263
3300	-0.1849	-0.0468	0.1902		22.36	-11.74	0.0941	0.0432	22	2	11	02263
3350	13.03	-15.71	12.1	320	136	-907	6.127	3.965	22	1	11	02263
3400	0.2347	0.0680	0.2443		27.72	-9.23	0.0538	0.0251	23	2	11	02263
3450	36.50	-8.91	22.2	283	261	-949	3.482	3.195	23	1	11	02263
3500	-0.2267	0.0600	0.2345		23.29	-6.72	-0.0443	0.0451	21	2	11	02263
3550	13.82	-2.91	8.9	281	364	-920	6.307	4.294	21	1	11	02263
3600	0.1971	-0.0972	0.2192		28.29	-13.06	0.0500	-0.0832	27	2	11	02263
ALT	EAST SHEAR	NORTH SHEAR	TOTAL SHEAR		AVG WE	AVG WN	AVG WE	AVG WN	N			ID
FEET	/SEC	/SEC	/SEC		FT/SEC	FT/SEC	/SEC	/SEC				

Figure 8. Sample Printout of First Degree Method

ALTITUDE	TIME	EAST	NORTH	SHEAR EAST	SHEAR NORTH			ID	
FEET	SEC	FEET	FEET	/SEC	/SEC				
1000.	1602.8	-1262.	261.					11	02263
1050.	4.6	-2.	-42.	-0.43	-9.13	5.41	2	2 11	02263
1100.	1607.4	-1264.	219.	0.1163	-0.0960			1 11	02263
1150.	4.2	47.	-79.	11.19	-18.81	12.96	329	2 11	02263
1200.	1611.6	-1213.	140.	-0.0786	0.1943			1 11	02263
1250.	4.4	16.	3.	3.33	0.62	2.01	259	2 11	02263
1300.	1616.4	-1201.	141.	-0.0647	-0.1609			1 11	02263
1350.	4.6	-5.	-72.	-1.16	-16.36	9.71	1	2 11	02263
1400.	1620.8	-1206.	91.	0.2423	0.0799			1 11	02263
1450.	4.7	93.	-36.	21.10	-8.57	14.59	290	2 11	02263
1500.	1625.0	-1109.	15.	-0.1173	0.1562			1 11	02263
1550.	4.4	50.	31.	11.36	2.05	7.62	238	2 11	02263
1600.	1629.4	-1056.	66.	0.0074	-0.3020			1 11	02263
1650.	1.8	46.	-28.	12.11	-23.16	19.67	332	2 11	02263
1700.	1633.2	-1013.	-22.	-0.0636	0.1716			1 11	02263
1750.	4.0	23.	-24.	5.75	-6.00	6.02	316	2 11	02263
1800.	1637.2	-990.	-46.	0.0360	-0.1422			1 11	02263
1850.	4.6	63.	-63.	9.35	-20.22	33.19	335	2 11	02263
1900.	1641.8	-943.	-136.	0.0651	0.4450			1 11	02263
1950.	5.2	75.	102.	17.06	24.26	17.85	218	2 11	02263
2000.	1646.8	-892.	-33.	-0.0468	-0.1951			1 11	02263
2050.	4.4	58.	-63.	13.18	-15.23	11.93	319	2 11	02263
2102.	1650.4	-814.	-104.	-0.0299	-0.0606			1 11	02263
2150.	4.2	43.	-81.	10.24	-19.29	12.93	332	2 11	02263
2202.	1654.6	-771.	-185.	0.0726	0.0176			1 11	02263
2250.	5.2	91.	-91.	17.50	-17.50	14.65	314	2 11	02263
2300.	1656.8	-680.	-276.	0.1083	0.1944			1 11	02263
2350.	4.2	116.	9.	28.33	2.14	16.82	265	2 11	02263
2402.	1664.0	-561.	-263.	-0.0290	-0.1123			1 11	02263
2450.	4.8	112.	-67.	25.43	-6.11	16.00	289	2 11	02263
2505.	1668.6	-444.	-306.	-0.1329	-0.0635			1 11	02263
2550.	4.2	51.	-65.	12.14	-15.48	11.85	321	2 11	02263
2604.	1672.8	-193.	-374.	0.0057	0.1023			1 11	02263
2650.	4.8	81.	-25.	12.71	-5.21	8.13	292	2 11	02263
2702.	1633.6	-132.	-109.	0.0881	-0.2001			1 11	02263
2750.	4.8	90.	-116.	21.57	-25.22	19.63	319	2 11	02263
2800.	1682.2	-231.	-515.	0.0403	0.1559			1 11	02263
2850.	5.4	130.	-52.	25.56	-9.63	16.17	290	2 11	02263
2903.	1683.6	-95.	-567.	-0.2656	-0.1662			1 11	02263
2950.	4.0	-4.	-105.	-1.00	-26.25	15.55	2	2 11	02263
3000.	1691.6	-66.	-632.	0.1403	0.1835			1 11	02263
3050.	4.8	76.	-36.	15.83	-7.50	10.37	295	2 11	02263
3104.	1696.4	-23.	-708.	-0.0324	-0.2250			1 11	02263
3150.	4.5	20.	-117.	4.59	-30.00	18.19	347	2 11	02263
3207.	1700.0	6.	-840.	0.2420	0.1816			1 11	02263
3250.	3.8	113.	-45.	30.79	-11.84	19.51	291	2 11	02263
3304.	1704.6	123.	-885.	-0.1674	0.0002			1 11	02263
3350.	4.4	53.	-52.	12.05	-11.82	9.09	314	2 11	02263
3403.	1709.0	136.	-913.	0.2252	0.0421			1 11	02263
3450.	4.6	159.	-35.	34.57	-7.61	20.96	282	2 11	02263
3501.	1713.6	335.	-897.	-0.1816	0.0404			1 11	02263
3550.	4.2	66.	-15.	16.43	-3.57	6.95	282	2 11	02263
ALTITUDE	DELTA TIME	DELTA EAST	DELTA NORTH	WIND EAST	WIND NORTH	WIND TOTAL	WIND ANG		
FEET	SEC	FEET	FEET	FT/SEC	FT/SEC	KNOTS	DEG		

Figure 9. Sample Printout of Finite Difference Method

Since the data was shown to be linear for the most part, it was decided to compute the winds from first finite differences of the 0.2 sec x, y, z coordinate data and to compare them with this linear method.

1.4 FINITE DIFFERENCES

The conclusions reached in the previous sections indicated that the data were linear for the most part with respect to time. If the data were truly linear, the slope with respect to time would be identical to the first finite difference. It is faster (and therefore cheaper) to compute finite differences than to fit a linear function and evaluate the first derivative. The finite difference winds and shears should be similar to the linear method.

1.4.1 WINDS

The winds in terms of finite differences are given by:

$$W_x = \frac{x_n - x_0}{t_n - t_0} \qquad W_y = \frac{y_n - y_0}{t_n - t_0} \qquad (63a)\ (63b)$$

since the data are equally spaced (0.2 sec between points) equations can be rewritten as:

$$W_x = \frac{x_n - x_0}{n} \cdot 5 \qquad W_y = \frac{y_n - y_0}{n} \cdot 5 \qquad (64a)\ (64b)$$

where the "5" is to convert to units of ft/sec.

1.4.2 SHEARS

The shears are computed using the alternate method:

$$S_q = \frac{W_{q_{\ell+100}} - W_{q_\ell}}{\Delta h} \qquad (61)$$

where again ℓ is the altitude of the mid point of the layer.

The component shears are given by:

$$S_x = \frac{W_{x_{\ell+100}} - W_{x_\ell}}{100} \quad \text{and} \quad S_y = \frac{W_{y_{\ell+100}} - W_{y_\ell}}{100} \qquad (62a)\ (62b)$$

for a 100-foot layer.

1.4.3 ELIMINATION OF STRAY DATA POINTS

The routine used to eliminate stray data points in the finite difference method is identical to that used in the quadratic and linear methods. The inclusion of a stray data point in a least-squares fit will cause a very bad value. In the finite difference method, however, a stray point will have no effect on the value of the winds and shears provided it is not the first or last point. There are on the average about twenty-five data points in a 100-foot layer; hence the probability that one data point is stray is 1/25 or .04. Since there are normally few stray points in the data, the elimination of stray data could have been skipped without great harm to the results.

1.4.4 RESULTS AND CONCLUSIONS FOR FINITE DIFFERENCES

The computer program was constructed as indicated in this section. A sample of the output is presented as Figure 9. As before, the title at the top of the figure is for the odd (100 foot) lines, while the title at the bottom is for the even (50 foot) lines. The results agree well with the linear method which indicates that this cheaper method can be used instead of the linear method with little change in the results. We base this conclusion, however, on examination of only a few soundings by unmodified ROSEs. Such opinion is therefore subject to possible future revision.

1.5 GENERAL COMPARISON OF ALL FITS

In order to summarize the results of the various type fits, two portions of the test flight processed by each method have been listed side by side for easy comparison. The two portions chosen were: 1) the lowest part of the flight which was the most erratic; 2) a portion near 50,000-feet altitude which was the smoothest. The east component was selected because its magnitude was larger, and it was generally smoother. Tables 1 and 2 are wind comparisons, while Tables 3 and 4 are shear comparisons. Tables 1 and 3 are the low altitude, and Tables 2 and 4 are the high altitude. In Tables 1 and 2, the column "Deg" indicates the highest degree used by the m th degree polynomial; the column "ANOVA" indicates the highest significant degree. The one sigma level is included for the linear and quadratic winds and the quadratic shears.

The values for the winds obtained by all the fits agree well with each other and with rawinsonde data. Since the method of finite difference is the quickest, it was decided to use this method in future work. The values for the shears seem to depend completely upon the fitting method used. No method seemed to produce values which were consistent from point to point even within that method.

TABLE 1. Comparison of Winds at Low Altitudes

ALTITUDE	Δa/Δt	Δā/Δt	EAST WINDS Feet/sec Linear and Quadratic	mth degree Poly	Deg	ANOVA
1000						
1050	-.43		-3.77 + 0.77	0.00	0	1
1100		6.07				
1150	11.19		13.23 + 0.91	13.27	1	1
1200		7.45				
1250	3.33		2.26 + 0.49	0.00	0	1
1300		1.23				
1350	-1.84		-0.58 + 0.23	0.00	0	1
1400		10.67				
1450	23.10		23.79 + 0.61	23.90	1	1
1500		16.93				
1550	11.36		9.37 + 0.90	8.41	1	1
1600		10.77				
1650	12.11		13.04 + 0.69	12.92	1	1
1700		7.42				
1750	5.75		7.72 + 0.69	7.42	1	2
1800		12.00				
1850	9.35		13.26 + 1.96	10.01	9	9
1900		10.75				
1950	17.86		22.38 + 1.59	10.96	9	1
2000		19.22				
2050	13.18		10.03 + 1.16	10.43	9	2
2100		7.96				
2150	10.24		14.19 + 0.99	13.95	1	1
2200		12.92				
2250	17.58		17.54 + 0.56	15.52	3	1
2300		23.62				
2350	29.33		29.96 + 0.52	29.44	1	1
2400		30.12				
2450	23.43		24.48 + 0.84	25.60	9	2
2500		15.36				
2550	12.14		12.06 + 0.43	12.11	1	1
2600		17.15				
2650	12.71		9.16 + 0.64	12.65	9	2
2700		10.49				
2750	21.52		20.45 + 0.69	21.19	9	2
2800		26.51				
2850	25.56		27.24 + 0.42	26.71	9	1

TABLE 2. Comparison of Winds at High Altitudes

ALTITUDE	Δa/Δt	Δā/Δt	EAST WIND Feet/sec Linear and Quadratic	mth degree Poly	Deg	ANOVA
48250	69.97		69.99 + 0.44	70.17	1	
48300		70.61				
48350	72.26		73.24 + 0.33	73.39	1	
48400		71.44				
48450	70.97		75.41 + 1.09	75.50	1	1
48500		70.17				
48550	70.61		70.44 + 0.62	70.63	1	1
48600		70.35				
48650	69.12		69.59 + 0.90	69.64	1	1
48700		71.99				
48750	70.64		74.30 + 0.94	74.16	1	1
48800		72.86				
48850	71.29		69.98 + 0.68	69.74	1	1
48900		71.98				
48950	67.59		68.92 + 0.98	69.08	1	1
49000		67.99				
49050	72.59		72.86 + 0.96	72.99	1	1
49100		72.01				
49150	74.44		76.32 + 0.38	76.32	1	1
49200		75.96				
49250	75.17		74.04 + 0.34	74.27	1	1
49300		73.18				
49350	75.00		73.39 + 1.31	72.79	1	1
49400		73.49				
49450	69.84		70.59 + 0.96	70.91	1	1
49500		72.25				
49550	71.00		67.49 + 0.99	67.68	1	1
49600		65.88				
49650	64.15		62.46 + 0.39	62.50	1	1
49700		62.97				
49750	60.81		61.22 + 0.96	61.27	1	1
49800		61.29				
49850	61.72		60.99 + 0.54	60.35	1	1
49900		59.41				
49950	60.13		60.32 + 0.32	60.05	1	1
50000		57.66				
50050	55.00		55.78 + 0.44	55.84	1	1
50100		54.04				

TABLE 3. Comparison of Shears at Low Altitudes

ALTITUDE	EAST SHEARS /sec $\Delta u/\Delta t$	$\Delta\bar{u}/\Delta t$	Linear	Quadratic
1000				
1050				*-.0971 * .0597
1100	.1163		.1702	
1150		.0138		*-.1239 * .0492
1200	-.0786		-.1099	
1250		-.0622		*-.1729 * .0417
1300	-.0447		-.0265	
1350		.0944		*-.2619 * .0309
1400	.2423		.2816	
1450		.0626		-.1260 * .0603
1500	-.1173		-.1562	
1550		-.0616		-.1534 * .0769
1600	.0678		.0487	
1650		-.0335		-.1322 * .0715
1700	-.0636		-.0531	
1750		.0844		.1805 * .0660
1800	.0360		.0543	
1850		-.0125		*-.7247 * .1532
1900	.0451		.0913	
1950		.0947		-.0192 * .0830
2000	-.0468		-.1235	
2050		-.1170		-.3572 * .0913
2100	-.0298		.0414	
2150		.0538		-.0794 * .0810
2200	.0726		.0335	
2250		.1090		.1051 * .0461
2300	.1093		.1282	
2350		.0650		.1022 * .0512
2400	-.0290		-.0564	
2450		-.1479		-.2296 * .0737
2500	-.1129		-.1242	
2550		.0180		-.0242 * .0472
2600	.0057		-.0298	
2650		-.0667		-.4889 * .0527
2700	.0991		.1130	
2750		.1603		.3422 * .0440
2800	.0403		.0674	
2850		-.1326		-.0636 * .0352

TABLE 4. Comparison of Shears at High Altitudes

ALTITUDE	EAST SHEARS /sec $\Delta u/\Delta t$	$\Delta\bar{u}/\Delta t$	Linear	Quadratic
44250		.0035		-.0768 * .0542
44300	.0339		.0325	
44350		.0082		-.1549 * .0658
44400	-.0130		.0217	
44450		.0127		-.0156 * .1383
44500	-.0036		-.0497	
44550		.0019		-.0699 * .0620
44600	-.0189		-.0185	
44650		.0154		-.0301 * .0914
44700	.0572		.0572	
44750		.0097		.0647 * .0559
44800	-.355		-.0422	
44850		-.0096		-.1191 * .0598
44900	-.2370		-.0896	
44950		-.0401		-.2697 * .1054
45000	.0499		.0194	
45050		-.0412		-.0383 * .1241
45100	.0140		.0346	
45150		.0396		-.0939 * .0655
45200	.0073		-.0208	
45250		-.0279		.1538 * .0715
45300	-.0017		-.0065	
45350		.0031		.0052 * .1546
45400	-.0514		-.0280	
45450		-.0128		.0046 * .1361
45500	.0118		-.0310	
45550		-.0643		-.0702 * .1270
45600	-.0645		-.0503	
45650		-.0283		-.0508 * .0663
45700	-.0334		-.0124	
45750		-.0168		-.0439 * .0468
45800	.0091		-.0054	
45850		-.0194		-.1075 * .0676
45900	-.0159		-.0057	
45950		-.0175		.0181 * .0379
46000	-.0833		-.0454	
46050		-.0072		-.0142 * .0753
46100	.0097		.0307	

2. SELF-INDUCED BALLOON MOTION

Wind and shear values produced by the various smoothing techniques indicated that the winds were very erratic at the bottom of the flight. This condition persisted until about 40,000 feet, where it suddenly vanished and the wind became smooth. Concurrently with our work, Murrow and Henry repeated an experiment first performed in 1958 on Radiosonde balloons[4]. The new experiment consisted in releasing ROSE and other smooth balloons in still air and tracking them with cameras. The results indicated that the spherical balloons experienced self-induced motions similar to those experienced by the earlier Radiosonde balloons. The direction of these motions is apparently random, but their magnitude seems to be a function of the vertical terminal velocity. A plan view of six balloon ascents presented in Murrow and Henry's paper shows that the balloon behaves very erratically and generally unpredictably[4]. When these results were made known, we plotted several actual ROSE launches from Eglin AFB. From concurrent Radiosonde releases we expected a predominantly westerly wind. The East vs North plot showed that superimposed on the eastward motion were various loops and spirals similar to those found by Murrow and Henry.

The reason for the self-induced motion has not been completely explained, but it is generally thought to be due to a type of turbulence in the wake of the balloon. Some work has been done on this problem and is presented as Appendix 2 and Appendix 5, but a satisfactory explanation has not been achieved.

The mathematical techniques selected for computing wind and shear values were based on the initial assumption that the balloon motion was very nearly the same as the motion of the wind. The self-induced motions caused this initial assumption to be invalid. It is felt that the mathematical techniques do describe the motion of the balloon; unfortunately, the values are not also the wind and shear values.

Two corrective approaches were taken to make the ROSE balloons useful wind sensors. The first corrective approach was an attempt to measure and analyze the self-induced motions by means of a Power Spectral Density Technique. The aim of this approach was to develop a model of the self-induced behavior for the purpose of removing its effect from the data. The result of this approach is presented in Section 3. The second (and eventually more successful) approach was a physical modification of the balloon itself to control the wake turbulence.

3. POWER SPECTRAL ANALYSIS OF BALLOON MOTION

The East vs North plots of the ROSE data indicated that the balloon motion was generally unpredictable in a small interval. However, when a plot of an entire flight was viewed there appeared to be a type of fairly regular oscillation. The technique commonly used to determine oscillatory changes in data is the Power Spectral Density Analysis. The basis for this technique is given in the standard work on time series analysis by Blackman and Tukey[5]. An excellent Time Series Analysis program has been prepared by Healy and Bogert[6] at Bell Telephone Laboratories and is available through SHARE[7]. The final output of the program is a table of Power at specific frequencies vs the frequencies. A spike in the curve indicates a predominance of that frequency in the data.

3.1 TIME SERIES ANALYSIS COMPUTER PROGRAM

Because of the sizable programming effort required to prepare a Time Series Analysis for a computer, a search of the available program libraries was made. From the several good methods available,[6,8,9] the one by Healy and Bogert[6] was selected because their approach seemed easiest to tailor to our particular problem. The time series analysis involves a large number of computations on a fairly large quantity of data. Healy and Bogert broke down the computations into separate numerical processes and wrote one FORTRAN subroutine for each process. The method was then to use each subroutine (with the necessary linkages) as a high level command. For example, to read the data into the machine the main program uses merely CALL READIN (A, NA, ANAME) to transfer the data to the array "A" where it is ready for computation. The main calling sequence gives the overall concept of the computation steps without regard to all of the FORTRAN mechanics necessary for the actual computer operation. This makes modification of the program very easy. One merely writes and debugs a new independent subroutine including only the "CALL" line in the main program.

The original version of the program contained 17 subroutines which may be found in Reference 6. For our analysis we decided to use just 5 of 17 subroutines. These 5 subroutines are presented as Appendix 3 with descriptions of their individual processes.

3.1.1 MODIFICATIONS TO THE HEALY-BOGERT PROGRAM

There were two major changes made to the basic program: the conversion of the compiler language and an increase in size. The original compiler language used was FORTRAN II, and all of the input, output, and computations were coded in FORTRAN. The program was converted to FORTRAN IV and operated under the IBSYS system in order to use the techniques provided by this more advanced system. The original program was limited to a maximum of 1500 points per analysis. By using fewer subroutines, we were able to increase this maximum to 5000 points per analysis. The other minor changes were the addition of different trend-removing techniques and the addition of pre-whitening and post-darkening subroutines. The input subroutine READIN was also changed to conform to our data. The additional subroutines are described in Appendix 4.

3.1.2 PROCEDURE TO TEST PROGRAM USING SIMULATED DATA

The programs received through SHARE are normally well documented and perform satisfactorily; therefore the program was tested by simulating data with known frequencies and processing it by using the PSD program. The manufactured data were a linear function with frequencies superimposed on it. The frequencies were: 1/187, 1/131, 1/43, 1/41, 1/37, 1/17, 1/7, and $1/(1+\sqrt{3})$ cycles per second. The main calling sequence used the following subroutines: READIN, DETRND (over the whole data set), AUTCOV (with 100 lags), FOURTR (using the hanned cosine transforms), and OUTPUT. The program performed very well in reporting all of the frequencies we had manufactured. The output from the test was plotted on rectangular scales (presented as Figure 10) and on semi-log scales (presented as Figure 11).

The ROSE data seemed to be essentially quadratic rather than linear; hence the same eight frequencies were superimposed on a parabola, and the PSD program was re-run with the QTRND subroutine (Appendix 4). All of the frequencies were reported again, and the shapes of the $P(\phi)$ vs ϕ curves were identical to those shown in Figures 10 and 11.

Since the program seemed to perform well on "clean" data, it was next decided to add to the quadratic data random noise of approximately 10% of the amplitude of the data. The pre-whitening (WHITN) and post-darkening (PDRKN) subroutines (Appendix 4) were then added in an attempt to remove the noise. The output again was almost identical to that shown in Figures 10 and 11.

The next step was to see if a method simpler than the least squares linear, or quadratic methods could remove the general trend and still produce results which would be satisfactory. The first method (TRNDR) was to remove a line determined by the first and last points of a five-second section. Then by using the last point of a section as the first point of the next section, continuity could be produced through all of the data. The results were again almost identical to those shown in Figures 10 and 11.

It was thought that perhaps a moving average would better remove the general trend from the data than a series of straight lines as in TRNDR. The subroutine MOVAVG was written and used with both 51- and 81-point averages. The number of lags was then reduced to 50--first because the number of points was reduced and secondly, in order to determine how the lower resolution would affect the shape and placement of the spikes. The result of the 51-point average is shown as Figure 12. This result is identical to the output from the 81-point average method. It will be noticed that the peaks have broadened slightly but are still very satisfactory in returning the frequencies known to be present in the data.

The results of these tests indicated that the program was performing satisfactorily and could be applied to actual data.

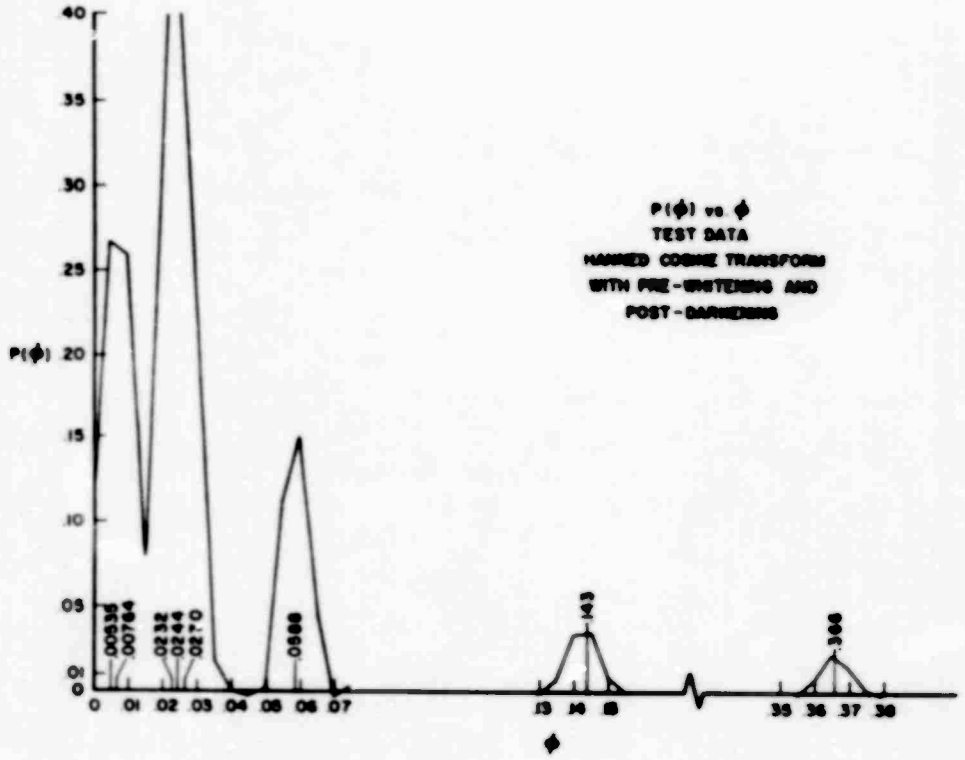

Figure 10. Test of Manufactured Data Processed by High Resolution PSD Program (Rectangular Scale)

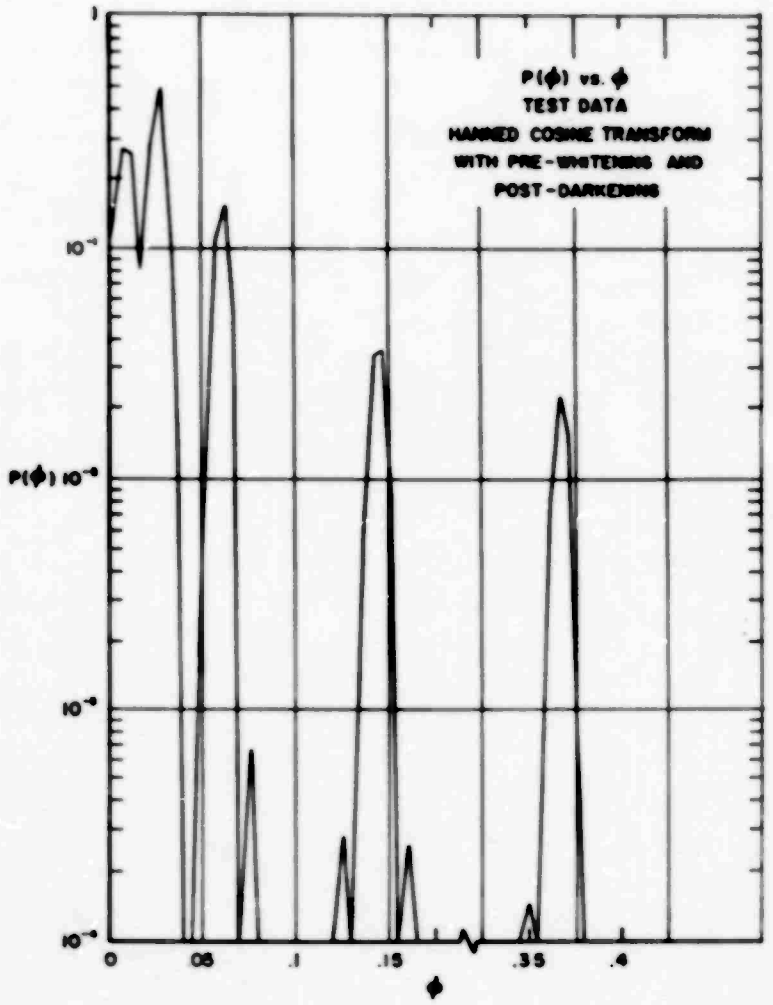

Figure 11. Test of Manufactured Data Processed by High Resolution PSD Program (Semi-log Scale)

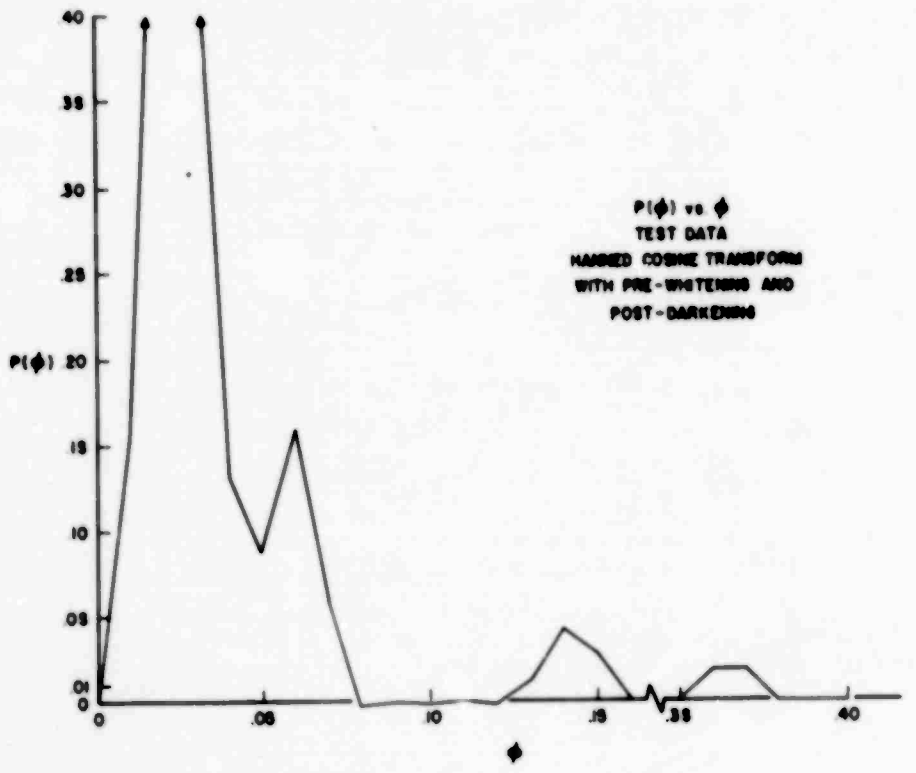

Figure 12. Test of Manufactured Data Processed by Low Resolution PSD Program (Rectangular Scale)

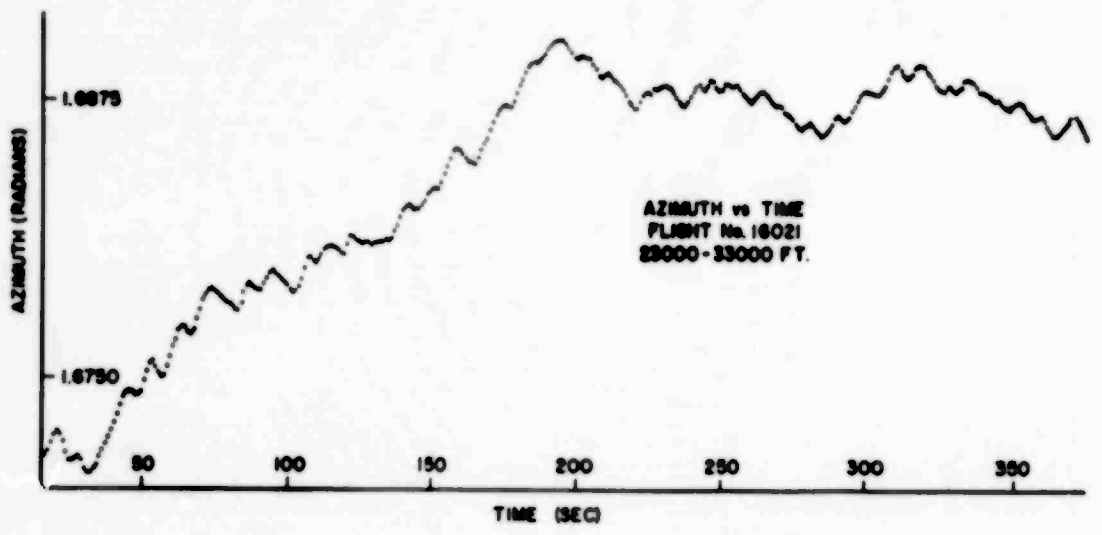

Figure 13. Azimuth vs Time for Flight 16021 23,000 to 33,000 Feet Altitude Layer

3.2 ANALYSIS OF ROSE DATA BY PSD PROGRAM

The vertical motion of a ROSE balloon is very smooth and does not exhibit any of the oscillatory motion found in the horizontal plane. Because of this the Azimuth angle of the radar was selected for analysis rather than the Elevation angle or Range. The program was set up for a computer run so that a ROSE packed binary tape was the input, and the PSD table with the history and identification of the run was the output.

3.2.1 STANDARD ROSE BALLOONS

The standard ROSE balloon results were achieved in two steps. The first was a control study using only one flight (16021) chosen at random. The second step was to apply the techniques developed in the first step to a series of standard balloons flown at nearly the same time as some of the modified balloons.

3.2.1.1 Control Study of Flight 16021

In order to obtain a better understanding of the actual ROSE data, a plot of Azimuth vs Time for flight 16021 was made. A portion, from 23 thousand to 33 thousand feet altitude, is presented as Figure 13. This portion of 400 seconds is essentially a quadratic with the familiar oscillations superimposed on it.

The data were processed four times, each using a different trend-removing technique. The main program used the following calling sequence:

1. READIN (400 points)
2. One of the trend-removing routines
3. WHITN (ALFA1 = - 1/2, ALFA2 = +1)
4. AUTCOV (50 lags)
5. FOURTR (Hanned cosine transform)
6. PDRKN (ALFA1 = - 1/2, ALFA2 = + 1)

The four trend-removing routines used were:

1. QTRND over the whole interval
2. TRNDR over 50 point lines
3. MOVAVG over 51 points
4. MOVAVG over 81 points

The results of all four runs were almost identical, and a representative plot of $P(\phi)$ vs ϕ is shown in Figure 14. The plot indicates that in this portion of the flight there was a much greater predominance of low frequencies than high frequencies, and as frequency increases the power diminishes approximately as the log of the frequency. It is interesting to note that the very slight peak at a frequency of 0.1 cps repeats itself in all four attempts. However, it is believed that the peak does not rise high enough above its surroundings to enable one to say that there is a predominant oscillation at a frequency of 0.1 cps.

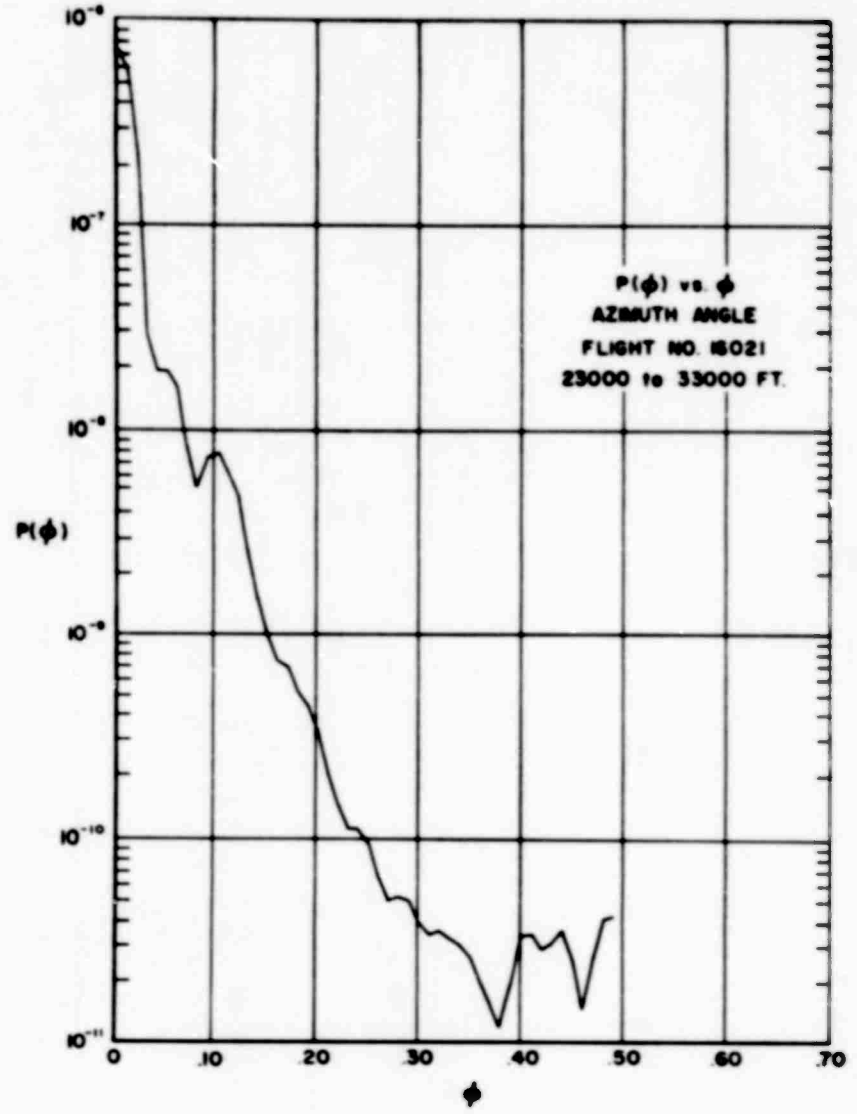

Figure 14. Results of PSD Analysis of Azimuth of Flight 16021 23,000 to 33,000 Feet Altitude

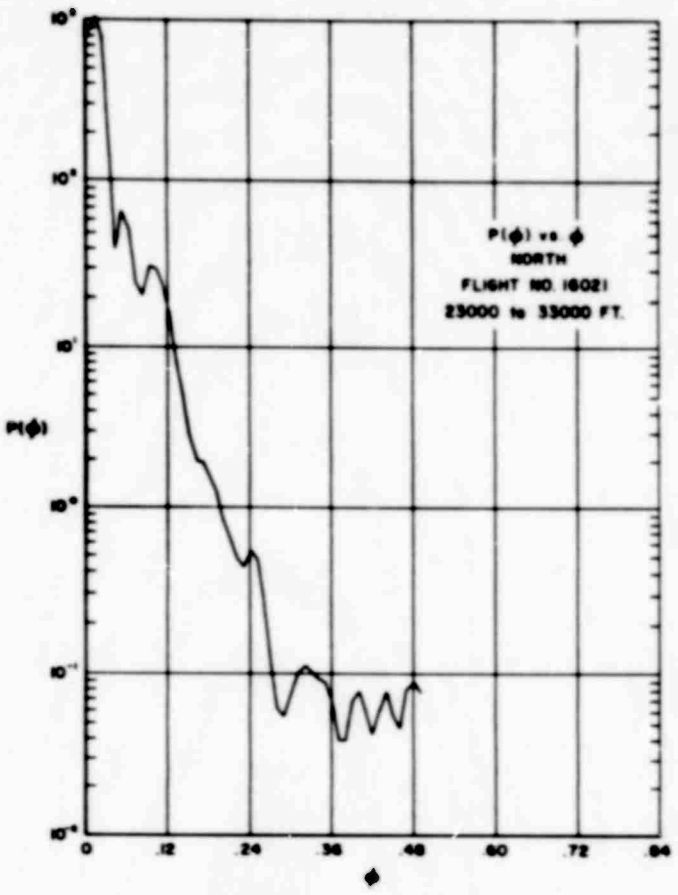

Figure 15. Results of PSD Analysis of North of Flight 16021 23,000 to 33,000 Feet Altitude

To determine the effect of the oscillating azimuth angle on the horizontal components, two analyses were run (each with a different trend remover) on each of the East and North components for the same altitude band. Although the balloon was launched near the radar site, a strong westerly at the time of this flight had pushed the balloon (at an altitude of 23,000 feet) much farther to the east but at about the same latitude. This resulted in the North component being more noticeably oscillatory than the East component. The different trend-removing routines again had no visible effect in producing a power curve of different shape. A typical result for the North component is presented as Figure 15; a result for the East component is shown as Figure 16. The slight increase in power is again noticed in the North component at 0.1 cps; because of the location of the balloon with respect to the radar, such increase is not perceived in the East component.

The next step was to work with various parts of the flight analyzing only the azimuth angle. First, the entire flight was analyzed (0 to 63,000 feet). The result was a very noisy linear function on semi-log scale similar to those shown in Figures 14 and 17. This function was not only noisier than those depicted in Figures 14 and 17, it also lacked the prominence at 0.1 cps. Analysis of the first half of the flight (0 to 33,000 feet) gave the same result as the analysis of the whole flight. When the Azimuth vs Time plot of the entire flight was studied, it was noticed that at about 42,000 feet the oscillations vanished (which coincided with the smoothing of the winds mentioned earlier). An analysis of the last portion of the flight (43,000 to 63,000 feet) was made. The results, presented as Figure 18, indicate the presence of very low frequency (below 0.03 cps) oscillations and essentially white noise at all frequencies above this--a result quite different from any obtained in previous analyses. This agrees with the observed fact that the winds suddenly became smooth at 42,000 feet. In order to check this result, the portion of the flight from 34,000 feet to 45,000 feet was analyzed. The result is presented as Figure 17 in which the whole first portion of the flight seems to confirm that the oscillations really do vanish above 42,000 feet for the standard ROSE balloon.

3.2.1.2 Series of Standard Flights

The results of the control study indicated that Azimuth should be analyzed and that the flight should be broken into two sections: 1) the portion containing the oscillations (the first of the lower half of the flight); 2) the part that is smoother (the second or upper half of the flight). The flights of several standard balloons were chosen for analysis of the azimuth both in the two altitude bands and over the entire flight. The flight numbers of the balloons chosen were 16053, 16074, 16083, 16114, and 16116. The output is presented as Figures 19, 20, 21, 22, and 23 respectively. The analysis of the entire flight is not shown because it is very similar to the lower-half analysis. It can be seen that while the general trend of the upper and lower portions are similar, the upper portions have none of the small peaks found in the lower portions. These small peaks are not sufficiently prominent to give assurance that these frequencies are always present in the data. If the frequencies are not always present, attempting to remove them could cause even more erratic data.

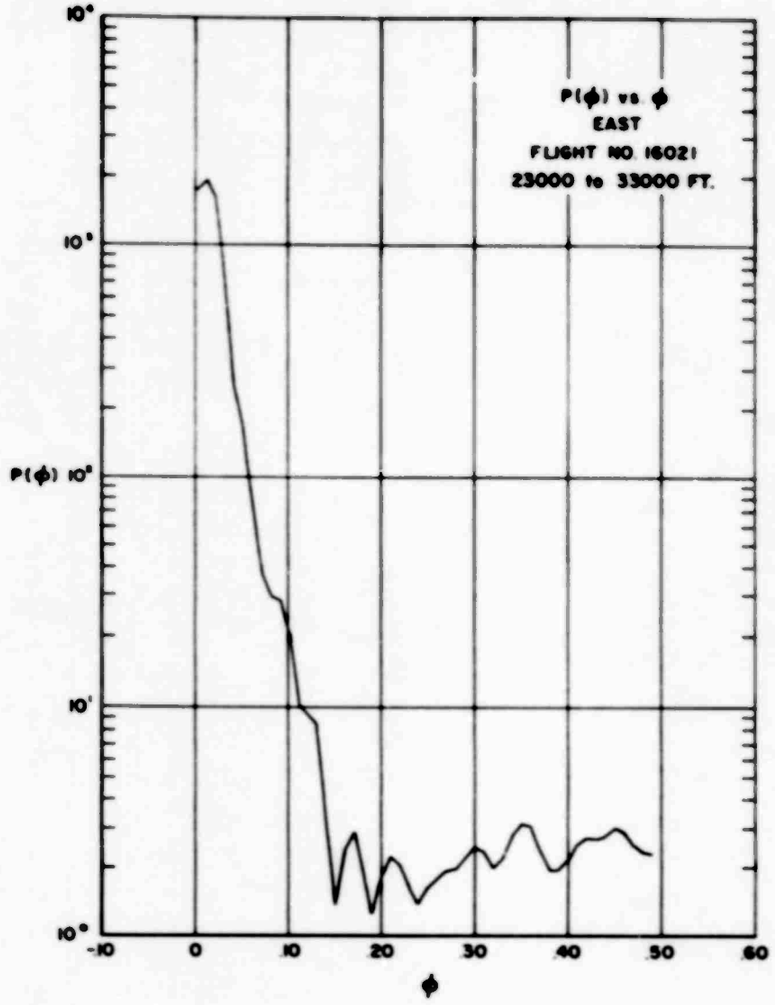

Figure 16. Results of PSD Analysis of East of Flight 16021 23,000 to 33,000 Feet Altitude

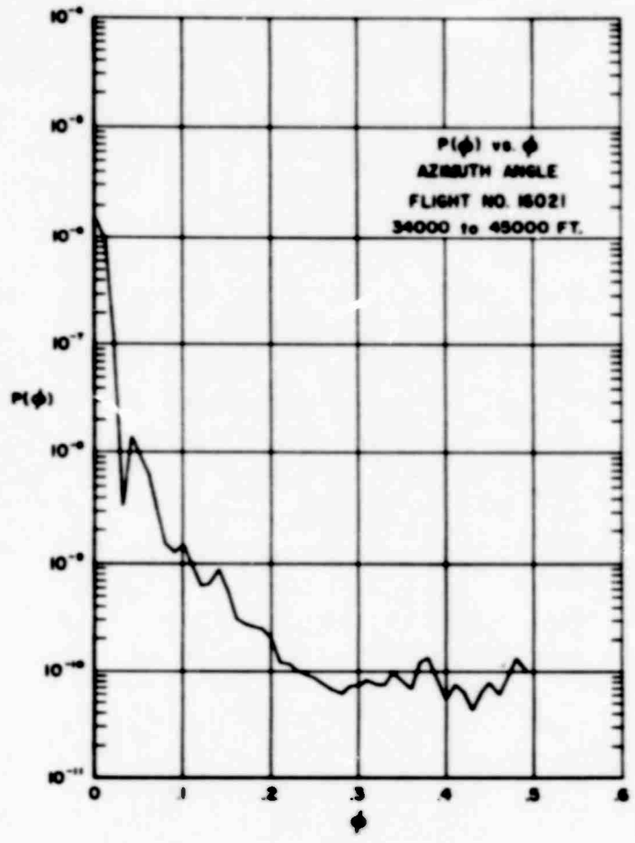

Figure 17. Results of PSD Analysis of Azimuth of Flight 16021 34,000 to 45,000 Feet Altitude

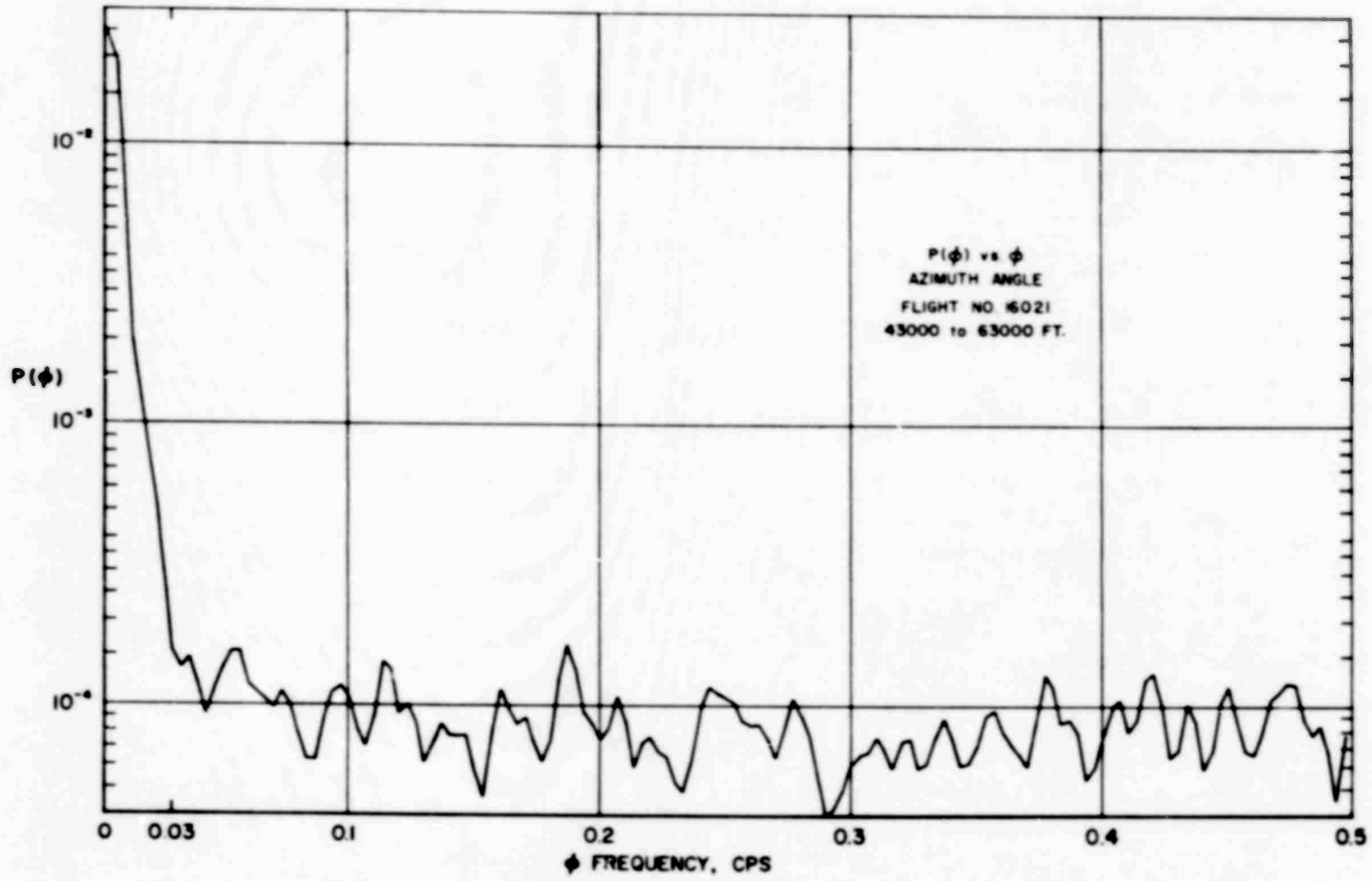

Figure 18. Results of PSD Analysis of Azimuth of Flight 16021 43,000 to 63,000 Feet Altitude

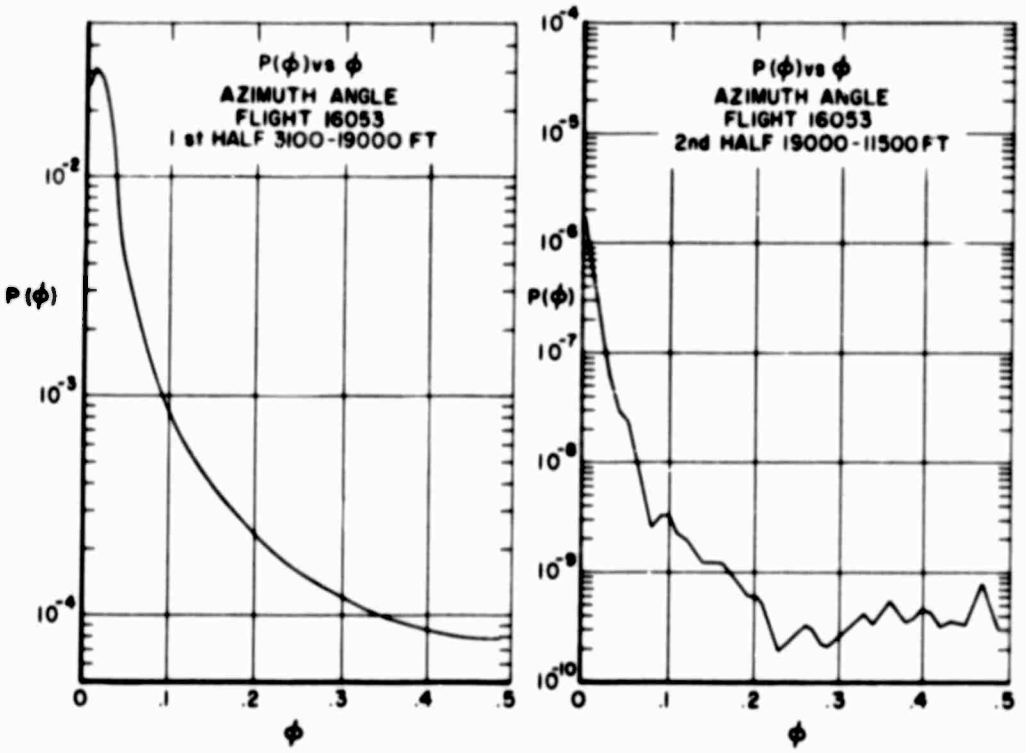

Figure 19. Results of Two PSD Analyses of Azimuth of Flight 16053

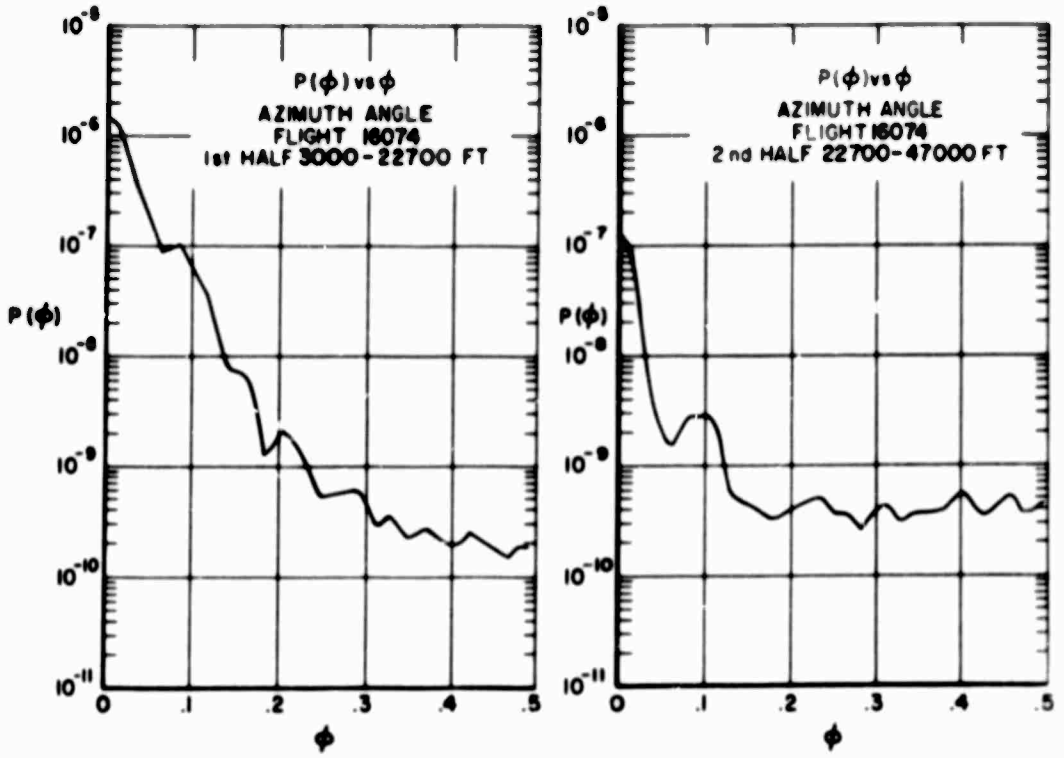

Figure 20. Results of Two PSD Analyses of Azimuth of Flight 16074

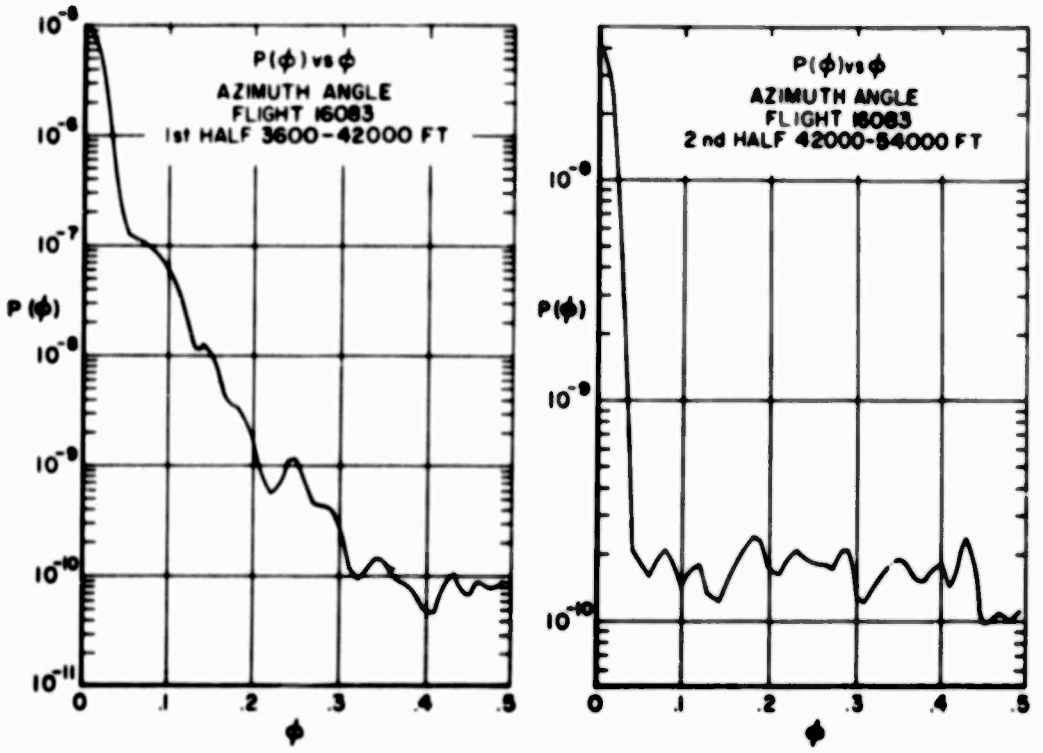

Figure 21. Results of Two PSD Analyses of Azimuth of Flight 16083

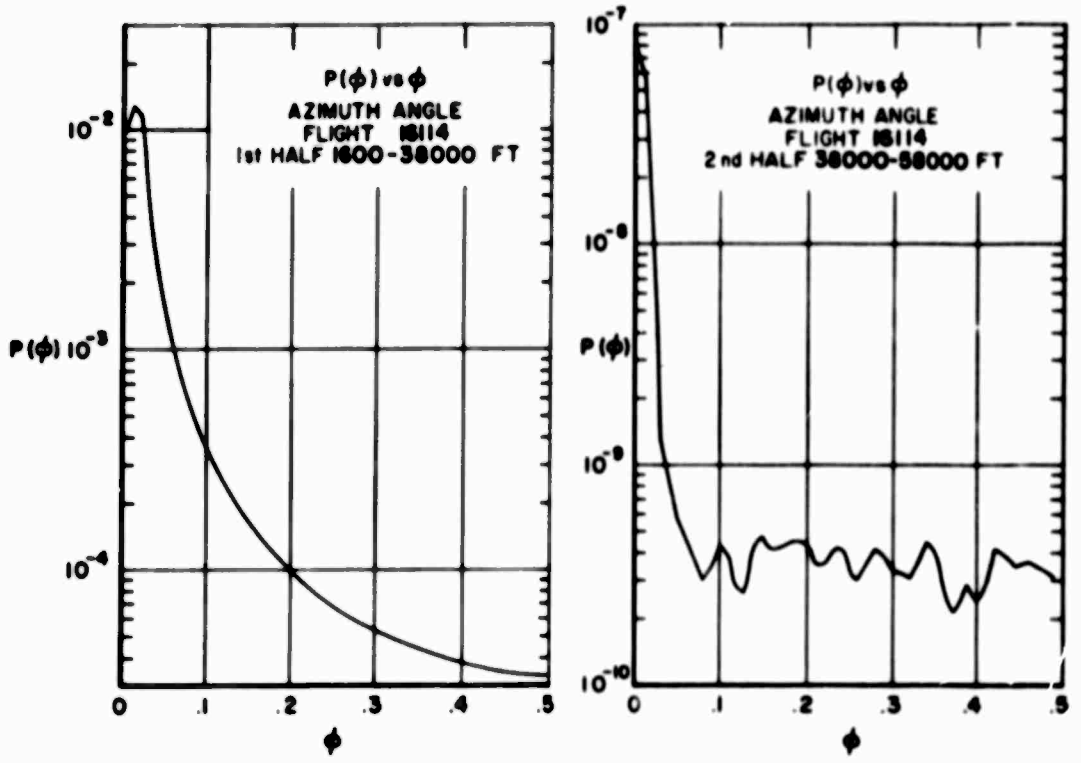

Figure 22. Results of Two PSD Analyses of Azimuth of Flight 16114

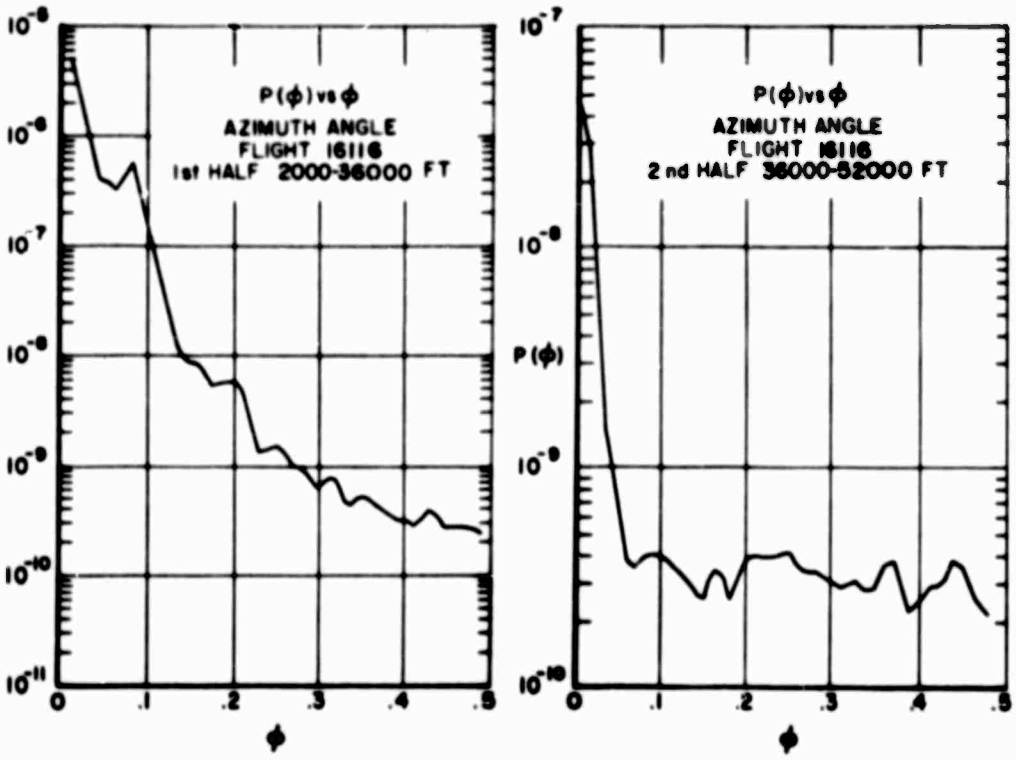

Figure 23. Results of Two PSD Analyses of Azimuth of Flight 16116

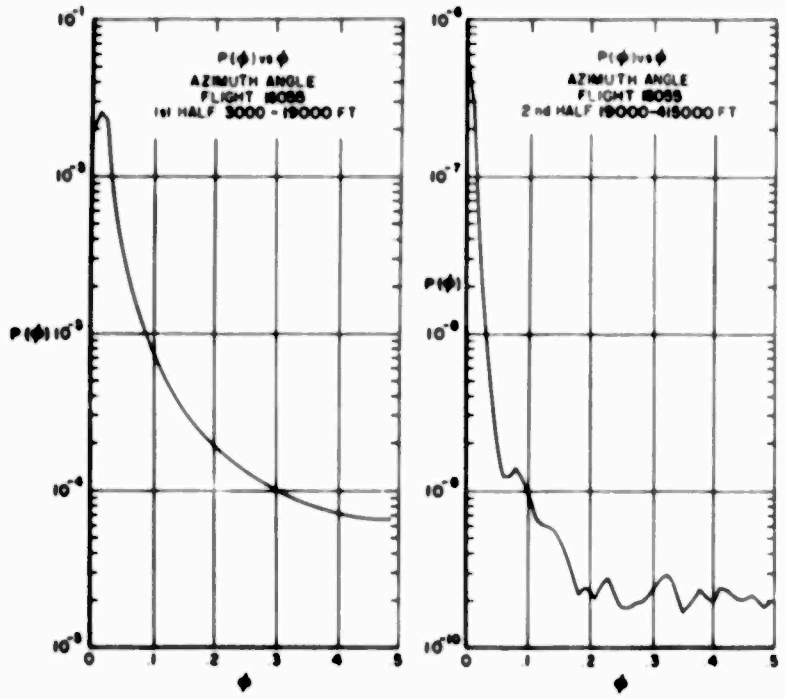

Figure 24. Results of Two PSD Analyses of Azimuth of Flight 16055

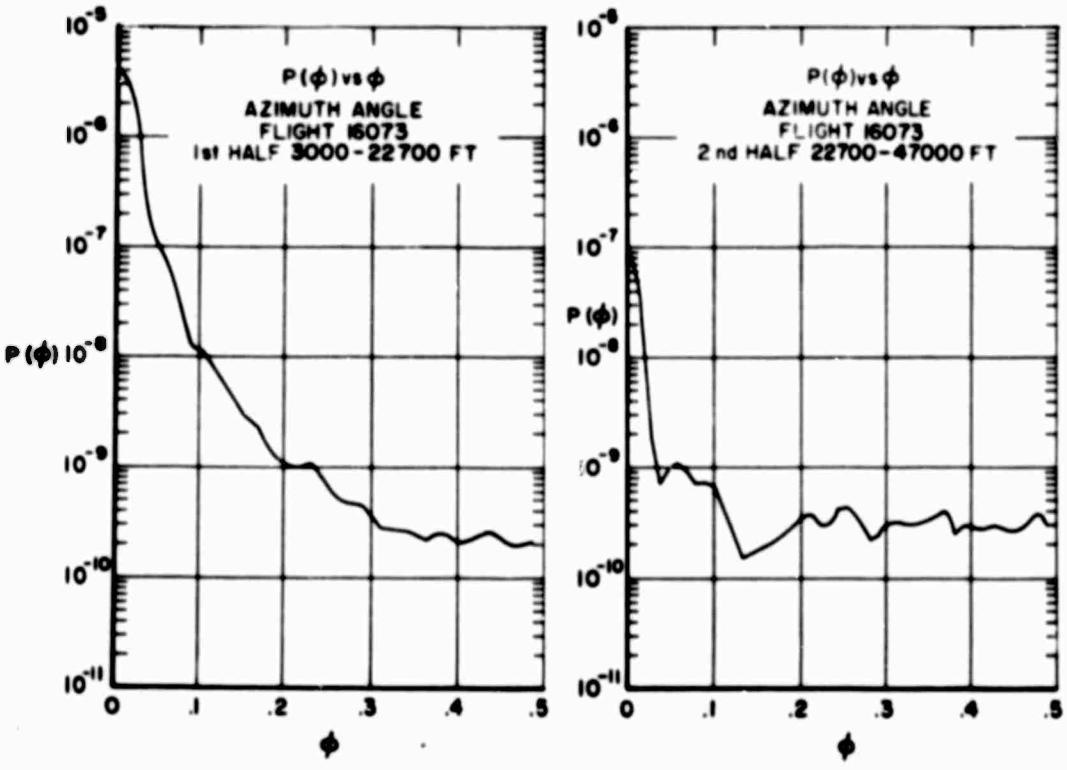

Figure 25. Results of Two PSD Analyses of Azimuth of Flight 16073

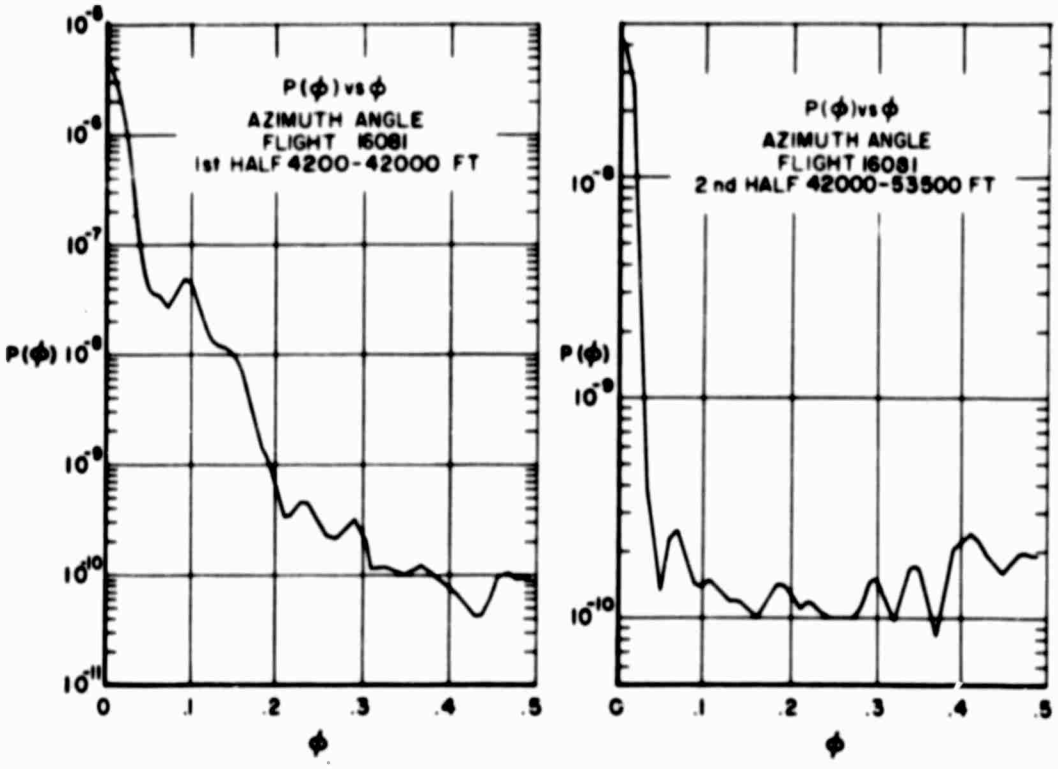

Figure 26. Results of Two PSD Analyses of Azimuth of Flight 16081

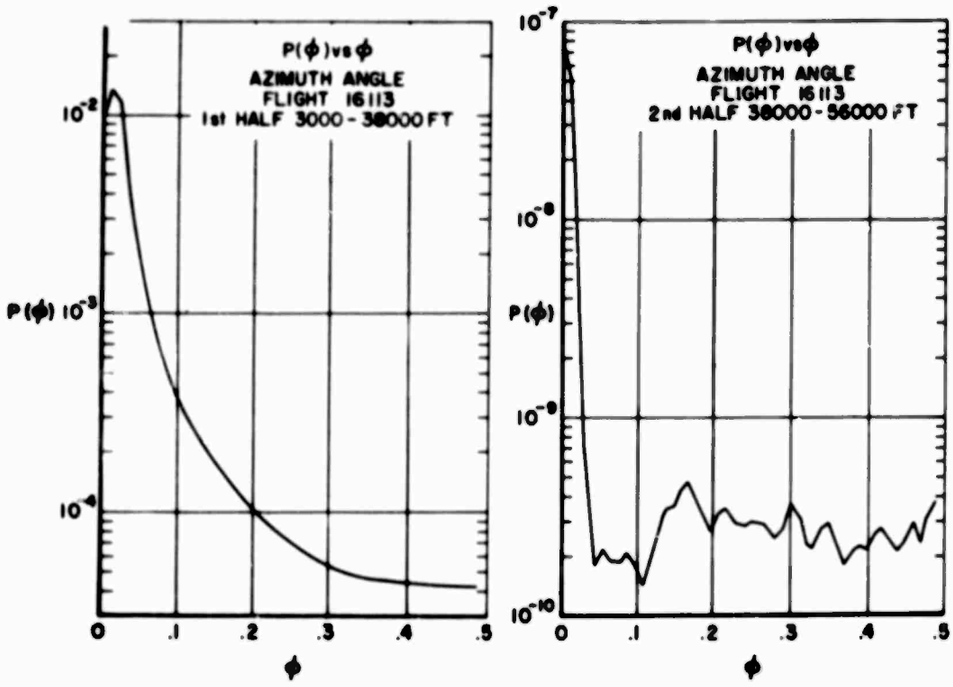

Figure 27. Results of Two PSD Analyses of Azimuth of Flight 16113

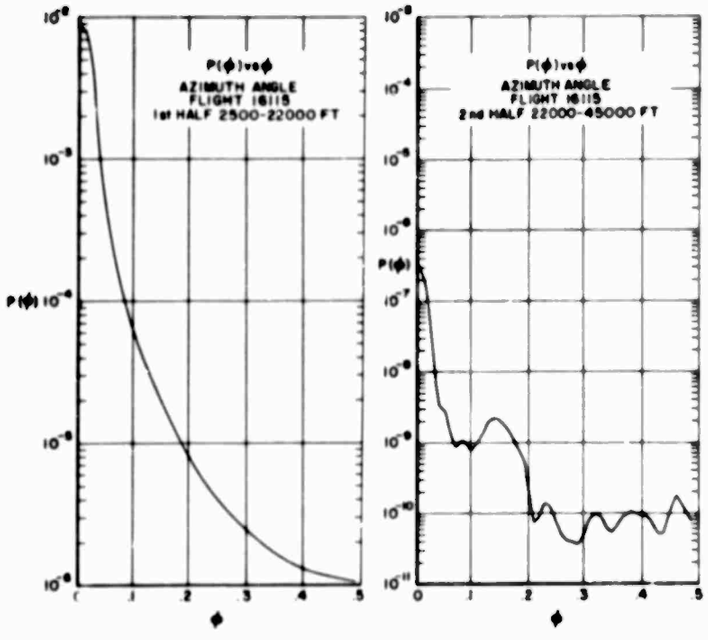

Figure 28. Results of Two PSD Analyses of Azimuth of Flight 16115

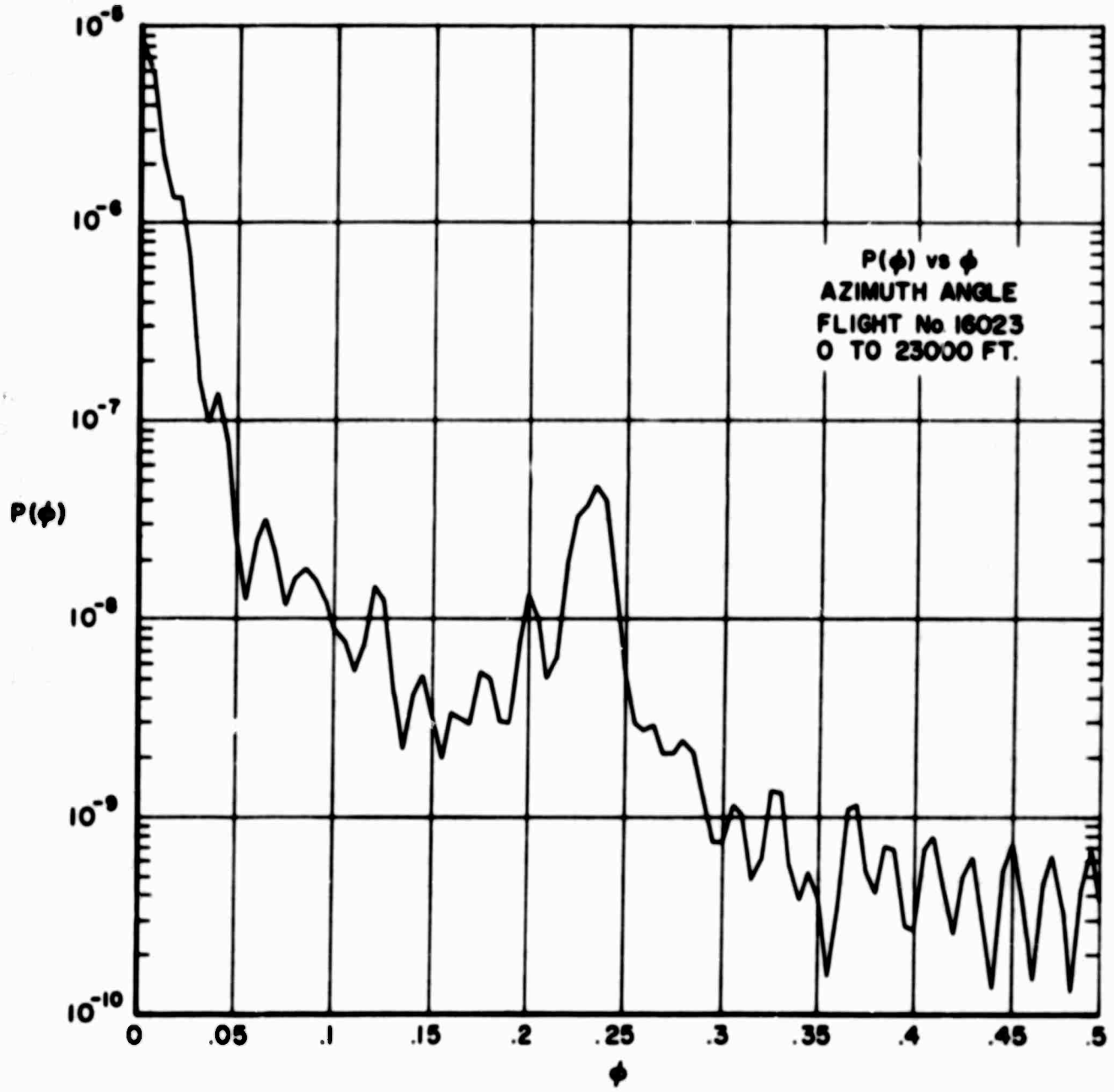

Figure 29. Results of PSD Analysis of Azimuth of Lower Part of Flight 16023

3.2.2 MODIFIED BALLOONS

The second approach to eliminating self-induced balloon motion was to physically modify the balloons. These modifications will be discussed in Section 4; for now it will be sufficient to indicate that there were basically three types of modified balloons: tails, fences, and roughening--plus two flights by a one-meter sphere with corner reflectors known as the ROBIN Balloon. Power spectral density analyses were performed on the two halves of at least one flight of each type of modified balloon. The $P(\phi)$ vs ϕ plots are presented for these representative flights:

Flight No.	Modification Type	Figure
16055	belts	24
16073	roughening	25
16081	belts	26
16113	tails	27
16115	tails	28

Upper portions of flights of modified balloons and standard balloons are very similar, but the similarity between the lower half-portions of flights of these balloons varies with the type of modification used. In all cases at least some of the smaller peaks were removed and in general the modified balloons resulted in a smoother PSD result.

3.2.3 MODIFIED ROBIN BALLOONS

In addition to the variously modified ROSE balloons two smooth, one-meter ROBIN balloons were also tested. The first had a two-inch inflation valve and a five-mb pressure-relief valve. The second had a two-inch combination inflation and relief valve. The flight was divided into two portions with the division at 23,000 feet. The results of the PSD analysis of the upper portion is very similar to the flight pattern shown in Figure 17. Except for the very low frequency peak, the data contained the same power at all frequencies. The lower portion is similar to the lower portions of the other flights with one distinction. There is a broad peak in the power curve from about 0.22 to 0.245 cps which rises high enough above its surrounding to give it a degree of credibility. The rise rate of the ROBIN is about 15 ft/sec in this region; therefore the oscillation covers 60 to 70 feet of altitude. However, the presence of the large amount of power at lower frequencies (as seen in Figure 29) makes this discovery impractical to apply in a data reduction technique.

3.3 GENERAL CONCLUSIONS

The purpose of this approach was to find a predictable periodicity which could be eliminated from the data in order to produce reliable winds and shears. We have not been able to find (with any degree of certainty) such a predictable periodicity since the motion of the balloon apparently contains no prominent frequencies.

4. PHYSICAL MODIFICATION TO THE STANDARD ROSE BALLOONS

The second approach to making the ROSE a more reliable wind sensor was to make various physical modifications to the shape of standard ROSE balloons in an attempt to control the wake separation.

The standard ROSE, as described previously, is a smooth sphere. A photograph of a standard ROSE taken immediately after launch is shown in Figure 30. The modifications were of three basic types: tails, orthogonal fences, and over-all roughening. The tail modifications were devices similar to those used with ordinary kites to improve the stability without changing the shape of the standard ROSE balloon. The orthogonal fence modifications (shown in Figure 31) consists of two orthogonal great circle strips of poly-film with lightweight drinking cups attached with their open end toward the balloon. The over-all roughening modification (shown in Figure 32) is popularly known as the "Jimsphere" and is generally attributed to Jim Scoggins. It consists of lightweight cups attached to the balloon in a fairly symmetrical design similar to a golf ball that had been turned inside out[12].

In addition to these modified ROSE balloons there were also two ROBIN balloons. The ROBIN balloon is a one meter diameter smooth sphere, as shown in Figure 33. They were modified from standard configuration by the addition of a pressure-relief valve so they could rise higher without bursting.

Each modified balloon was flown and tracked in a program testing the effectiveness of the modification. The testing program is described in Section 5.

Figure 30. Photograph of Standard ROSE in Flight

Figure 31. Photograph of Modified ROSE with Orthogonal Fences

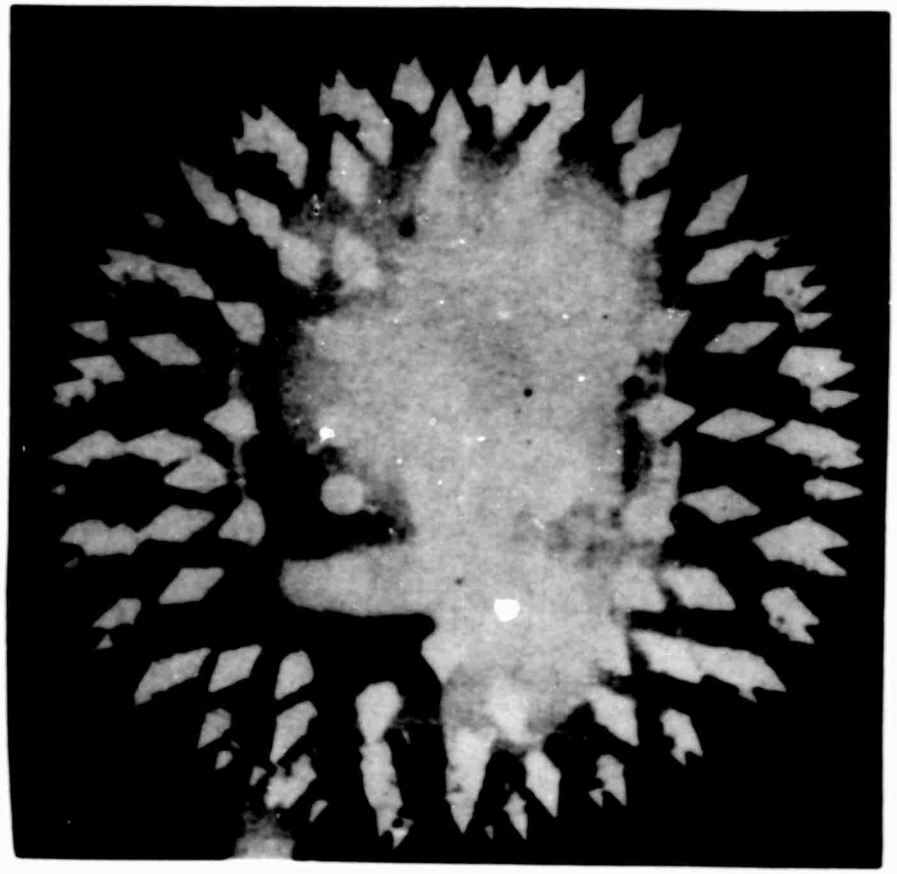

Figure 32. Photograph of Modified ROSE with Over-all Roughening

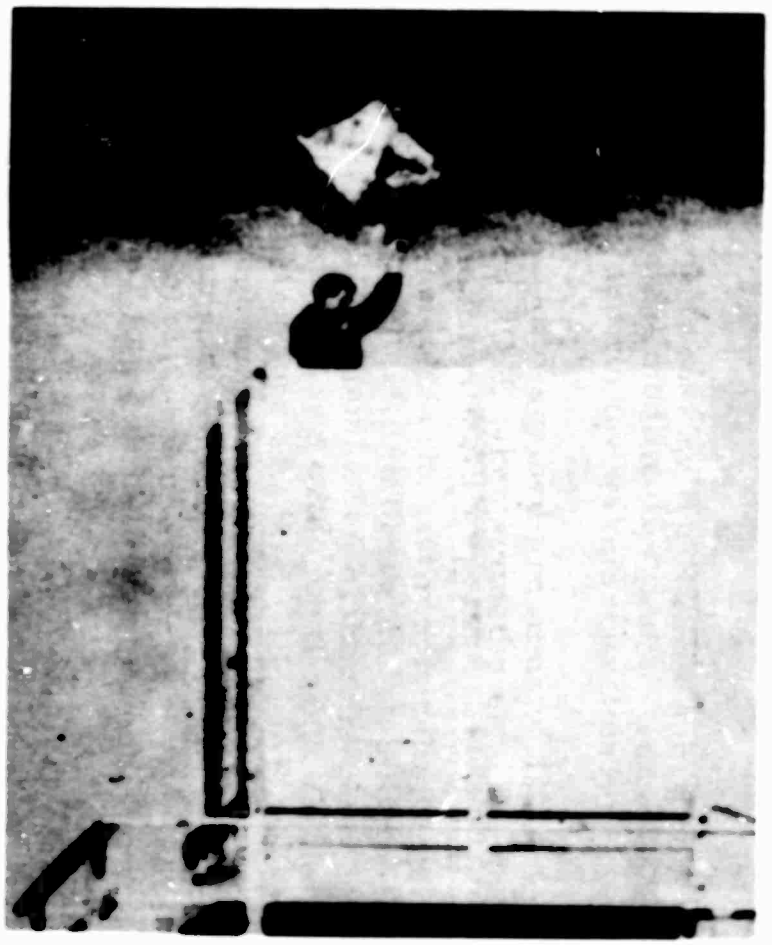

Figure 33. Photograph of Modified ROBIN Balloon

5. TESTING OF MODIFIED ROSE BALLOONS

In order to evaluate the effects of the ROSE modifications, a series of 89 test flights were flown at Eglin AFB where a standard and a modified ROSE balloon were flown at about the same time. A comparison involving the variances of the winds was made.

5.1 COLLECTION OF DATA

Each flight of a balloon was tracked with the AN/FPS-16 radar, and the data was processed by Eglin's standard xyz reduction program. When a group of processed flights was completed, they were stored serially on a binary magnetic tape. The binary tape was then forwarded to the University of Dayton Research Institute together with a BCD listing of every tenth point (in order to reduce the volume of the paper). An inventory of this test program is presented as Table 5 and includes all the pertinent information concerning the flights.

5.2 COMPUTATION OF WINDS AND THEIR VARIANCES

The conclusions reached in the studies of the various fits indicated that the finite-difference method of computing wind is normally adequate. Finite-difference Winds over 100-foot layers of altitude were computed for each flight of the series. When the mean winds over the 1000-foot layer were computed, the variances of both components and the wind vector over the same 1000-foot layer were also computed. This was done in order to quantify the effect of the modification. A sample of this type of printout is presented as Figure 34. A plot of the Wind Vector vs Altitude was drawn for each flight. Samples of portions of these plots are shown as Figures 35 to 38. The large dot shown in these figures represents the average over 1000 feet altitudes while the x'ed, dashed line is the value reported by standard rawinsonde balloon launched at about the same time as the test balloon. Figure 35 describes the wind reported by a standard ROSE balloon at the altitude at which oscillations disappear. Figures 36 to 38 are plots of the variously modified ROSE balloons which present a general view of the effect of the modifications on the computation of the Wind Vector.

5.3 COMPARISON OF VARIANCES

A representative variance of the wind vector over a 10000-foot altitude layer was computed using the following equation:

$$\sigma^2 = \frac{\Sigma(\sigma W_E)^2 + \Sigma(\sigma W_N)^2}{n} , \tag{65}$$

where $\Sigma\sigma W_E^2$ and $\Sigma\,\sigma W_N^2$ are the sums of the individual 1000-foot variances over each 10000-foot layer. These variances were computed for four layers from 0 to 40000-foot altitude and are presented as Table 6. The comparison

of variances was performed by computing the Ratio ($\overline{R}$) given by the following equation:

$$\overline{R} = \frac{\sigma^2_{Std} - \sigma^2_{modified}}{\sigma^2_{Std}} \tag{66}$$

where σ^2_{Std} and $\sigma^2_{modified}$ are the variances over 10000-foot altitude layer of a standard ROSE and a modified ROSE respectively, flown at nearly the same time. The ratio for each of the four altitude layers for each modified balloon is presented as Table 7. The Ratio ($\overline{R}$) is a type of percent-reduction equation, and the values of $\overline{R}$ for a modified balloon can be interpreted as follows: a small value for $\overline{R}$ indicates that there is very little difference between a standard balloon and this modified balloon; a large value for $\overline{R}$ indicates that there was a significant change due to the modification. When the value of $\overline{R}$ approaches 1.0 the variance of the modified balloon approaches zero--which is just about as unrealistic as the winds reported by the unmodified ROSE balloon. It was determined that a 0.7 to 0.9 reduction in variance would indicate a successful modification. Some of the more successful modifications would then be applied to the remaining standard ROSE balloons in the Air Force stocks so they could be used to produce reliable wind values. Care must be used in the selection of the modification because the balloon's wind response can be adversely affected. [10]

TABLE 5. Flights Conducted in Comparison Tests of Modified ROSEs

ID	DATE	TIME	BALLOON	MODIFICATION
16001	12/13/63	1603	Std 125	
16002	12/13/63	1606	B-24	25 ft. nylon cord with 2.5 ft x 2 in 6 mil bows every 2 ft.
16003	12/16/63	1402	Std 136	
16004	12/16/63	1403	B-22	25 ft nylon cord
16011	1/2/64	1422	B-12	10 ft. x 2 in 1.5 mil
16012	1/2/64	1800	Std 17	
16013	1/6/64	1718	D 7	Belts 6 mil w 19 large cut cups
16014	1/6/64	1812	Rawinsonde	
16015	1/6/64	1744	Std 14	
16021	12/10/63	1348	Std 36	
16022	12/10/63	1354	B-23	10 ft. nylon cord with 2.5 ft. x 2 in 6 mil bows every 2 ft.
16023	12/10/63	1511	Robin No. 1	
16024	12/10/63	1725	Robin No. 2	
16031	12/11/63	[illegible]	A 1	"Jimsphere" 230 large cups
16032	12/11/63	1601	D	Belts 6 mil w triangular tents every 1 ft.
16033	12/11/63	1723	D 6	Belts 1.5 mil w 96 small cut cups
16034	12/11/63	1828	B-25 High Altitude	10 ft. x 1.5 ft. 1.5 mil tail with 3 large cut cups
16035	12/11/63	1327	Std 50	
16036	12/11/63	1444	Std 22	
16037	12/11/63	1701	Std 21	
16038	12/11/63	1810	B-25 Low Altitude	10 ft x 1.5 ft, 1.5 mil tail with 3 large cut cups
16039	12/11/63	1835	Std 11	
16041	1/14/64	1729	Std 3	
16042	1/14/64	1657	B-15	10 ft x 6 in 2.5 mil
16043	1/14/64	1802	B-14	10 ft x 6 in 4 mil
16044	1/15/64	1331	Std 5	
16045	1/15/64	1334	B-3	5 ft x 2 in 2.5 mil
16046	1/16/64	1327	Std 10	
16047	1/16/64	1334	A 12	"Jimsphere" 75 large cut cups
16051	1/7/64	1556	Std 1	
16052	1/7/64	1602	B-9	10 ft x 2 in 6 mil
16053	1/10/64	1529	Std 9	
16054	1/10/64	1457	D 4	Belts 1.5 mil w 48 small cut cups
16055	1/10/64	1605	D 3	Belts 1.5 mil w 48 small cups
16056	1/13/64	1701	B-11	10 ft x 2 in 2.5 mil
16057	1/13/64	1656	Std 19	
16061	12/12/63	1336	A 4	"Jimsphere" 300 large cups
16062	12/12/63	1446	C 8	Belts 1.5 mil 3, 10 ft x 2 in loops
16063	12/12/63	1600	A 9	"Jimsphere" 75 large cut cups
16064	12/12/63	1702	D 8	Belts mil w 20 V-cut large cups
16065	12/12/63	1825	B-26	Parachute with 8 in. vent (ML-132)
16066	12/12/63	1404	Std 128	
16067	12/12/63	1530	Std 133	
16068	12/12/63	1746	Std 135	
16071	12/17/63	1735	B-8	5 ft x 6 in 1.5 mil
16072	12/17/63	1733	Std 12	
16073	12/20/63	1553	A 3	"Jimsphere" 75 large cups
16074	12/20/63	1547	Std 17	
16075	12/22/63	1431	A 7	"Jimsphere" 230 large cut cups
16076	12/20/63	1427	Std 9	
16081	12/18/63	1715	C 4	Belts 1.5 mil w 10, 2 ft. x 2 in. ribbons
16082	12/18/63	1836	D 5	Belts 1.5 mil w 96 small cups
16083	12/18/63	1746	Std 137	
16084	12/20/63	1401	Std 140	
16085	12/20/63	1405	B-12	10 ft x 2 in 1.5 mil
16086	12/20/63	1413	B-4	5 ft x 2 in 1.5 mil
16087	12/20/63	1424	Std 146	
16091	1/29/64	1332	B-18	25 ft x 4 in 1.5 mil
16092	1/29/64	1328	Std 47	
16093	1/30/64	1334	B-2	5 ft x 2 in 4 mil
16094	1/30/64	1328	Std 21	
16095	1/31/64	1350	B-5	5 ft x 6 in 6 mil
16096	1/31/64	1328	Std 42	
16101	12/26/63	1406	B-7	5 ft x 6 in 2.5 mil
16102	12/26/63	1359	Std 144	
16103	12/27/63	1403	B-17	25 ft x 2 in 1.5 mil
16104	12/27/63	1359	Std 5	
16105	12/30/63	1400	Std 12	
16106	12/30/63	1403	B-1	5 ft x 2 in 6 mil
16111	1/21/64	1423	A 8	"Jimsphere" 150 large cut cups
16112	1/21/64	1420	Std 16	
16113	1/23/64	1531	B-19	47 ft x 2 in 1.5 mil
16114	1/23/64	1520	Std 47	
16115	1/28/64	1331	B-16	10 ft x 6 in 1.5 mil
16116	1/28/64	1329	Std 43	
16121	2/18/64	1731	B-20	47 ft x 4 in 1.5 mil
16122	2/18/64	1726	Std 38	
16123	2/19/64	1635	B-6	5 ft x 6 in 4 mil
16124	2/19/64	1626	Std 42	
16125	2/24/64	1856	C 9	Belts 1.5 mil 5 ft x 2 in loops, every 2 ft
16126	2/24/64	1851	Std 33	
16127	2/20/64	1706	B-13	10 ft x 6 in 6 mil
16128	2/20/64	1703	Std 45	
16129	2/25/64	1754	B-10	10 ft x 2 in 4 mil
16130	2/25/64	1749	Std 31	
16131	2/28/64	1830	Std	
16132	2/28/64	1820	A 2	"Jimsphere" 150 large cups
16133	3/2/64	1432	Std 34	
16134	3/2/64	1427	A 6	"Jimsphere" 75 large cups

Alt	North	East	Δt	WN	WE	WT	$\dot{h}$	ID
3200.	-3605.	-3618.	4.4	-31.59	-29.32	43.10	22.50	16004
3301.	-3718.	-3716.	4.1	-27.56	-23.90	36.48	24.63	16004
3400.	-3833.	-3839.	4.4	-26.14	-27.96	38.27	22.50	16004
3500.	-3960.	-3967.	4.1	-30.97	-31.22	43.98	24.39	16004
3600.	-4069.	-4091.	4.4	-24.77	-28.18	37.52	22.73	16004
3702.	-4181.	-4224.	4.1	-27.32	-32.44	42.41	24.88	16004
3800.	-4276.	-4323.	3.9	-24.36	-25.39	35.18	25.13	16004
3900.	-4410.	-4450.	4.3	-31.16	-29.53	42.93	23.25	16004
4001.	-4511.	-4550.	4.1	-24.64	-24.39	34.67	24.64	16004
4100.	-4621.	-4643.	4.2	-26.19	-22.14	34.29	23.57	16004
-27.45	-27.47	38.88	23.82	3.36792	2.81500	3.84505	1.02967	
4200.	-4728.	-4708.	3.9	-27.44	-16.67	32.10	25.64	16004
4300.	-4837.	-4780.	3.9	-27.95	-18.46	33.50	25.64	16004
4403.	-4957.	-4859.	4.3	-27.91	-18.37	33.41	23.95	16004
4500.	-5082.	-4938.	4.2	-29.76	-18.81	35.21	23.10	16004
4601.	-5170.	-5016.	4.0	-22.00	-19.50	29.40	25.25	16004
4700.	-5244.	-5048.	3.6	-20.55	-8.89	22.39	27.50	16004
4800.	-5327.	-5111.	4.4	-18.86	-14.32	23.68	22.73	16004
4900.	-5436.	-5178.	4.2	-25.95	-15.95	30.46	23.81	16004
5002.	-5544.	-5185.	3.5	-30.86	-2.00	30.92	29.14	16004
5100.	-5671.	-5181.	4.2	-30.24	0.95	30.25	23.33	16004
-13.20	-26.15	30.13	25.01	7.38435	4.23666	4.14293	2.06504	
5201.	-5757.	-5216.	4.3	-20.00	-8.14	21.59	23.49	16004
5300.	-5874.	-5176.	4.3	-27.21	9.30	28.76	23.02	16004
5401.	-5972.	-5130.	4.2	-23.33	10.95	25.77	24.05	16004
5501.	-6089.	-5140.	4.3	-27.21	-2.33	27.31	23.26	16004
5600.	-6204.	-5145.	4.1	-28.05	-1.22	28.07	24.15	16004
5702.	-6320.	-5141.	4.2	-27.62	0.95	27.63	24.28	16004
5802.	-6420.	-5144.	4.7	-21.28	-0.64	21.29	21.28	16004
5901.	-6487.	-5167.	4.1	-16.34	-5.61	17.28	24.15	16004
6002.	-6538.	-5188.	4.2	-12.14	-5.00	13.13	24.05	16004
6100.	-6593.	-5190.	4.2	-13.10	-0.48	13.10	23.33	16004
-0.22	-21.63	22.39	23.51	6.12064	6.10848	6.10956	0.90043	
6200.	-6647.	-5196.	4.3	-12.56	-1.40	12.63	23.25	16004
6301.	-6711.	-5192.	4.0	-16.00	1.00	16.03	25.25	16004
6404.	-6775.	-5174.	4.3	-14.88	4.19	15.46	23.95	16004
6500.	-6837.	-5141.	4.2	-14.76	7.86	16.72	22.86	16004
6600.	-6901.	-5129.	4.1	-15.61	2.93	15.88	24.39	16004
6703.	-6962.	-5099.	4.1	-14.88	7.32	16.58	25.12	16004
6800.	-7017.	-5082.	4.2	-13.09	4.05	13.71	23.09	16004
6901.	-7061.	-5049.	4.1	-10.73	8.05	13.41	24.63	16004
7000.	-7100.	-5036.	4.3	-9.07	3.02	9.56	23.02	16004
7101.	-7145.	-4998.	4.4	-10.23	8.64	13.39	22.96	16004
4.56	-13.18	14.34	23.85	3.34717	2.45280	2.23882	0.93670	
7200.	-7161.	-4957.	3.8	-4.21	10.79	11.58	26.05	16004
7300.	-7211.	-4901.	4.0	-12.50	14.00	18.77	25.00	16004
7400.	-7269.	-4849.	4.4	-13.18	11.82	17.70	22.73	16004
7500.	-7270.	-4808.	4.5	-0.22	9.11	9.11	22.22	16004
7601.	-7303.	-4765.	4.2	-7.86	10.24	12.90	24.05	16004
7703.	-7323.	-4732.	3.9	-5.13	8.46	9.89	26.15	16004
7801.	-7341.	-4669.	3.8	-4.74	16.58	17.24	25.79	16004
7900.	-7372.	-4574.	4.3	-7.21	22.09	23.24	23.02	16004
8000.	-7398.	-4481.	4.1	-6.34	22.69	23.55	24.39	16004
8103.	-7423.	-4381.	3.9	-6.41	25.64	26.43	26.41	16004
15.14	-6.78	17.04	24.58	6.26976	3.82808	6.08491	1.54065	
$\overline{WE}$	$\overline{WN}$	$\overline{WT}$	$\bar{h}$	σ_{WE}	σ_{WN}	σ_{WT}	$\sigma_{\dot{h}}$	

Figure 34. Sample Output of Program to Compute Winds for the Evaluation of the Modified ROSE's

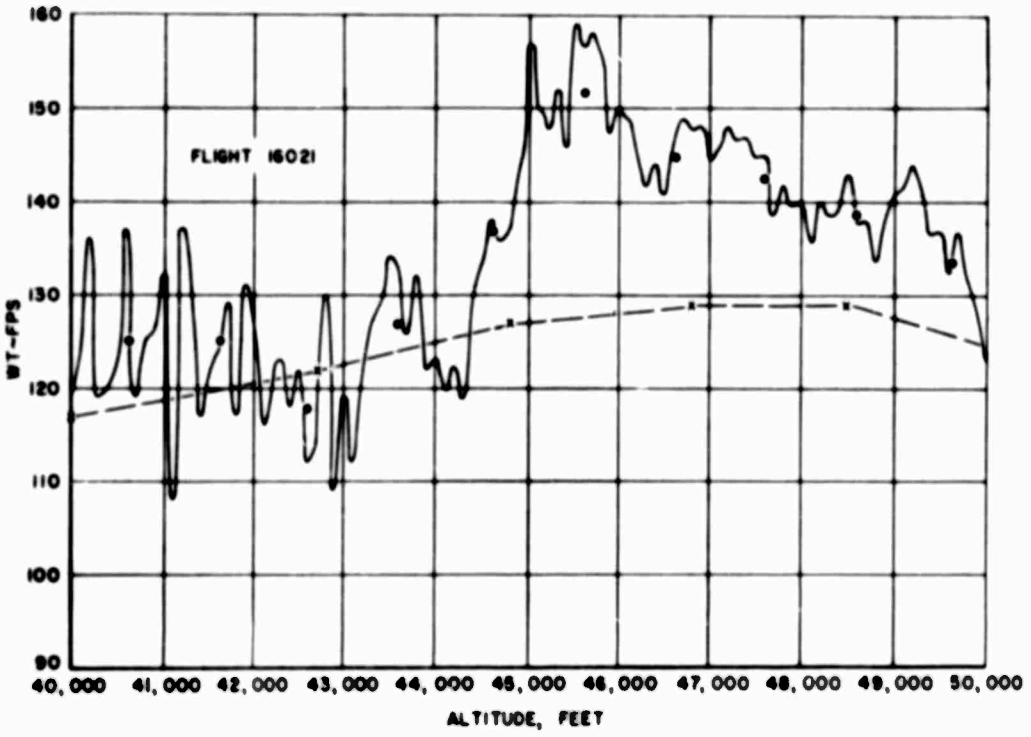

Figure 35. Wind Vector vs Altitude Flight 16021; 40,000 to 50,000 Feet

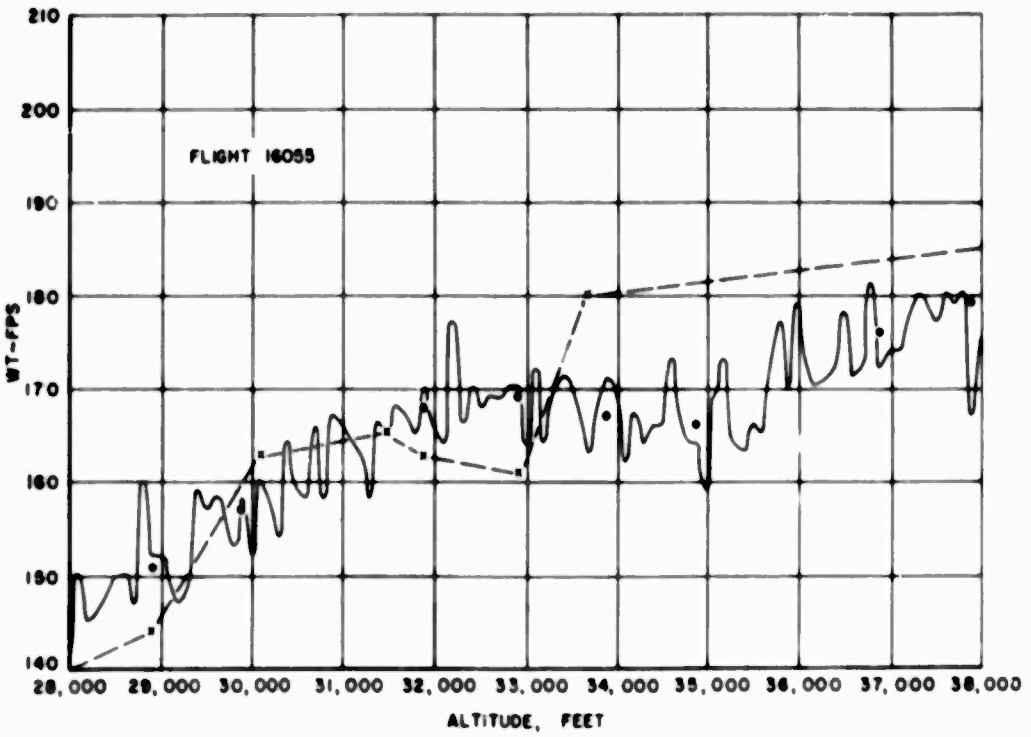

Figure 36. Wind Vector vs Altitude Flight 16055; 28,000 to 38,000 Feet

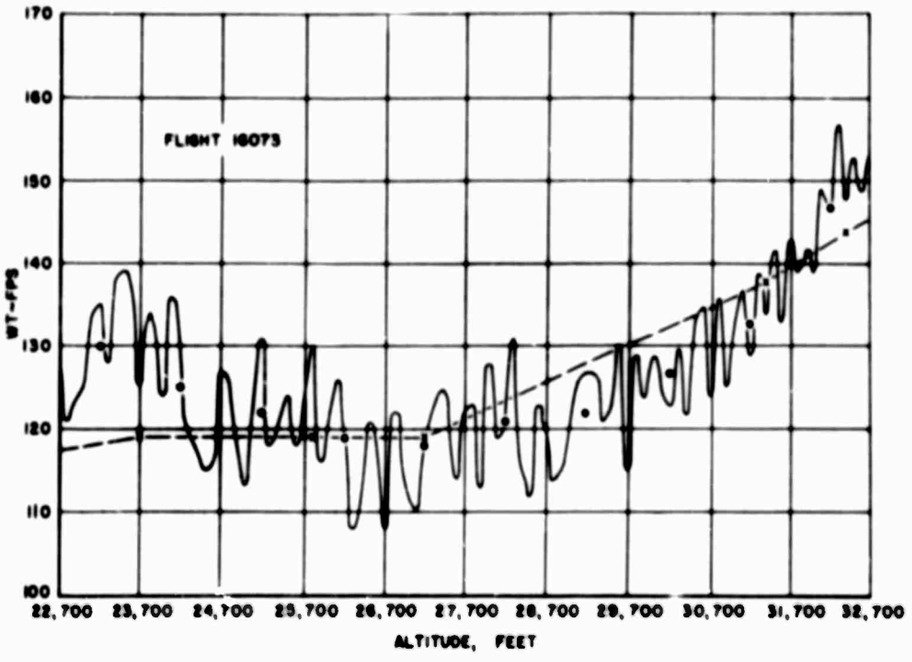

Figure 37. Wind Vector vs Altitude Flight 16073; 22, 700 to 32, 700 Feet

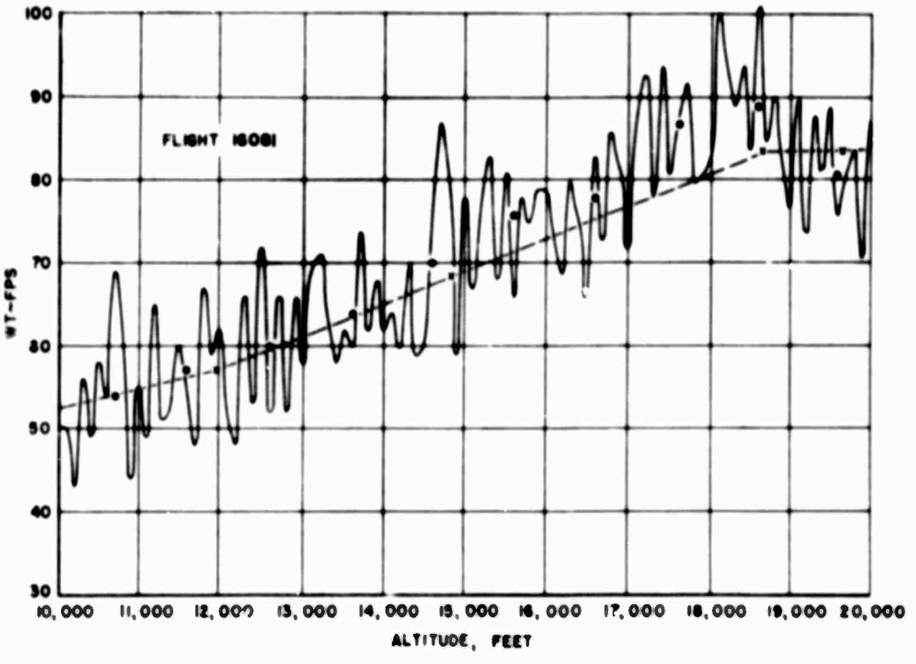

Figure 38. Wind Vector vs Altitude Flight 16081; 23, 600 to 33, 600 Feet

TABLE 6. 1000 ft Variances from Comparison Tests

Balloon No.	Alt. Layer 0-10,000	Alt. Layer 11-20,000	Alt. Layer 21-30,000	Alt. Layer 31-40,000
16001	129.615	16[illegible] 186	176.883	204.081
16002	64.797	39.908	76.261	188.950
16003	178.718	179 378	166.460	191.239
16004	42.320	36.273	78.845	128.492
16011		164.099	142.158	136.319
16012	175.592	230.033	239.258	166.090
16013	388.098	43.815	1041.031	1014.910
16015	446.345	638.065	1630.862	1121.300
16021	174.491	176 242	140.990	172.152
16022	60.584	51.360	66.298	141.130
16023	33.776	16.969	13 358	61.240
16024	57.438	31 380	29.727	626.023
16031	20.068	14 760	17.808	249 496
16032	65.151	41.873	66.613	95 386
16033	28.072	21.510	24.699	124.921
16034			64.951	99.118
16035	248.416	227.294	191.824	159 941
16036	178.886	186.392	176.271	161.335
16037	230.497	207.902	229.423	158.235
16038	317 564	155.284		
16039	644 403	213.834	224.064	172.814
16041	165.437	201.851	187 135	151.789
16042			67 825	128.891
16043	43.622	72.774	61.657	112.201
16044	184.049	254.485	210.621	206.589
16045	340.375	118.415	131.174	220.195
16046	204 878	240.254	229.510	267.949
16047	137.524	106.950	72.108	38.486
16051	287.254	764 953	1499 344	2793.860
16052	213.694	599 700	1274.509	990.025
16053	172.293	192.845	156.406	439.924
16054		105.788	78.056	25.626
16055	45.678	56.976	36.279	150.733
16056	100.465	119.620	602.444	
16057	155.928	159 140	175.210	424 082
16061	14.205	18.165	25.528	201.618
16062	58 828	87.833	82.082	100.526
16063	78 051	73.439	90.048	89 901
16064	58.726	28.682	43.270	118.167
16065	152.018	144.710	118.822	322.135
16066	133.382	153.494	137 110	82 322
16067	136.62	147.185	177 515	155.314
16068	172.262	129.446	144.356	161.839
16071	146.110	167.125	74.440	189.007
16072	140.611	209.041	206.546	155.942

Balloon No.	Alt. Layer 0-10,000	Alt. Layer 11-20,000	Alt. Layer 21-30,000	Alt. Layer 31-40,000
16073	137.475	68.988	82.401	75.920
16074	443.321	140.655	205.293	1949.966
16075	19.764	25.313	23.709	23.341
16076	229 054	219 925	255.635	189 535
16081	118.155	111.305	76 057	108.157
16082	28.320	26.173	25.238	16.604
16083	224.967	202.275	183.894	140.065
16084	179.508	175.470	174.057	165.526
16085	43.235	39.781	57 464	82.380
16086	161 184	211.810	205.457	740.655
16091	75.555	60.839	76.164	73.384
16092	201.553	184.535	188 624	158 246
16093	185.047	156.770	215.043	95.427
16094	180.158	200.442	207.504	179.720
16095	71.508	35.048	174.124	1098.681
16096	147.008	137.189	159.475	95.427
16101	75.508	[illegible] 839	76.167	73.365
16102	203.897	184 575	188.644	158.232
16103	185.087	156.755	215.043	196.427
16104	180.158	200.422	207.525	179.702
16105	71.508	35.005	123.035	1098.681
16106	146.990	139.454	159.475	95 427
16111		16.254	16.658	30.487
16112	167.162	186.443	213.536	192.431
16113	63 [illegible]	87.868	96.427	85.908
16114	125.[illegible]	194.962	213.536	1 2.431
16115	105.415	81.357	87.170	417.695
16116	219.361	973.716	195.021	193.967
16122	55.472	56.553	481.748	1353 074
16123	151.020	122.904	192.261	971.753
16124	85.324	157.853	1183.668	
16125	209.154	258.551	244.989	320.483
16126	109.303	71.065	107.332	835.047
16132	62.460	95.313	4705.237	2702.001
16127	255.635	247.722	258.547	641.556
16128	44.216	58.136	50.584	372.821
16129	159.613	175.163	633.116	158.795
16130	127.566	99.371		
16131		495 045	2589.034	
16132	62.460	95.313	4705.237	2702.001
16133	179.357	196.173	198.327	1030.809
16134	29.579	65.709	81.144	70.866

TABLE 7. Comparison of Variances for Modified ROSE Balloons

Modified	Std	Alt. Layer 0-10,000	Alt. Layer 11-20,000	Alt. Layer 21-30,000	Alt. Layer 31-40,000
16002	16001	0.500	0.760	0.569	0.074
16004	16003	0.763	0.809	0.526	0.328
16011	16012	N.G.	0.287	0.406	0.179
16013	16015	0.130	0.148	0.362	0.095
16023	16021	0.806	0.904	0.926	0.644
16031	16035	0.919	0.935	0.907	N.G.
16032	16037	0.717	0.606	0.710	0.397
16033	16037	0.878	0.897	0.892	0.211
16034	16039	N.G.	N.G.	0.710	0.426
16038	16039	0.507	0.274	N.G.	N.G.
16042	16041	N.G.	N.G.	0.638	0.151
16043	16041	0.736	0.639	0.671	0.389
16045	16044	N.G.	0.535	0.377	N.G.
16047	16046	0.329	0.555	0.686	0.856
16052	16051	0.256	0.216	0.150	0.649
16054	16053	N.G.	0.452	0.501	0.942
16055	16053	0.735	0.705	0.768	0.657
16056	16057	0.356	0.248	N.G.	N.G.
16061	16066	0.894	0.882	0.814	N.G.
16062	16066	0.559	0.428	0.401	N.G.
16063	16067	0.429	0.501	0.493	0.421
16064	16068	0.659	0.778	0.708	0.270
16065	16068	0.118	N.G.	0.119	N.G.
16071	16072	0.191	0.201	0.155	N.G.
16073	16074	0.690	0.618	0.599	0.961
16075	16074	0.955	0.860	0.885	0.988
16081	16083	0.475	0.450	0.586	0.274
16082	16083	0.874	0.871	0.863	0.889
16085	16084	0.759	0.773	0.670	0.502
16091	16092	0.625	0.670	0.596	0.536
16093	16094	N.G.	0.218	N.G.	0.469
16095	16096	0.514	0.745	N.G.	N.G.
16101	16102	0.630	0.607	0.596	0.536
16103	16104	N.G.	0.218	N.G.	N.G.
16106	16105	N.G.	N.G.	N.G.	0.913
16111	16112	N.G.	0.913	0.922	0.842
16113	16114	0.489	0.549	0.548	0.554
16115	16166	0.519	0.916	0.553	N.G.
16123	16124	N.G.	0.221	0.838	N.G.
16125	16126	N.G.	N.G.	N.G.	0.616
16129	16130	N.G.	N.G.	N.G.	0.934
16132	16131	N.G.	0.803	N.G.	N.G.
16134	16133	0.835	0.665	0.591	0.931

6. SMALL LIGHTWEIGHT ROSE BALLOONS

The two approaches initially suggested to make the ROSE system reliable wind sensors met with limited success. A new approach which involved designing an entirely new balloon sensor was suggested by Reid. Experiments tend to confirm that the self-induced balloon motion can be related to the Reynolds Number, a unitless ratio of inertial to viscous forces. When the Reynolds Number is greater than 250000 the balloon experiences considerable instability, but when the Reynolds Number is less than 250000 the instability is negligible. The value of 250000 will be known as the critical Reynolds Number. The change from supercritical to subcritical occurs at about 42,000 feet altitude for the standard ROSE balloon. Reynolds Number for a sphere is given by

$$Re = \frac{|v| \rho D}{\mu} \tag{67}$$

$|v|$ is the velocity with respect to the surrounding air mass, ρ is the density of the air mass, D the diameter, and μ the coefficient of viscosity. Since the density or coefficient of viscosity of the air mass is obviously uncontrollable, Reynolds Number must be affected by changing the velocity or the diameter of the balloon. The velocity could be decreased by adding weight to the balloon, but this is not practical because it also increases the lag distance and the length of time required for a sounding. Decreasing the diameter of the balloon lowers the maximum altitude the balloon can attain but improves its wind response. Reid has shown that a balloon having a diameter of approximately 1 meter and weighing less than 100 gms should produce detailed winds from altitudes of 10000 to 50000 feet[10]. A series of 12 such balloons, designated as GT balloons, were fabricated for testing in comparative flight tests with standard two-meter ROSE balloons.

6.1 COMPUTATION OF WINDS, VARIANCES AND REYNOLDS NUMBERS OF GT BALLOONS

The program to test the GT balloons was identical to the one used to test the modified ROSE balloons. A list of the GT balloons and the standard ROSEs flown in the test series is presented as Table 8. Wind values were computed by the finite-difference method for 100-foot layers of atmosphere. Average winds for the 1000-foot layers with their variances were then computed.

In addition to the normal output (Figure 34), two extra parameters Rise Rate and Reynolds Number, were added to the printout shown in Figure 39. Rise Rate was computed by finite-differences, and Reynolds Number was computed from the following equation:

$$R_e = \frac{(\text{Rise Rate}) \cdot \rho_m \cdot D}{\mu_m} , \tag{68}$$

where ρ_m and μ_m are the density and the coefficient of viscosity respectively. They were obtained from the 1962 Model Atmosphere[11].

In addition, four flights (16141, 16142, 16143, and 16144) were recomputed using the linear fit method of computation described in Section 1.3. Values obtained by these various methods were then compared.

6.2 COMPARISON OF VARIANCES

The method used to compare the variances for the GT balloons was identical (computing the $\bar{R}$ values) to that used for the modified ROSE balloons. The values for the ratios are presented as Table 9. The values for the ratios for flights 16141 to 16144 are presented as Table 10.

The tables show a generally high reduction in the wind variance. Based on these values and their own independent calculations, the scientists at AFCRL have made a tentative selection of a new standard ROSE balloon. It was the balloon designated as GT59 in the test series and is a 0.25-mil, 40-inch balloon with a standard pop-out valve.

Alt	N	E	Δt	WN	WE	WT	Ż	ḧ	Re	ID
5301.	-1650.	-1850.	5.9	-11.87	-8.04	14.33	16.34	16.33	268903.	16147
5401.	-1725.	-1940.	8.0	-10.43	-11.99	15.89	12.52	12.51	205460.	16147
5503.	-1786.	-2054.	7.1	-7.66	-15.47	17.26	14.33	14.33	234528.	16147
5604.	-1879.	-2174.	7.4	-12.33	-17.19	21.16	13.69	13.68	223411.	16147
5705.	-1959.	-2296.	7.4	-9.87	-16.63	19.34	13.57	13.57	220916.	16147
5802.	-2022.	-2413.	7.2	-9.50	-16.40	18.95	13.45	13.45	218350.	16147
5901.	-2109.	-2535.	7.7	-11.27	-16.20	19.73	12.86	12.86	208220.	16147
6000.	-2176.	-2654.	6.4	-10.77	-18.81	21.67	15.53	15.53	250772.	16147
6103.	-2252.	-2832.	9.7	-7.25	-17.45	18.90	10.63	10.63	171124.	16147
6205.	-2325.	-2959.	7.1	-11.10	-17.90	21.07	14.33	14.32	229971.	16147
-15.61	-10.20	18.83	13.72	3.23062	1.67954	2.37866	1.58765			
6303.	-2396.	-3085.	7.3	-8.94	-17.70	19.83	13.50	13.50	216118.	16147
6400.	-2445.	-3208.	6.7	-7.02	-17.46	18.81	14.46	14.46	230909.	16147
6504.	-2502.	-3339.	8.2	-7.98	-16.21	18.07	12.61	12.61	200767.	16147
6605.	-2551.	-3466.	6.8	-6.43	-15.44	16.72	14.85	14.85	235748.	16147
6701.	-2622.	-3531.	6.6	-10.39	-13.77	17.25	14.55	14.54	230300.	16147
6800.	-2676.	-3621.	6.1	-7.43	-14.18	16.01	16.29	16.29	257236.	16147
6900.	-2750.	-3723.	5.9	-13.77	-17.35	22.15	16.94	16.93	266699.	16147
7000.	-2838.	-3827.	5.9	-14.70	-16.12	21.82	16.99	16.98	266698.	16147
7102.	-2924.	-3934.	7.2	-11.96	-14.20	18.57	14.15	14.15	221550.	16147
7201.	-3006.	-4044.	8.1	-10.23	-13.79	17.17	12.15	12.14	189688.	16147
-15.62	-9.88	18.64	14.65	1.56986	2.86178	2.07954	1.68174			
7304.	-3095.	-4145.	7.2	-12.59	-13.50	18.46	14.32	14.31	222937.	16147
7407.	-3203.	-4245.	7.8	-13.90	-12.05	18.40	13.22	13.21	205192.	16147
7501.	-3320.	-4340.	8.2	-14.10	-11.72	18.34	11.44	11.44	177148.	16147
7601.	-3417.	-4431.	6.2	-15.06	-13.43	20.18	16.21	16.20	250250.	16147
7705.	-3526.	-4533.	8.3	-13.04	-12.24	17.89	12.50	12.49	192412.	16147
7803.	-3643.	-4631.	8.0	-14.59	-12.40	19.15	12.24	12.23	187875.	16147
7904.	-3753.	-4715.	7.3	-14.64	-12.36	19.16	13.89	13.88	212686.	16147
8000.	-3847.	-4807.	8.0	-12.02	-11.39	16.56	12.02	12.02	183571.	16147
8101.	-3946.	-4894.	7.2	-12.47	-11.49	16.96	14.00	14.00	213252.	16147
8205.	-4062.	-4987.	8.0	-15.16	-10.78	18.60	12.96	12.97	197038.	16147
-12.14	-13.76	18.37	13.28	0.86115	1.14707	1.05807	1.38660			
8300.	-4187.	-5072.	8.5	-15.45	-10.52	18.69	11.22	11.22	169928.	16147
8408.	-4300.	-5134.	7.0	-15.52	-8.46	17.68	15.34	15.34	231704.	16147
8500.	-4430.	-5199.	7.9	-15.42	-7.15	17.00	11.74	11.73	176802.	16147
8600.	-4560.	-5251.	7.8	-16.79	-7.41	18.35	12.83	12.83	192737.	16147
8702.	-4680.	-5303.	7.8	-16.28	-5.93	17.32	13.01	13.01	194881.	16147
8801.	-4808.	-5351.	7.6	-16.95	-6.63	18.20	13.01	13.01	194369.	16147
8900.	-4925.	-5393.	7.2	-16.53	-6.71	17.84	13.84	13.83	206132.	16147
9001.	-5050.	-5445.	8.5	-15.01	-5.84	16.11	11.86	11.86	176217.	16147
9105.	-5160.	-5506.	7.9	-12.43	-7.40	14.46	13.10	13.10	194068.	16147
9203.	-5266.	-5560.	7.8	-13.76	-6.67	15.29	12.56	12.55	185499.	16147
-7.27	-15.41	17.09	12.85	1.37133	1.41739	1.39190	1.16702			
9301.	-5368.	-5624.	8.0	-13.74	-8.68	16.25	12.25	12.24	180431.	16147
9404.	-5462.	-5681.	7.6	-12.27	-8.04	14.67	13.57	13.57	199393.	16147
9503.	-5580.	-5740.	8.0	-14.91	-7.02	16.48	12.43	12.42	182098.	16147
9601.	-5697.	-5814.	7.9	-15.36	-9.65	18.15	12.51	12.51	182816.	16147
9703.	-5815.	-5980.	7.1	-16.73	-8.65	18.83	14.42	14.41	210076.	16147
9802.	-5935.	-5935.	7.6	-15.77	-8.00	17.68	13.06	13.05	189727.	16147
9901.	-6064.	-5996.	6.9	-18.23	-8.04	19.92	14.26	14.25	206557.	16147
10000.	-6204.	-6076.	7.4	-19.88	-10.46	21.58	13.44	13.43	194131.	16147
10103.	-6353.	-6173.	7.5	-19.18	-12.91	23.11	13.65	13.64	196701.	16147
10201.	-6501.	-6270.	7.6	-20.57	-12.88	24.27	12.93	12.92	185786.	16147
-9.43	-16.56	19.10	13.25	2.05403	2.62858	3.11266	0.74837			
$\overline{WE}$	$\overline{WN}$	$\overline{WT}$	$\bar{h}$	σ_{WE}	σ_{WN}	σ_{WT}	$\sigma_{\dot{h}}$			

Figure 39. Sample Output of Wind Computation for Standard and Modified Test Series

TABLE 8. Flights Conducted in Comparison Tests of GT Balloons

Flights Conducted in Comparison Test of GT Balloons

Flight	Balloon	Diameter Inches	Gauge mil	Weight Valve gms	Time and Date of Launch	
16141	GT-62	40	.25	48.1 Weightless	1242	26 May 64
16142	GT-59	40	.25	73.1 Std	1429	26 May 64
16143	13	78.5	.50	350 Std	1742	26 May 64
16144	30	78.5	.50	350 Std	1406	26 May 64
16145	29	78.5	.50	350 Std	1528	26 May 64
16146	GT-56	36	.25	29.3 Weightless	1629	26 May 64
16147	GT-52	36	.35	74.9 Std	1608	26 May 64
16151	GT-61	40	.50	73.7 Weightless	1237	27 May 64
16152	41	78.5	.50	350 Std	1428	27 May 64
16153	19	78.5	.50	350 Std	1532	27 May 64
16154	GT-58	40	.35	84.8 Std	1659	27 May 64
16155	GT-55	36	.50	62.3 Weightless	1451	27 May 64
16156	GT-53	36	.25	67.2 Std	1926	27 May 64
16157	48	78.5	.50	350 Std	1814	27 May 64
16161	GT-57	40	.50	100.6 Std	1346	28 May 64
16162	23	78.5	.50	350 Std	1251	28 May 64
16163	14	78.5	.50	350 Std	1409	28 May 64
16164	GT-60	40	.50	97.5 Std	1244	28 May 64
16171	7	78.5	.50	350 Std	1332	1 June 64
16172	GT-54	36	.50	85.5 Std	1443	1 June 64
16173	46	78.5	.50	350 Std	1610	1 June 64
16174	GT-51	36	.50	89.9 Std	1327	1 June 64

Table 9

Comparison of Variances for GT Balloons

GT Balloons	Std.	Alt 0-10,000	Alt 11-20,000	Alt 20-30,000	Alt 31-40,000
16141 (GT 62-11)	16144	0.037	0.942	0.894	0.739
*16142 (GT 59-9)	16144	0.812	0.947	0.954	0.842
16146 (GT 56-6)	16145	0.834	0.950	0.896	0.810
16147 (GT 52-2)	16145	0.928	0.953	0.940	0.691
16151 (GT 61-12)	16152	0.892	0.903	0.817	0.740
16154 (GT 58-8)	16157	0.890	0.965	0.961	0.915
16155 (GT 55-5)	16152	0.771	0.891	0.821	0.870
16156 (GT 53-3)	16153	0.894	0.963	0.972	0.904
16161 (GT 57-10)	16163	0.733	0.945	0.958	0.956
16164 (GT 60-7)	16162	0.863	0.920	0.960	0.934
16172 (GT 54-4)	16171	0.784	0.926	0.765	N.G.

* Indicates the type that is tentatively chosen as the new standard ROSE balloon.

Table 10

Comparison of Variances for GT Balloons Using Linear Winds

GT Balloons	Std	Alt 0-10,000	Alt 11-20,000	Alt 21-30,000	Alt 31-40,000
16141 (GT 62-11)	16144	0.945	0.953	0.929	0.769
16142 (GT 59-9)	16144	0.770	0.929	0.965	0.879
16146 (GT 56-6)	16145	0.988	0.963	0.957	0.860
16147 (GT 52-2)	16145	0.940	0.962	0.950	0.784

7. GENERAL CONCLUSIONS

The highest degree polynomial necessary to describe the motion of the ROSE balloon is in almost all instances the first degree. If the data contains extraneous points, they should either be eliminated before fitting a linear function or the method of finite-differences can be used--the latter being faster and more economical.

The Power Spectral Density Analysis Technique when applied to the balloon data produced no useable results. It was therefore suggested that physical methods of reducing the oscillations be pursued rather than trying to remove them mathematically from the radar data.

Some of the modified ROSE balloons show significant reductions of self-induced motion. Extreme care must be used in selecting the type of modification to be applied to the remaining standard ROSE balloons. With the proper modifications, the standard ROSE balloon can be used to measure the detail winds with fair reliability.

The smaller lightweight balloons seem to reduce wind variance most consistently. They also have better wind response and are much simpler to manufacture than the modified ROSE balloons.

8. FUTURE WORK

Future work will be in two areas: The first will be a more complete analysis of the modified ROSE balloons selected by scientists at AFCRL to be flown for a study which would determine a typical wind profile. The second will be to develop a more convenient data-handling system for the new lightweight ROSE balloons. Such a system will permit computations at the sounding site and will eliminate the delay involved in data reduction at a remote location.

APPENDIX I

INDUCED MASS

The values presented by Leviton for the wind response errors in the spherical balloon technique for measuring winds were questioned by Reed[13,14]. The basis for the difference between values computed by Leviton and Reed was attributed to the fact that Leviton assumed the apparent mass term to be zero.

A basic reference in aerodynamics, "Theory of Flight" by R. von Mises, page 573, provides the basis for the additional term in the expression for mass.

"In this argument, as well as in the preceding section, it has been assumed that the air reactions on a moving body depend on the instantaneous state of velocity only, not on the accelerations (and higher derivatives). It is obvious that this can be only an approximation and that some influences on the acceleration must exist. The theory of irrotational flow of a perfect fluid gives a certain answer to this question. According to this theory, a body moving in a fluid originally at rest behaves like a body of increased inertia: There is a term of apparent mass to be added to its real mass w/g, the reaction of the surrounding fluid would be taken intoaccount when the sphere is assumed to have the mass

$$\frac{W}{g} + \frac{2}{3} \pi \, pa^3$$

and to move under the influence of the other forces (weight, etc.) alone. This includes (for the case of a sphere) the result expressed in D'Alembert's paradox (Sec. IX. 3) that no reaction exists if the motion is uniform."

The volume of radius a is given by

$$V_B = \frac{4}{3} \pi a^3 \tag{69}$$

Solving for a^3 gives

$$a^3 = \frac{3 \cdot V_B}{4\pi} \tag{70}$$

Substituting in the expression for mass by von Mises gives

$$M = \frac{w}{g} + \frac{2}{3} \pi \rho \left(\frac{3 \cdot V_B}{4\pi} \right) \tag{71}$$

simplifying

$$M = \frac{w}{g} + \frac{1}{2} \rho \cdot V_B \tag{72}$$

The term $\frac{1}{2} \rho \cdot V_B$ is equal to one half the mass of the air displaced by the sphere. The equations of motion must therefore include the mass of the balloon and the mass of the air that is accelerated as though it were part of the body.

APPENDIX 2

AN ANALYSIS OF THE OSCILLATORY MOTION OBSERVED IN THE RISE OF A SPHERICAL BALLOON

In the course of this work it has become apparent that certain assumptions must be made if the analysis is to be mathematically tractable.

From wind-tunnel pressure measurements it is well known that the fluid flow at the front of a spherical object is essentially incompressible and inviscid for Mach Numbers appreciably less than one. However, at the rear of a sphere the wake is turbulent or at least rotational for Re greater than 100-200. In the case of ROSE, Re $\doteq 10^6$ after the first 0.5 second or so of travel. Because of this turbulence, we must resort to approximate methods since not even the simplest turbulent motion has yet lent itself to a strict mathematical analysis.

However, a certain amount of information may be obtained by a consideration of the supposedly potential flow at the front of the balloon. In doing this, of course, no information as to the causes of any oscillatory motion is obtained since these causes are tied up (apparently) in the unstable wake.

What is done to overcome this lack of information is to accept the oscillation as a fact and to apply it as a boundary condition to the equations governing the flow at the front of the balloon. Due to a lack of experimental data, the precise form of the balloon's oscillation is not known; it has, however, been assumed that this oscillation is in the form of a helical spiral.

We take axes at the center of the balloon as shown:

The x-axis is horizontal, and the y-axis is vertical. The z-axis is normal to the helical axis.

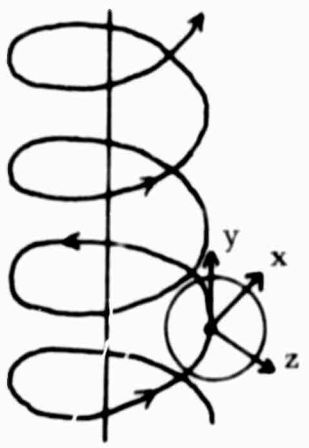

The angular velocity of the balloon is denoted by $\overline{\Omega}$, the vertical velocity of rise by $\overline{W}$, and the radius of the spiral by $\overline{d}$. The radius of the balloon is R. Hence, the axes are translating with velocity $\overline{W}$ and rotating with angular velocity $\overline{\Omega}$. The velocity of the air relative to axes fixed in space is given by the gradient of the velocity potential, U. The velocity of the fixed axes relative to the moving axes is $-\overline{W} - \overline{\Omega} \times (\overline{r} + \overline{d})$ where $\overline{r}$ is the radius vector from the moving axes to the point in question. Hence, the velocity of the fluid relative to the moving axes ($\overline{V}$) is given by

$$\overline{V} = \overline{\nabla} U - \overline{W} - \overline{\Omega} \times (\overline{r} + \overline{d}) \qquad (73)$$

Since we have assumed the flow to be inviscid, the boundary condition on the surface of the balloon is

$$V_r = 0 \tag{74}$$

where V_r = the radial component of velocity relative to balloon, and on the surface $r = R$. The above vectors have the components:

$$\overline{W} = (0, W, 0) \tag{75a}$$

$$d = (0, 0, d) \tag{75b}$$

$$\overline{\Omega} = (0, \Omega, 0) \tag{75c}$$

$$\overline{r} = (x, y, z) \tag{75d}$$

$$\overline{\Omega} \times (\overline{d} + \overline{r}) = \left| \Omega(z + d),\ 0,\ \Omega x \right| \tag{75e}$$

We use spherical coordinates defined by $x = r \sin\theta \cos\phi$, $y = r \sin\theta \sin\phi$, $z = r \cos\theta$. Now, $V_r = 0$ on $r = R$, so

$$V_r = 0 = \nabla_r U - \left[\overline{W} + \Omega \times (\overline{r} + \overline{d}) \right]_r \text{ at } r = R. \tag{76}$$

We have the general relationship:

$$v_r = v_x \sin\theta \cos\phi + v_y \sin\theta \sin\phi + v_z \cos\theta \tag{77}$$

Hence $$\nabla_r U = \frac{\partial U}{\partial r}_{r = R} = \Omega(z + d) \sin\theta \cos\phi + W \sin\theta \sin\phi - \Omega x \cos\theta \tag{78}$$

or $$\frac{\partial U}{\partial r}_{r = R} = \Omega d \sin\theta \cos\phi + W \sin\theta \sin\phi \tag{79}$$

This last condition along with the fact that $U \to 0$ as $r \to \infty$ makes up the boundary conditions on U. The velocity potential (U) must satisfy Laplace's equation:

$$\nabla^2 U = 0 \tag{80}$$

A solution to this equation which satisfies the above boundary conditions is

$$U = \frac{1}{r^2} (A \sin\theta \cos\phi + B \sin\theta \sin\phi). \tag{81}$$

It follows that

$$\frac{\partial U}{\partial r}_{r = R} = -\frac{2}{R^3} (A \sin\theta \cos\phi + B \sin\theta \sin\phi) \tag{82}$$

$$= \Omega d \sin\theta \cos\phi + W \sin\theta \sin\phi$$

The above equality must hold for all θ and ϕ, hence:

$$-\frac{2}{R^3} A = \Omega d \qquad \text{and} \qquad -\frac{2}{R^3} B = W$$

$$\text{or } A = -\frac{1}{2} R^3 \Omega d \qquad \text{and} \qquad B = -\frac{1}{2} R^3 W$$

Thus, the final expression for the potential becomes

$$U = -\frac{1}{2} \frac{R^3}{r^2} (\Omega d \sin\theta \cos\phi + W \sin\theta \sin\phi) \tag{83}$$

Two equations connecting the four unknowns: Ω, d, θ, and ϕ may be obtained by finding the coordinates of the stagnation point. We do this by finding V_θ and V_ϕ at $r = R$ and equating them to zero.

$$V_\theta = \overline{\nabla}_\theta U - \left[\overline{W} + \Omega \times (\overline{r} + \overline{d})\right]_\theta \tag{84}$$

$$\text{In general, } v_\theta = v_x \cos\theta \cos\phi + v_y \cos\theta \sin\phi - v_z \sin\theta \tag{85}$$

$$\text{Hence, } V_\theta = \frac{1}{r} \frac{\partial U}{\partial \theta} - \Omega(r\cos\theta + d)\cos\theta\cos\phi - W\cos\theta\sin\phi - \Omega r \sin^2\theta \cos\phi \tag{86}$$

$$V_{\theta\,r=R} = -\frac{3}{2}(\Omega d \cos\theta \cos\phi + W \cos\theta \sin\phi) - \Omega R \cos\phi \tag{87}$$

$$V_\phi = \overline{\nabla}_\phi U - \left[\overline{W} + \overline{\Omega} \times (\overline{r} + \overline{d})\right]_\phi \tag{88}$$

$$\text{in general, } v_\phi = v_y \cos\phi - v_x \sin\phi \tag{89}$$

$$\text{therefore } V_\phi = \frac{1}{r \sin\theta} \frac{\partial U}{\partial \phi} - W\cos\phi + \Omega(r\cos\theta + d)\sin\phi \tag{90}$$

$$(V_\phi)_{r=R} = \frac{3}{2}\left[\Omega d \sin\phi - W\cos\phi\right] + \Omega R \cos\theta \sin\phi \tag{91}$$

We now equate expression (87) and (91) to zero and obtain:

$$3\cos\theta(\Omega d \cos\phi + W \sin\phi) + 2\Omega R \cos\phi = 0 \tag{92}$$

$$3(\Omega R d \sin\phi - W\cos\phi) + 2\Omega R \cos\theta \sin\phi = 0 \tag{93}$$

These two equations contain the four unknowns: Ω (balloon angular velocity), d (radius of spiral), and θ, ϕ (coordinates of stagnation point).

As is well-known, however, two equations in four unknowns are a rather useless bit of symbolism in themselves. With this in mind, we come to the main problem of this paper: How to find something which occurs at the stagnation point, and how to express this something in the form of two or more analytic expressions.

We have at our disposal another hydrodynamic equation, namely Euler's equation of motion or, in its first integral form, Bernoulli's equation. For a system of rotating and translating axes such as those employed in this problem, Bernoulli's equation takes the form:

$$p = \frac{1}{2} \rho \Omega^2 D^2 \theta \rho g y - \frac{1}{2} \rho V^2 + f(t) \tag{94}$$

where p = pressure, ρ = density, f(t) = function of time, y = height above center of balloon, $D = \left[(d + z)^2 + x^2\right]^{1/2}$ = perpendicular distance from axis of spiral.

There are good physical reasons for believing that the pressure is maximum at the stagnation point (where V = 0). This may be rationalized by considering that the stagnation point is the most physically significant point on the top-half of the balloon. Since the pressure has a maximum at some point on the balloon, we would expect that this maximum would occur at the stagnation point. Furthermore, it is generally known that in the case of any solid body moving in an airstream with constant velocity the stagnation point and pressure maximum occur at the same point. With this bit of justification behind us, we now proceed to maximize the pressure:

The pressure is a maximum if

$$\frac{\partial p}{\partial \theta} = \frac{\partial p}{\partial \phi} = 0 \text{ on } r = R.$$

Substituting for D and y in (3) we get

$$p = \frac{1}{2} \rho \Omega^2 (d^2 + 2 rd \cos \theta + r^2 \cos^2 \theta + r^2 \sin^2 \theta \cos^2 \phi) \tag{95}$$
$$- \rho gr \sin \theta \sin \phi - \frac{1}{2} \rho V^2 + f(t)$$

$$\frac{\partial p}{\partial \theta} = \frac{1}{2} \rho \Omega^2 (-2 rd \sin \theta - 2r^2 \sin \theta \cos \theta + 2r^2 \sin \theta \cos \theta \cos^2 \phi) \tag{96}$$
$$- \rho gr \cos \theta \sin \phi$$

$$\frac{\partial p}{\partial \phi} = \frac{1}{2} \rho \Omega^2 (-2r^2 \sin^2 \theta \cos \phi \sin \phi) - \rho gr \sin \theta \cos \phi \tag{97}$$

These last two expressions, when evaluated at r = R and equated to zero, give

$$\Omega^2 \sin\theta\,(R\cos\theta\sin^2\phi + d) + g\cos\theta\sin\phi = 0 \tag{98}$$

$$\Omega^2 R\sin\theta\sin\phi + g = 0, \text{ provided } \sin\theta\cos\phi \neq 0 \tag{99}$$

We now have at our disposal four equations: namely, 92, 93, 98, and 99 in the four unknowns Ω, d, θ, and ϕ. It is possible, in principle, to solve these four equations for the unknowns.

Equations 93, 98, and 99 are easily solved by eliminating θ and ϕ. However, the inevitable conclusion reached is that

$$\Omega d^2 = 0 \tag{100}$$

and upon further analysis we see that this implies that $\Omega \neq 0$, but that d = 0. This is interpreted as meaning that the balloon is rotating about its axis and rising vertically. We can only conclude from this that (1) a rising balloon cannot spiral or (2) the assumption made about the pressure at the stagnation point is false. If we accept conclusion (2) as more likely and shelve our conceptual misgivings, we can search for another set of relationships.

If the pressure is not a maximum at the stagnation point as defined above, where is it a maximum? There is one other physically significant point on the upper half of the balloon. This point, which we might call the null-disturbance point, is that point at which the hydrodynamic disturbance in the air due to the balloon is zero. That is to say, it is the point at which the air motion relative to the balloon axes is purely helical. The fact that the disturbance is zero at this point is expressed mathematically by the equation

$$\overline{\nabla} U = 0 \tag{101}$$

This implies that $\overline{\nabla}_\theta U = \overline{\nabla}_\phi U = \overline{\nabla}_r U = 0$, and that $\overline{\nabla}_r U \equiv 0$ identically on r = R.

$$\nabla_\theta U = -\frac{1}{2}\cos\theta\,(\Omega d\cos\phi + W\sin\phi) \tag{102}$$

$$\nabla_\phi U = \frac{1}{2}\,(\Omega d\sin\phi - W\cos\phi) \tag{103}$$

The above two expressions when equated to zero yield:

$$\cos\theta\,(\Omega d\cos\phi + W\sin\phi) = 0 \quad \text{and} \tag{104a}$$

$$\Omega d\sin\phi - W\cos\phi = 0 \tag{104b}$$

These two equations will be supplemented by the two pressure conditions used before, namely

$$\frac{\partial p}{\partial\theta} = \frac{\partial p}{\partial\phi} = 0 \quad \text{at the null-disturbance point.}$$

The pressure is given as before by

$$p = \frac{1}{2}\rho\Omega^2(d^2 = 2dr\cos\theta + r^2\cos^2\theta + r^2\sin^2\theta\cos^2\phi) \qquad (105)$$

$$-\rho\, gr\sin\theta\sin\phi - \frac{1}{2}\rho V^2 + f(t)$$

$$\frac{\partial p}{\partial\theta} = \rho\Omega^2(-dr\sin\theta - r^2\sin\theta\cos\theta + r^2\sin\theta\cos\theta\cos^2\phi) \qquad (106)$$

$$-\rho\, gr\cos\theta\sin\phi - \rho\overline{V}\cdot\frac{\partial\overline{V}}{\partial\theta}$$

and $$\frac{\partial p}{\partial\phi} = -\rho\Omega^2 r^2\sin^2\theta\sin\phi\cos\phi - \rho\, g\, r\sin\theta\cos\phi - \rho\overline{V}\cdot\frac{\partial\overline{V}}{\partial\phi} \qquad (107)$$

A little algrebra gives:

$$\overline{V}\cdot\frac{\partial\overline{V}}{\partial\theta} = -\frac{3}{2}\Omega^2 Rd\sin\theta\cos^2\phi - \frac{3}{2}W\Omega R\sin\theta\sin\phi\cos\phi \qquad (108)$$

$$-\Omega^2 R^2\sin\theta\cos\theta\sin^2\phi$$

and

$$\overline{V}\cdot\frac{\partial\overline{V}}{\partial\phi} = \frac{3}{2}W\Omega R\cos\theta\cos^2\phi - \Omega^2 R^2\sin\phi\cos\phi \qquad (109)$$

$$+\frac{3}{2}W\Omega R\cos\theta\sin^2\phi + \Omega^2 R^2\cos^2\theta\sin\phi\cos\phi$$

These substituted into equations 106 and 107 give, along with the condition that $\frac{p}{\theta} = \frac{p}{\phi} = 0$, that

$$-\Omega^2 d\sin\theta - g\cos\theta\sin\phi + \frac{3}{2}\Omega^2 d\sin\theta\cos^2\phi \qquad (110a)$$

$$+\frac{3}{2}W\Omega\sin\theta\sin\phi\cos\phi = 0$$

$$g\sin\theta\cos\phi + \frac{3}{2}W\Omega\cos\theta = 0 \qquad (110b)$$

The preceding four equations (104a, 104b, 110a, and 110b) are analogous to 92, 93, 98, and 99 of the previous analysis although it is apparent there is little similarity between the forms of the two sets of equations.

Equations 104a and 104b yield one physically significant solution, namely,

$$\cos\theta = 0 \text{ and } \tan\phi = \frac{W}{\Omega d}$$

These two conditions when substituted in equations 110a and 110b yield

$$\Omega^2 d = 0 \tag{111}$$

which is identical with the result obtained under the assumption that the pressure is maximum with $\nabla = 0$.

Thus, two essentially different sets of assumptions lead to the same physically insignificant result--namely that the balloon does not spiral. We are again left with the two alternate conclusions mentioned previously: (1) that the balloon can't spiral and (2) that the pressure assumption is false.

If we again accept conclusion (2) as correct, we are once more left with but two valid equations (either 92 and 93 or 104a and 104b), and the problem again is to find two more. This could easily be done if an expression could be found for the pressure in the vicinity of the stagnation point (or null-disturbance point). First, we recall Bernoulli's equation is

$$p - \frac{1}{2} \rho \Omega^2 D^2 + \rho g y + \frac{1}{2} \rho V^2 = f(t) \tag{112}$$

The above-mentioned expression for the pressure could be substituted in Bernoulli's equation, and the entire system of equations could be differentiated with respect to the space coordinates of the balloon and equated to zero.

This method depends upon the fact that f(t) is only a function of t and therefore:

$$\frac{\partial f}{\partial \theta} = \frac{\partial f}{\partial \phi} = \frac{\partial f}{\partial r} = \frac{\partial^2 f}{\partial \theta \, \partial \phi} = \frac{\partial^2 f}{\partial \theta \, \partial r} = \frac{\partial^2 f}{\partial \phi \, \partial r} = \frac{\partial^2 f}{\partial \theta^2} = \frac{\partial^2 f}{\partial \phi^2} = \frac{\partial^2 f}{\partial r^2} = 0 \tag{113}$$

Although all the above equations are not independent, at least three of them would most likely be so. It is therefore possible that they could yield at least three more equations in the unknowns.

APPENDIX 3

TIME SERIES ANALYSIS BY HEALY AND BOGERT

1. READIN (A, NA, ANAME)

This Subroutine reads in NA values of the sequence A from punch cards. NA is read from columns 1-6 of the first card and the BCD characters in columns 7-80 are stored in the vector ANAME for future references. ANAME must be given the dimension 13 in the main program. The second card of the deck carries the format of the data cards in ordinary FORTRAN form omitting the word FORMAT but including the parentheses.

2. OUTPUT (A, NA, ANAME, INDIC)

This Subroutine prints NA values of the sequence A in floating form (without starting a new page). The printout is preceded by the name held in BCD characters in the vector ANAME which must be given the dimension 13 in the main program. If INDIC is negative, the series will be punched out five to a card with the two preceding cards required by READIN; if INDIC is a positive number, the series will be written on the corresponding tape as three binary records--the first containing NA, the second ANAME.

3. DETRND (A, NA, B, NDEG)

The mean (NDEG = 0) or a least-square linear trend (NDEG = 1) is subtracted from the NA values of the sequence A, and the residuals are stored as the sequence B.

4. AUTCOV (A, NA, B, L)

This Subroutine calculates the series B as the autocovariances of the series A (of length NA) from lags 0 to L. Owing to the nature of FORTRAN indexing, B(J) corresponds to lag (J - 1), and the sequence B is of length L + 1. The formula used is

$$B(J) = \sum_{I=1}^{NA - J+1} A(I) * A(I + J - 1) \; / \; (NA - J + 1) - AVE^2, \qquad J = 1, \; L + 1 \tag{114}$$

when AVE denotes the average values of the sequence A.

5. FOURTR (A, L, B, INDIC)

Form the sequence B as the Fourier transform of the sequence A of length L + 1. For INDIC = 1,

$$B(K) = A(1) + \sum_{I=2}^{L} A(I) * \cos \frac{(I - 1)(K - 1)}{L} \pi + (-1)^{K-1} A(L+1) \; / \; L, \qquad K=1, \; L+1. \tag{115}$$

For INDIC = 2 the cosines are replaced by sines, and the end terms are omitted. INDIC = 3 or 4 provides these same transforms smoothed ("hanned") with coefficients 1/4, 1/2, 1/4, the end terms being found from symmetry considerations. Note that the sequences are not of length L+1 to match AUTCOV and CRSCOV. N must not exceed 1500.

APPENDIX 4

ADDITIONAL SUBROUTINES ADDED BY WILLIAM E. BROCKMAN TO THE ORIGINAL PROGRAM BY HEALY AND BOGERT

1. QTRND (A, NA, B)

The least-squares quadratic trend is subtracted from the NA values of the sequence A, and the residuals are stored as the sequence B. Orthogonal polynomial coefficients are used.

2. WHITN (A, NA, ALFA1, ALFA2, B)

The data in the sequence A of length NA is prewhitened using the coefficients ALFA1 and ALFA2; the whitened data is then stored in sequence B. The prewhitening equation is given by:

$$B(I) = ALFA1 * A(I) + ALFA2 * A(I + 1) \quad I = 1, N-1 \tag{116}$$

3. PDRKN (A, NA, ALFA1, ALFA2, B)

The data in the sequence A of length NA is post-darkened (also known as "recoloring") using the coefficients ALFA1 and ALFA2; the post-darkened data is then stored in sequence B. The post-darkening equation used is

$$B(I) = \frac{A(I)}{ALFA1^2 + ALFA2^2 + 2 * ALFA1 * ALFA2 * \cos(\pi * (I-1) / N)} \qquad I=1, N-1 \tag{117}$$

4. TRNDR (A, NA, L, B)

Straight line segments containing L points are subtracted from corresponding points in the sequence A of length NA; the residuals are stored as the sequence B.

5. MOVAVG (A, NA, L, B)

Moving averages over L points are subtracted from the point corresponding to the mid-point of the L points of sequence A of length NA. Again the residuals are stored as the sequence B.

APPENDIX 5

APPROXIMATE VALUES OF AERODYNAMIC FORCES ACTING ON THE ROSE BALLOON

The results of our work thus far in explaining mathematically the balloon's self-induced motion have yielded very little useful information. The plots of the space coordinates of a ROSE sounding which first revealed loops and spirals in an altitude band which rawinsonde reported to be calm were indeed surprising. Curiosity was the motivation for our attempt to compute the magnitude of the forces necessary to produce such motions.

The equations of motion for the three coordinates can be written as:

$$M\ddot{x} = 1/2\ \rho \cdot A \cdot C_D\ |v|\ (\dot{x} - W_x) + A_x \tag{118}$$

$$M\ddot{y} = 1/2\ \rho \cdot A \cdot C_D\ |v|\ (\dot{y} - W_y) + A_y \tag{119}$$

$$M\ddot{z} = -1/2\ \rho \cdot A \cdot C_D\ |v|\ (\dot{z} - W_z) + A_z + mg - g\rho V_B \tag{120}$$

M is the total (system plus induced) mass, and A_q is the Aerodynamic Force in the q component. We can assume that $W_z = {}^{q}z = A_z = 0$, and we have shown that a good approximation for M (the total mass) is

$$M = m + 1/2\ \rho\ V_B \tag{121}$$

where m is the mass of the system.

Making the substitutions and rearranging the equations become:

$$-1/2\ \rho \cdot A \cdot C_D\ |v| = \frac{(m+1/2\rho V_B)\ \ddot{x} - A_x}{\dot{x} - W_x} \tag{122}$$

$$-1/2\ \rho \cdot A \cdot C_D\ |v| = \frac{(m+1/2\rho V_B)\ \ddot{y} - A_y}{\dot{y} - W_y} \tag{123}$$

$$-1/2\ \rho \cdot A \cdot C_D\ |v| = \frac{-mg + g\rho\ V_B}{\dot{z}} \tag{124}$$

Since the left side of all three equations are now identical, the right sides can be equated:

$$\frac{(m+1/2\ \rho\ V_B)\ \ddot{x} - A_x}{\dot{x} - W_x} = \frac{-mg + g\rho\ V_B}{\dot{z}} \tag{125a}$$

$$\frac{(m + 1/2\ \rho\ V_B)\ddot{y} - A_y}{\dot{y} - W_y} = \frac{-mg + g\rho\ V_B}{\dot{z}} \tag{125b}$$

and solving these 2 equations for A_x and A_y respectively gives:

$$A_x = (m + 1/2\ \rho\ V_B)\ddot{x} + (mg - g\rho\ V_B) \cdot \frac{(\dot{x} - W_x)}{\dot{z}} \tag{126a}$$

$$A_y = (m + 1/2\ \rho\ V_B)\ddot{y} + (mg - g\rho\ V_B) \cdot \frac{(\dot{y} - W_y)}{\dot{z}} \tag{126b}$$

The values used for the accelerations and velocities were obtained from a randomly selected standard ROSE flight. The data was fitted with a second-degree orthogonal polynomial. The first derivative evaluated at the mid-point of the 100-foot interval produced the velocities, and the second derivative produced the accelerations. The density (ρ) was obtained from the 1962 Model Atmosphere, and the gravity (g) was taken to be -9.8 m/sec^2. The winds (W_x and W_y) were average value of the winds on the layer 500 feet above and below the particular altitude. The vector sum of A_x and A_y was then computed. The results were as follows:

Altitude (feet)	Aerodynamic Force (newtons)
500	27.5
5,000	45.1
10,000	28.1
20,000	10.4
30,000	11.5
40,000	3.2
50,000	5.5

The values seem to agree with the spirals in the data, but their accuracy is suspect because of approximations and assumptions. The trend of lower forces at the higher altitudes also agrees with the theory that the critical value of Reynolds Number occurs at about 40,000 feet.

This approach was not pursued because of reasoning similar to that given for not pursuing the questionable results of Power Spectral Density Analysis.

APPENDIX 6

LEGENDRE POLYNOMIALS

This appendix is included in order to give the reader easy access to the actual numbers used in the polynomials. $P_{m,n}(i)$ is a Legendre polynomial of degree m, of the form

$$P_{m,n}(i) = \sum_{k=0}^{m} (-1)^k \binom{m}{k} \binom{m+k}{k} \frac{i^{[k]}}{n^{[k]}} \tag{13}$$

where $i^{[k]} = i\,(i-1)(i-2)\ldots(i-k+1)$ and $i^{[0]} = 1$ (14a)

and $$\binom{m}{k} = \frac{m!}{(m-k)!\;k!} \tag{14b}$$

The first few polynomials are:

$$P_{0,n}(i) = 1 \tag{33a}$$

$$P_{1,n}(i) = 1 - 2\frac{i}{n} \tag{33b}$$

$$P_{2,n}(i) = 1 - 6\frac{i}{n} + 6\,\frac{i(i-1)}{n(n-1)} \tag{33c}$$

Now make the following substitution:

$$C_1 = \frac{i}{n} \tag{127a}$$

$$C_2 = C_1\,(\frac{i-1}{n-1}) \tag{127b}$$

$$C_3 = C_2\,(\frac{i-2}{n-2}) \tag{127c}$$

$$\vdots$$

$$C_m = C_{m-1}(\frac{i-m+1}{n-m+1}) \tag{127d}$$

gives this simpler form for the polynomials.

$$P_{0,n}(i) = 1 \tag{128a}$$

$$P_{1,n}(i) = 1 - 2C_1 \tag{128b}$$

$$P_{2,n}(i) = 1 - 6C_1 + 6C_2 \tag{128c}$$

$$P_{3n,}(i) = 1 - 12C_1 + 30\,C_2 - 20C_3 \tag{128d}$$

$$P_{4,n}(i) = 1 - 20C_1 + 90\,C_2 - 140C_3 + 70C_4 \tag{128e}$$

$$P_{5,n}(i) = 1 - 30C_1 + 210C_2 - 560C_3 + 630C_4 - 252C_5 \tag{128f}$$

$$P_{6,n}(i) = 1 - 42C_1 + 420C_2 - 1680C_3 + 3150C_4 - 2772C_5 + 924C_6 \tag{128g}$$

$$P_{7,n}(i) = 1 - 56C_1 + 756C_2 - 4200C_3 + 11550C_4 - 16632C_5 + 12012C_6 - 3432C_7 \tag{128h}$$

$$P_{8,n}(i) = 1 - 72C_1 + 1260C_2 - 9240C_3 + 34650C_4 - 72072C_5 + 64084C_6 - 51480C_7 + 12870C_8 \tag{128i}$$

$$P_{9,n}(i) = 1 - 90C_1 + 1980C_2 - 18480C_3 + 90090C_4 - 252252C_5 + 420420C_6 - 411840C_7 + 218790C_8 - 48620C_9 \tag{128j}$$

The first derivative of the orthogonal polynomial

$$\hat{q}_i = A_{0,n}(i) + A_1P_{1,n}(i) + A_2P_{2,n}(i) + \ldots + A_mP_{m,n}(i) \tag{11}$$

is given by

$$\dot{\hat{q}}_i = A_0P'_{0,n}(i) + A_1P'_{1,n}(i) + A_2P'_{2,n}(i) + \ldots + A_mP'_{m,n}(i) \tag{30}$$

where $P'_{m,n}(i)$ is the first derivative of the Legendre polynomial

It is a characteristic of Legendre polynomials that if m is even and the first derivative is evaluated at the mid-point (n/2) of the interval with length n, then

$$P'_{m,n}\left(\frac{n}{2}\right) = 0 \tag{38}$$

Therefore, the derivative of an even degree polynomial is equivalent to the derivative of a polynomial of one degree less. For example, if m = 2, then

$$P_{2,n}(i) = 1 - 6\frac{i}{n} + 6\,\frac{i^2 - i}{n^2 - n} \tag{33c}$$

and the first derivative with respect to i is given by:

$$P'_{2,n}(i) = -6 \cdot \frac{1}{n} + 6 \cdot \frac{2i - 1}{n^2 - n} \tag{34c}$$

At $i = n/2$

$$P'_{2,n}\left(\frac{n}{2}\right) = -\frac{6}{n} + \frac{6\left(2 \cdot \frac{n}{2} - n\right)}{n\,(n-1)} \tag{129a}$$

$$P'_{2,n}\left(\frac{n}{2}\right) = -\frac{6}{n} + \frac{6}{n}\,\frac{(n-1)}{n-1} = -\frac{6}{n} + \frac{6}{n} = 0. \tag{129b}$$

The derivatives are taken with respect to the index (i); therefore the denominator which contains only functions of n does not change. To simplify, the following substitution will be made: Let

$$NB\,(1) = n \tag{130a}$$

$$NB\,(2) = n\,(n-1) \tag{130b}$$

$$NB\,(3) = n\,(n-1)\,(n-2) \tag{130c}$$

$$\vdots \qquad\qquad \vdots$$

$$NB\,(j) = n(n-1) \ldots (n+1-j) \tag{130d}$$

The Legendre polynomial general derivatives and the derivatives evaluated at $i = n/2$ are listed below:

$$P'_{1,n}(i) = -\frac{2}{NB(1)} \qquad P'_{1,n}\left(\frac{n}{2}\right) = -\frac{2}{NB(1)} \tag{131a, 131b}$$

$$P'_{3,n}(i) = -12\,\frac{1}{NB(1)} + 30\,\frac{2i-1}{NB\,(2)} - 20\,\frac{(3i^2 - 6i + 2)}{NB\,(3)} \tag{132a}$$

$$P'_{3,n}\left(\frac{n}{2}\right) = \frac{-12}{NB\,(1)} + 30\,\frac{1}{NB(2)}\left[n - 1\right] - 20\,\frac{1}{NB(3)}\left[2 + \frac{n}{4}\,(-12 + 3n)\right] \tag{132b}$$

$$P'_{5,n}(i) = -30\,\frac{1}{NB\,(1)} + 210\,\frac{1}{NB\,(2)}\left[2i - 1\right] - 560\,\frac{1}{NB\,(3)}\left[2 + \frac{i}{2}\,(-12 + 6i)\right] \tag{133a}$$

$$+ 630\,\frac{1}{NB\,(4)}\left[-6 + i(22 + 2i(-9 + 2i))\right] - 252\,\frac{1}{NB\,(5)}\cdot$$

$$\left[24 + \frac{i}{8}\,(-800 + 2i\,(420 + 2i(-80 + 10i)))\right]$$

$$P'_{5,n}\left(\frac{n}{2}\right) = -30\,\frac{1}{NB\,(1)} + 210\,\frac{1}{NB\,(2)}\left[n - 1\right] - 560\,\frac{1}{NB\,(3)}\left[2 + \frac{n}{4}\,(-12 + 3n)\right] \tag{133b}$$

$$+ 630 \frac{1}{NB(4)} \left[-6 + \frac{n}{2}(22 + n(-9 + n))\right] - 252 \frac{1}{NB(5)} \cdot$$

$$\left[24 + \frac{n}{16}(-800 + n(420 + n(-80 + 5n)))\right]$$

$$P'_{7,n}\left(\frac{n}{2}\right) = -56 \frac{1}{NB(1)} + 756 \frac{1}{NB(2)} \left[-1 + n\right] - 4200 \frac{1}{NB(3)} \cdot \quad (134)$$

$$\left[2 + \frac{n}{4}(-12 + 3n)\right] + 1150 \frac{1}{NB(4)} \left[-6 + \frac{n}{2}(22 + n(-9 + n))\right]$$

$$- 16632 \frac{1}{NB(5)} \left[24 + \frac{n}{16}(-800 + n(420 + n(-80 + 5n)))\right]$$

$$+ 12012 \frac{1}{NB(6)} \left[-120 + \frac{n}{16}(4348 + n(-2700 + n(-75 + 3n))))\right]$$

$$-3432 \frac{1}{NB(7)} \left[720 + \frac{n}{64}(-112896 + n(77952 + 7(-12000 + n$$

$$(3500 + n(252 + 7n)))))\right]$$

$$P'_{9,n}\left(\frac{n}{2}\right) = -90 \frac{1}{NB(1)} + 1980 \frac{1}{NB(2)} \left[-1 + n\right] - 18480 \frac{1}{NB(3)} \cdot \quad (135)$$

$$\left[2 + \frac{n}{4}(-12 + 3n)\right] + \frac{90090}{NB(4)} \left[-6 + \frac{n}{2}(22 + n(-9 + n))\right]$$

$$-252252 \frac{1}{NB(5)} \left[24 + \frac{n}{16}(-800 + n(420 + n(-80 + 5n)))\right]$$

$$+ 420420 \frac{1}{NB(6)} \left[-120 + \frac{n}{16}(4384 + n(-2700 + n(-75 + 3n))))\right]$$

$$-411840 \frac{1}{NB(7)} \left[720 + \frac{n}{64}(-112896 + n(77952 + n$$

$$(-12000 + n(3500 \cdot n(252 + 7n)))))\right] + 218790 \frac{1}{NB(8)} \cdot$$

$$\left[-5040 + \frac{n}{16}(209088 = n(-157584 + n(54152 + n(-980 + n$$

$$(966 + n(-9 + n))))))\right] -48620 \frac{1}{NB(9)} \left[40320 + \frac{n}{256}\right.$$

$$(-28053504 + n(22679808 + n(-8612352 + n(1795920 + n \cdot$$

$$(-217728 + n(15288 + n(-576 + 9)))))))\Big]$$

A still more convenient form for computing can be obtained by the following substitution:

Let $(FCR)_1 = \frac{1}{NB\ (1)}$ (136a)

$$(FCR)_2 = \frac{1}{NB\ (2)}\left[\ -1 + n\ \right] \quad (136b)$$

$$(FCR)_3 = \frac{1}{NB\ (3)}\left[\ -12 + 3n\right] \quad (136c)$$

$$(FCR)_4 = \frac{1}{NB\ (4)}\left[\ -6 + \frac{n}{2}(22 + n(-9 + n))\ \right] \quad (136d)$$

$$(FCR)_5 = \frac{1}{NB\ (5)}\left[\ 24 + \frac{n}{16}(-800 + n(420 + n(-80 + 5n)))\ \right] \quad (136e)$$

$$(FCR)_6 = \frac{1}{NB\ (6)}\left[\ -120 + \frac{n}{16}\ (4384 + n(-2700 + n(680 - n(-75 + 3n))))\right] \quad (136f)$$

$$(FCR)_7 = \frac{1}{NB\ (7)}\left[\ 720 + \frac{n}{64}(-112896 + n(77952 + n(-12000 + n\ (3500 + n(252 + 7n)))))\ \right] \quad (136g)$$

$$(FCR)_8 = \frac{1}{NB\ (8)}\left[\ -5040 + \frac{n}{16}(209088 = n(-157584 + n(54152 + n(-9800 + n(966 + n(-49 + n))))))\ \right] \quad (136h)$$

$$(FCR)_9 = \frac{1}{NB\ (9)}\left[\ 40320 + \frac{n}{265}(-28054504 + n(22679808 + n(-8612352 + n(1795920 + n(-217728 + n(15288 + n(-576 + 9n)))))))\ \right] \quad (136i)$$

The polynomials evaluated at the mid-point (n/2) then become:

$$P'_{1,n}\left(\frac{n}{2}\right) = -2\ (FCR)_1 \quad (137a)$$

$$P'_{3,n}\left(\frac{n}{2}\right) = -12\ (FCR)_1 + 30\ (FCR)_2 - 20\ (FCR)_3 \quad (137b)$$

$$P'_{5,n}\left(\frac{n}{2}\right) = -30\ (FCR)_1 + 210\ (FCR)_2 - 560\ (FCR)_3 + 630\ (FCR)_4 \quad (137c)$$

$$-252\ (FCR)_5$$

$$P'_{7,n}(\frac{n}{2}) = -56\,(FCR)_1 + 756\,(FCR)_2 - 4200\,(FCR)_3 + 11550\,(FCR)_4 \quad (137d)$$

$$-16632\,(FCR)_5 + 12012\,(FCR)_6 - 3432\,(FCR)_7$$

$$P'_{9,n}(\frac{n}{2}) = -90\,(FCR)_1 + 1980\,(FCR)_2 - 18480\,(FCR)_3 = 90090\,(FCR)_4 \quad (137e)$$

$$-252252\,(FCR)_5 + 420420\,(FCR)_6 - 411840\,(FCR)_7$$

$$+ 218790\,(FCR)_8 - 48620\,(FCR)_9$$

Acknowledgments:

The author wishes to express his appreciation to Major Robert Lenhard for his many helpful suggestions and his assistance in coordinating the efforts of the data processing system; to Mr. Nicholas Engler for his constructive criticisms and suggestions; to Mr. Anthony Grandillo and Mr. Yong W. Lim for their assistance in preparing the error analysis and orthogonal polynomial coefficients; to Mr. Lawrence Jehn for assistance in applying the PSD technique; to Mr. Robert Willis for his work on balloon motions; and to Mrs. Robert Murphy and Miss Sue Bledsoe for their assistance in preparing this manuscript.

References

1. Scoggins, James R., "An Evaluation of Detail Wind Data as Measured by the FPS-16 Radar/Spherical Balloon Technique," NASA TN D. 1572, NASA, May 1963.

2. Crow, E. L., Davis, Maxfield, Statistics Manual, S599, Dover Publications, Inc., N.Y., N.Y., 1960.

3. Brockman, William E., "Computer Programs in FORTRAN and BALGOL for Determining Winds, Density, Pressure, and Temperature from the ROBIN Falling Balloon," University of Dayton Research Institute report for Contract AF 19(604)-7450, AFCRL, Hanscom Field, Massachusetts.

4. Murrow, Harold N., and Robert M. Henry, "Self-Induced Balloon Motion and Their Effects on Wind Data," presented at American Meteorological Society 5th Conference on Applied Meteorology, Atlantic City, N.J., March 2-6, 1964.

5. Blackman, R. B., and J. W. Tukey, "The Measurement of Power Spectra," Dover Publications, Inc., N.Y., 1959.

6. Healy, M. J. R., and B. P. Bogert, "FORTRAN Subroutines for Time Series Analysis," Communications of the Association for Computing Machinery, Vol. 6, No. 1, (January, 1963) pages 32-34.

7. SHARE Distribution No. 1406 BE TISR (PA) and (LS), SHARE General Program Library.

8. Gauss, E. J., "Estimation of Power Spectral Density by Filters," Journal of the Association for Computing Machinery, Vol. 11, No. 1, (January, 1964) pages 98-103.

9. BIMD Computer Programs Manual, Health Sciences Computing Facility, Department of Preventive Medicine and Public Health, School of Medicine, University of California, Los Angeles.

10. Reid, Daniel F., "The ROSE Wind Sensor," presented at American Meteorological Society 5 th Conference on Applied Meteorology, Atlantic City, N.J., March 2-6, 1964.

11. U.S. Standard Atmosphere, 1962, prepared by NASA, USAF, and USWB, December, 1962, Washington, D.C.

12. Scoggins, James R., "Aerodynamics of Spherical Balloon Wind Sensors," Journal of Geophysical Research, 69 (4), February 15, 1964.

13. Leviton, R. "A Detailed Wind Profile Sounding Technique," Proceedings of the National Symposium on Winds for Aerospace Vehicle Design, Air Force Surveys in Geophysics, No. 140, Geophysics Research Directorate, Bedford, Mass., March, 1962.

14. Reed, W.H. III, "Comments on the FPS-16/Spherical Balloon Technique for Measuring Detailed Wind Profiles," a Memorandum commenting on Reference 13, NASA, Langley, Virginia.

Unclassified

Security Classification

DOCUMENT CONTROL DATA - R&D

(Security classification of title, body of abstract and indexing annotation must be entered when the overall report is classified)

1 ORIGINATING ACTIVITY (Corporate author) University of Dayton Research Institute University of Dayton, Dayton, Ohio	2a REPORT SECURITY CLASSIFICATION Unclassified 2b GROUP

3 REPORT TITLE

SMALL SCALE WIND SHEARS FROM ROSE BALLOON TRACKED BY AN/FPS 16 RADAR

4 DESCRIPTIVE NOTES (Type of report and inclusive dates)

Scientific Report. Final. December 1964

5 AUTHOR(S) (Last name, first name, initial)

Brockman, William E.

6 REPORT DATE December 1964	7a TOTAL NO OF PAGES 96	7b NO OF REFS 14
8a CONTRACT OR GRANT NO. AF 19(604)-7450 b PROJECT NO 6682 c TASK 668203 d	9a ORIGINATOR'S REPORT NUMBER(S) 9b OTHER REPORT NO(S) (Any other numbers that may be assigned this report) AFCRL-65-99	

10 AVAILABILITY/LIMITATION NOTICES

Qualified requestors may obtain copies of this report from DDC. Other persons or organizations should apply to U. S. Department of Commerce, Office of Technical Services, Washington, D. C. 20230

11 SUPPLEMENTARY NOTES	12 SPONSORING MILITARY ACTIVITY Air Force Cambridge Research Labs. Hq AFCRL, (CRER) USAF Waltham 54, Massachusetts

13 ABSTRACT

The ROSE balloon / AN-FPS-16 radar system is designed to report small-scale winds and shears by polynomial smoothing of the radar tracking data. The most successful mathematical technique for fitting the data and computing wind and shears is presented along with other techniques which were considered but ultimately rejected.

Analysis of self-induced balloon motion is attempted by classical physical methods and by a Power Spectral Density Technique.

A criterion for evaluating the effect of modification to the standard ROSE is developed and applied to modified ROSE's and the newer small light-weight balloon.

14 KEY WORDS	LINK A		LINK B		LINK C	
	ROLE	WT	ROLE	WT	ROLE	WT
ROSE Balloon Winds Wind Shears Power Spectral Density Radar Tracking						

INSTRUCTIONS

1. ORIGINATING ACTIVITY: Enter the name and address of the contractor, subcontractor, grantee, Department of Defense activity or other organization *(corporate author)* issuing the report.

2a. REPORT SECURITY CLASSIFICATION: Enter the overall security classification of the report. Indicate whether "Restricted Data" is included. Marking is to be in accordance with appropriate security regulations.

2b. GROUP: Automatic downgrading is specified in DoD Directive 5200.10 and Armed Forces Industrial Manual. Enter the group number. Also, when applicable, show that optional markings have been used for Group 3 and Group 4 as authorized.

3. REPORT TITLE: Enter the complete report title in all capital letters. Titles in all cases should be unclassified. If a meaningful title cannot be selected without classification, show title classification in all capitals in parenthesis immediately following the title.

4. DESCRIPTIVE NOTES: If appropriate, enter the type of report, e.g., interim, progress, summary, annual, or final. Give the inclusive dates when a specific reporting period is covered.

5. AUTHOR(S): Enter the name(s) of author(s) as shown on or in the report. Enter last name, first name, middle initial. If military, show rank and branch of service. The name of the principal author is an absolute minimum requirement.

6. REPORT DATE: Enter the date of the report as day, month, year, or month, year. If more than one date appears on the report, use date of publication.

7a. TOTAL NUMBER OF PAGES: The total page count should follow normal pagination procedures, i.e., enter the number of pages containing information.

7b. NUMBER OF REFERENCES: Enter the total number of references cited in the report.

8a. CONTRACT OR GRANT NUMBER: If appropriate, enter the applicable number of the contract or grant under which the report was written.

8b, 8c, & 8d. PROJECT NUMBER: Enter the appropriate military department identification, such as project number, subproject number, system numbers, task number, etc.

9a. ORIGINATOR'S REPORT NUMBER(S): Enter the official report number by which the document will be identified and controlled by the originating activity. This number must be unique to this report.

9b. OTHER REPORT NUMBER(S): If the report has been assigned any other report numbers *(either by the originator or by the sponsor)*, also enter this number(s).

10. AVAILABILITY/LIMITATION NOTICES: Enter any limitations on further dissemination of the report, other than those imposed by security classification, using standard statements such as:

(1) "Qualified requesters may obtain copies of this report from DDC."

(2) "Foreign announcement and dissemination of this report by DDC is not authorized."

(3) "U. S. Government agencies may obtain copies of this report directly from DDC. Other qualified DDC users shall request through _____."

(4) "U. S. military agencies may obtain copies of this report directly from DDC. Other qualified users shall request through _____."

(5) "All distribution of this report is controlled. Qualified DDC users shall request through _____."

If the report has been furnished to the Office of Technical Services, Department of Commerce, for sale to the public, indicate this fact and enter the price, if known.

11. SUPPLEMENTARY NOTES: Use for additional explanatory notes.

12. SPONSORING MILITARY ACTIVITY: Enter the name of the departmental project office or laboratory sponsoring *(paying for)* the research and development. Include address.

13. ABSTRACT: Enter an abstract giving a brief and factual summary of the document indicative of the report, even though it may also appear elsewhere in the body of the technical report. If additional space is required, a continuation sheet shall be attached.

It is highly desirable that the abstract of classified reports be unclassified. Each paragraph of the abstract shall end with an indication of the military security classification of the information in the paragraph, represented as (TS), (S), (C), or (U).

There is no limitation on the length of the abstract. However, the suggested length is from 150 to 225 words.

14. KEY WORDS: Key words are technically meaningful terms or short phrases that characterize a report and may be used as index entries for cataloging the report. Key words must be selected so that no security classification is required. Identifiers, such as equipment model designation, trade name, military project code name, geographic location, may be used as key words but will be followed by an indication of technical context. The assignment of links, rules, and weights is optional.